

ABSTRACT

Minarets are tall and slender structures. They are vulnerable to fail or get damaged under lateral loads. In recent years, the number of reinforced concrete (RC) minarets in North Cyprus has increased significantly. Owing absence of structural code about how to design a minaret, forced us to revise our knowledge about these structures. Door openings, geometry changes in the cross-sectional size and additional mass at balconies are one of the most frequently encountered problems in these unique structures. The main purpose is to make a comparison and discuss the results of wind and seismic analysis of selected RC minarets according to ACI307-98, NCSC2015 and TS498, in order to clarify weaknesses and critical points. For this reason four RC minarets of heights 26.0 m, 33.2 m, 61.45 m and 76.2 m which exist in North Cyprus have been modelled by using SAP2000, v19.0 package program. Two types of analysis adopted; static wind analysis and dynamic earthquake response spectrum analysis. The results obtained from both static and dynamic loads are presented in the form of top displacements, base reactions and internal forces for selected RC minaret for different codes. The major findings of this study indicate that the dynamic elastic response spectrum analysis according to ACI307-98 is forming the major lateral design load for the RC minarets and an additional concern should be given in the crucial points in order to preserve ductility of these structures.

Keywords: RC minarets; wind load; earthquake load; response spectrum method; finite element method; SAP2000

ÖZET

Minareler uzun ve narin yapılardır. Yanal yükler altında zarar görebilme veya hasar görmeye eğilimi olan yapılardır. Son yıllarda Kuzey Kıbrıs'taki betonarme minarelerin sayısı önemli ölçüde artmıştır. Minarelerin nasıl tasarlanacağına dair yol gösterici yapısal yönetmeliklerin eksikliği bizleri bu yapılar hakkındaki bilgimizi gözden geçirmemize zorlamıştır. Kapı boşlukları, enine kesitteki geometri değişiklikler ve balkonlardaki ek kütleler, bu eşsiz yapılarda en sık karşılaşılan sorunlu noktalardır. Zayıf noktaları ve kritik noktaları açıklığa kavuşturmak için ACI307-98, NCSC2015 ve TS498'e göre seçilen betonarme minarelerin rüzgar ve deprem analizinin sonuçlarını karşılaştırmalı olarak tartışmak ana hedeftir. Bu temel amaca göre, Kuzey Kıbrıs'ta var olan 26.0 m, 33.2 m, 61.45 m ve 76.2 m yüksekliğindeki dört adet betonarme minare, SAP2000, v19.0 paket programı kullanılarak modellenmiştir. İki tip analiz tatbik edilmiştir; Statik rüzgar analizi ve dinamik deprem spektrum analizi. Hem statik hem de dinamik yüklerden elde edilen sonuçlar, farklı yönetmeliklere göre seçilmiş betonarme minareler için, tepe deplasmanları, taban reaksiyon kuvvetleri ve iç kuvvetler şeklinde sunulmuştur. Bu çalışmanın başlıca bulguları, ACI307-98'e göre dinamik elastik tepki spektrum analizinin, betonarme minarelerinin ana yanal tasarım yükünü oluşturduğunu ve bu yapıların sünekliliğini korumak için kritik noktalarda ek bir hassasiyet gösterilmesi gerekliliğidir.

Anahtar Kelimeler: Betonarme minareler; rüzgar yükü; deprem yükü; tepki spektrum yöntemi; sonlu elemanlar yöntemi; SAP2000

**ANALYSIS OF RC MINARETS UNDER WIND
AND EARTHQUAKE LOADING IN NORTH
CYPRUS**

**A THESIS SUBMITTED TO THE GRADUATE
SCHOOL OF APPLIED SCIENCES
OF
NEAR EAST UNIVERSITY**

**By
LOUAY KARAKER**

**In Partial Fulfillment of the Requirements for
the Degree of Master of Science
in
Civil Engineering**

NICOSIA, 2018

LOUAY KARAKER

**ANALYSIS OF RC MINARETS UNDER WIND AND EARTHQUAKE
LOADING IN NORTH CYPRUS**

**NEU
2018**

**ANALYSIS OF RC MINARETS UNDER WIND AND
EARTHQUAKE LOADING IN NORTH CYPRUS**

**A THESIS SUBMITTED TO THE GRADUATE
SCHOOL OF APPLIED SCIENCES
OF
NEAR EAST UNIVERSITY**

**By
LOUAY KARAKER**

**In Partial Fulfillment of the Requirements for
the Degree of Master of Science
in
Civil Engineering**

NICOSIA, 2018

**Louay KARAKER: ANALYSIS OF RC MINARETS UNDER WIND
AND EARTHQUAKE LOADING IN NORTH CYPRUS**

**Approval of Director of Graduate School of
Applied Sciences**

Prof. Dr. Nadire ÇAVUŞ

**We certify that, this thesis is satisfactory for the award of the degree of Master of
Science in Civil Engineering**

Examining Committee in Charge:

Prof. Dr. Kabir Sadeghi

Department of Civil Engineering, Near
East University

Assoc. Prof. Dr. Mehmet Cemal Geneş

Department of Civil Engineering, Eastern
Mediterranean University

Assoc. Prof. Dr. Rifat Reşatoğlu

Supervisor, Department of Civil
Engineering, Near East University

I hereby declare that all information in this document has been obtained and presented in accordance with academic rules and ethical conduct. I also declare that, as required by these rules and conduct, I have fully cited and referenced all material and results that are not original to this work.

Name, Last name: Louay KARAKER

Signature:

Date:

ACKNOWLEDGEMENTS

At the outset, I would like to present my deepest thanks for my first and dependable supporters, my parents.

Sincere thanks go to all my respectable teachers in Near East University who helped me change not only my vision of engineering but also of life. Over and above I would like to express my deep and sincere gratitude to the examining committee of my thesis, Prof. Dr. Kabir Sadeghi as a head of jury and Assoc. Prof. Dr. Mehmet Cemal Geneş, as a jury member, for their efforts and interest. My deepest thanks go to my research supervisor Assoc. Prof. Dr. Rifat Reşatoğlu for his support that allowed me to overcome every possible problem in every step of my academic life and broadening my vision. I would also like to thank him for his patience, friendship and empathy.

My special appreciation and thanks go to my brothers, for their direct and indirect motivation and supporting to complete my master degree.

Last but not the least; I would like to thank my colleagues and friends for supporting me physically and spiritually throughout my life.

To my family...

ABSTRACT

Minarets are tall and slender structures. They are vulnerable to fail or get damaged under lateral loads. In recent years, the number of reinforced concrete (RC) minarets in North Cyprus has increased significantly. Owing absence of structural code about how to design a minaret, forced us to revise our knowledge about these structures. Door openings, geometry changes in the cross-sectional size and additional mass at balconies are one of the most frequently encountered problems in these unique structures. The main purpose is to make a comparison and discuss the results of wind and seismic analysis of selected RC minarets according to ACI307-98, NCSC2015 and TS498, in order to clarify weaknesses and critical points. For this reason four RC minarets of heights 26.0 m, 33.2 m, 61.45 m and 76.2 m which exist in North Cyprus have been modelled by using SAP2000, v19.0 package program. Two types of analysis adopted; static wind analysis and dynamic earthquake response spectrum analysis. The results obtained from both static and dynamic loads are presented in the form of top displacements, base reactions and internal forces for selected RC minaret for different codes. The major findings of this study indicate that the dynamic elastic response spectrum analysis according to ACI307-98 is forming the major lateral design load for the RC minarets and an additional concern should be given in the crucial points in order to preserve ductility of these structures.

Keywords: RC minarets; wind load; earthquake load; response spectrum method; finite element method; SAP2000

ÖZET

Minareler uzun ve narin yapılardır. Yanal yükler altında zarar görebilme veya hasar görmeye eğilimi olan yapılardır. Son yıllarda Kuzey Kıbrıs'taki betonarme minarelerin sayısı önemli ölçüde artmıştır. Minarelerin nasıl tasarlanacağına dair yol gösterici yapısal yönetmeliklerin eksikliği bizleri bu yapılar hakkındaki bilgimizi gözden geçirmemize zorlamıştır. Kapı boşlukları, enine kesitteki geometri değişiklikler ve balkonlardaki ek kütleler, bu eşsiz yapılarda en sık karşılaşılan sorunlu noktalardır. Zayıf noktaları ve kritik noktaları açıklığa kavuşturmak için ACI307-98, NCSC2015 ve TS498'e göre seçilen betonarme minarelerin rüzgar ve deprem analizinin sonuçlarını karşılaştırmalı olarak tartışmak ana hedeftir. Bu temel amaca göre, Kuzey Kıbrıs'ta var olan 26.0 m, 33.2 m, 61.45 m ve 76.2 m yüksekliğindeki dört adet betonarme minare, SAP2000, v19.0 paket programı kullanılarak modellenmiştir. İki tip analiz tatbik edilmiştir; Statik rüzgar analizi ve dinamik deprem spektrum analizi. Hem statik hem de dinamik yüklerden elde edilen sonuçlar, farklı yönetmeliklere göre seçilmiş betonarme minareler için, tepe deplasmanları, taban reaksiyon kuvvetleri ve iç kuvvetler şeklinde sunulmuştur. Bu çalışmanın başlıca bulguları, ACI307-98'e göre dinamik elastik tepki spektrum analizinin, betonarme minarelerinin ana yanal tasarım yükünü oluşturduğunu ve bu yapıların sünekliliğini korumak için kritik noktalarda ek bir hassasiyet gösterilmesi gerekliliğidir.

Anahtar Kelimeler: Betonarme minareler; rüzgar yükü; deprem yükü; tepki spektrum yöntemi; sonlu elemanlar yöntemi; SAP2000

TABLE OF CONTENTS

ACKNOWLEDGMENTS.....	i
ABSTRACT.....	iii
ÖZET	iv
TABLE OF CONTENTS	v
LIST OF TABLES	viii
LIST OF FIGURES	x
LIST OF ABBREVIATIONS	xii
LIST OF SYMBOLS	xiii

CHAPTER 1: INTRODUCTION

1.1 Background	1
1.2 Effect of Lateral Loads on Minarets	4
1.3 Significance of the Study.....	7
1.4 Objectives of the Study.....	11

CHAPTER 2: LITERATURE REVIEW

2.1 Overview	12
--------------------	----

CHAPTER 3: METHODOLOGY

3.1 Overview.....	15
3.2 Methodology of the Study	15
3.3 Case Study	16
3.4 Modelling of RC Minarets	16
3.5 Evaluation of Stairs Effect on the Modal Periods and Frequencies of the Modelled RC Minarets	20
3.6 Slenderness Evaluation of the Modelled RC Minarets	23

CHAPTER 4: WIND LOAD ANALYSIS

4.1 Overview	24
--------------------	----

4.2 Wind Load Effects on RC Minarets	24
4.3 Wind Load Calculation Procedure According to TS498.....	26
4.4 Wind Load Calculation Procedure According to ACI307-98	28
4.4.1 Along wind load calculation procedure	30
4.4.2 Across wind load calculation procedure	33
4.4.3 Combination of across wind and along wind load	38

CHAPTER 5: EARTHQUAKE LOAD ANALYSIS

5.1 Overview	39
5.2 Earthquake Load Effects on RC Minarets	39
5.3 Response Spectrum Method	40
5.4 Response Spectrum Method According to NCSC2015.....	41
5.5 Response Spectrum Method According to ACI307-98	48

CHAPTER 6: CALCULATIONS AND RESULTS

6.1 Overview	53
6.2 Wind Load Calculations	53
6.2.1 Wind load calculations according to TS498	53
6.2.2 Wind load calculations according to ACI307-98	56
6.2.2.1 Along wind load calculations according to ACI307-98	56
6.2.2.2 Across wind load calculations according to ACI307-98	62
6.2.3 Comparison between wind load calculation results according to TS498 & ACI307-98.....	63
6.3 Earthquake Load Calculation	72
6.3.1 Earthquake load calculations according to NCSC2015	72
6.3.2 Earthquake load calculations according to ACI307-98	73
6.4 Applying Wind and Earthquake Loads on the Modelled Minarets	75
6.5 Analysis Results	77
6.5.1 Top displacements	78
6.5.2 Base reactions	82
6.5.3 Stress contours analysis	83

CHAPTER 7: CONCLUSIONS	85
REFERENCES	87
 APPENDICES	
Appendix 1: SOIL INVESTIGATION REPORT	93
Appendix 2: LIST OF NORTH CYPRUS MOSQUES	95
Appendix 3: A TYPICAL MINARET PROJECT PLAN	97
Appendix 4: THE STUDIED MINARETS PLANS	98
Appendix 5: ESTIMATING OF VORTEX SHEDDING EFFECTS ON TALL STRUCTURES.....	102
Appendix 6: SAP2000 ANALYSIS AND RESULTS	104

LIST OF TABLES

Table 1.1:	Largest earthquakes in Cyprus	10
Table 1.2:	Statistical analysis of the historical seismicity data in Cyprus	10
Table 3.1:	Modal periods and frequencies of the 76.2 m minaret	22
Table 3.2:	First mode natural frequencies of the representative minarets	23
Table 4.1:	Wind velocity and wind pressure for different heights	27
Table 4.2:	Importance factor for wind design (I)	29
Table 5.1:	The effective ground acceleration coefficient	42
Table 5.2:	Building importance factor	44
Table 5.3:	The spectrum characteristic periods	45
Table 5.4:	Ground (soil) types	45
Table 5.5:	Local site classes	46
Table 5.6:	Structural behaviour factor R for non-building structures	47
Table 5.7:	Soil site class	50
Table 5.8:	The corresponding site coefficients at short period F_a	50
Table 5.9:	The corresponding site coefficients at long period F_v	51
Table 5.10:	Long period, transition period	52
Table 6.1:	Wind load calculation for 26.0 m minaret according to TS498	54
Table 6.2:	Wind load calculation for 33.2 m minaret according to TS498	54
Table 6.3:	Wind load calculation for 61.45 m minaret according to TS498	55
Table 6.4:	Wind load calculation for 76.2 m minaret according to TS498	56
Table 6.5:	Mean wind load calculation for 26.0 m minaret according to ACI307-98	57
Table 6.6:	Fluctuating wind load calculation for 26.0 m minaret according to ACI307-98	57
Table 6.7:	Along wind load calculation for 26.0 m minaret according to ACI307-98	58
Table 6.8:	Mean wind load calculation for 33.2 m minaret according to ACI307-98	58

Table 6.9: Fluctuating wind load calculation for 33.2 m minaret according to ACI307-98	58
Table 6.10: Along wind load calculation for 33.2 m minaret according to ACI307-98	59
Table 6.11: Mean wind load calculation for 61.45 m minaret according to ACI307-98	59
Table 6.12: Fluctuating wind load calculation for 61.45 m minaret according to ACI307-98	60
Table 6.13: Along wind load calculation for 61.45 m minaret according to ACI307-98	60
Table 6.14: Mean wind load calculation for 76.2 m minaret according to ACI307-98	61
Table 6.15: Fluctuating wind load calculation for 76.2 m minaret according to ACI307-98	61
Table 6.16: Along wind load calculation for 76.2 m minaret according to ACI307-98	62
Table 6.17: Condition of consideration of across wind load according to ACI307-98	63
Table 6.18: Comparison of wind load intensities for 26.0 m minaret	64
Table 6.19: Comparison of wind load intensities for 33.2 m minaret	66
Table 6.20: Comparison of wind load intensities for 61.45 m minaret	68
Table 6.21: Comparison of wind load intensities for 76.2 m minaret	70
Table 6.22: Top displacements due to wind and earthquake loads	80
Table 6.23: Maximum top displacement limit for the modelled minarets	81
Table 6.24: Shear force and bending moment due to wind and earthquake loads ..	82

LIST OF FIGURES

Figure 1.1:	Minaret styles of different countries	2
Figure 1.2:	Component segments of a typical Ottoman minaret	3
Figure 1.3:	The collapsed minaret of the Ebubekir Sıddık Mosque, Kayaş, Ankara, Turkey	5
Figure 1.4:	The collapsed minarets in Erdemli, Mersin, Turkey	5
Figure 1.5:	The two collapsed minarets of Ulu Mosque, Kahramanmaraş, Turkey	5
Figure 1.6:	The collapsed minaret of Şafak Mosque, Izmir, Turkey	6
Figure 1.7:	Minarets collapsed during Kocaeli and Düzce earthquakes	6
Figure 1.8:	Number of constructed RC minarets in North Cyprus since 1983 .	7
Figure 1.9:	Disasters frequency between 1990 and 2014 in Cyprus	8
Figure 1.10:	Economic damage frequency due to disasters between 1990 and 2014 in Cyprus	8
Figure 1.11:	Seismicity of Cyprus between 1896 and 2010	9
Figure 3.1:	Geometrical and cross sectional properties of the selected minarets	18
Figure 3.2:	3-D SAP2000 FEM of the representative minarets	20
Figure 3.3:	Models of 76.2 m minaret	21
Figure 4.1:	Wind load effect on a tall freestanding structure	24
Figure 4.2:	Along and across wind directions	25
Figure 4.3:	Wind profile for tall body structures with circular section.....	27
Figure 4.4:	Basic wind speed map for Cyprus	29
Figure 4.5:	Simplified representation of mean and gust wind effects	30
Figure 4.6:	Schematic representations for along wind load calculations as per ACI307-98.....	32
Figure 4.7:	Across wind effect “vortex shedding”	33
Figure 4.8:	Schematic representations for across wind load calculations as per ACI307-98.....	37
Figure 5.1:	Graphical description of response spectrum	40
Figure 5.2:	A typical design spectrum	41

Figure 5.3:	Seismic map zones according to NCSC2015	43
Figure 5.4:	Design acceleration spectra according to NCSC2015	48
Figure 5.5:	Design response spectrum according to ACI307-98	52
Figure 6.1:	Comparison of wind load intensities for 26.0 m minaret	64
Figure 6.2:	Comparison of wind load intensities for 33.2 m minaret	66
Figure 6.3:	Comparison of wind load intensities for 61.45 m minaret	68
Figure 6.4:	Comparison of wind load intensities for 76.2 m minaret	70
Figure 6.5:	Response spectrum function definition on SAP2000 according to NCSC2015.....	72
Figure 6.6:	Response spectrum curve according to NCSC2015.....	73
Figure 6.7:	Response spectrum function definition on SAP2000 according to ACI307-98.....	74
Figure 6.8:	Response spectrum curve according to ACI307-98.....	74
Figure 6.9:	Applying wind loads according to ACI307-98 on the modelled minarets	75
Figure 6.10:	Applying wind loads according to TS498 on the modelled minarets	76
Figure 6.11:	Deformed shapes of the modelled minarets after applying the loads	77
Figure 6.12:	Displacements over the height of 26.0 m Minaret	78
Figure 6.13:	Displacements over the height of 33.2 m Minaret	78
Figure 6.14:	Displacements over the height of 61.45 m Minaret	79
Figure 6.15:	Displacements over the height of 76.2 m Minaret	79
Figure 6.16:	Top displacements due to wind and earthquake loads	80
Figure 6.17:	Normal stress distribution of 76.2 m minaret	83
Figure 6.18:	Shear stress distribution of 76.2 m minaret	84

LIST OF ABBREVIATIONS

ACI307-98	American Concrete Institute Code No. 307
ASCE7-16	American Society of Civil Engineers Code No. 7
CRED	Centre for Research on the Epidemiology of Disasters
FEM	Finite Element Models
MCER	Risk-Targeted Maximum Considered Earthquake
NCSC2015	North Cyprus Seismic Code 2015
PGA	Peak Ground Acceleration
RC	Reinforced Concrete
RSM	Response Spectrum Method
RMS	Root Mean Square
SAP2000	Structural Analysis Program
TS498	Turkish Code No. 498

LIST OF SYMBOLS

γ	Unit weight
E	Young's modulus
ν	Poisson's ratio
A	Thermal expansion coefficient
f_{ck}	Compressive strength of concrete
f_{cd}	Design strength of concrete
f_y	Bending reinforced yield stress
f_{yd}	Expected reinforced yield stress
f	First mode frequency
C_f	Aerodynamic factor
q	Wind pressure
ρ	Air density
V_R	Reference design wind speed
v	Basic wind speed
I	Importance factors
$W(z)$	Along wind load
$\bar{w}(z)$	Mean along wind load
$w'(z)$	Fluctuating along wind load
$C_{dr}(z)$	Drag coefficient
$\bar{p}(z)$	Pressure due to mean hourly design wind speed
$M_w(b)$	Base bending moment due to mean along wind load
G_w	Gust factor
T_1	Natural period
V_{cr}	Critical wind speed
S_t	Strouhal number
M_a	Peak base moment due to across wind load
C_L	RMS lift coefficient
β_S	Fraction of critical damping
β_a	Aerodynamic damping

$S_{Pa}(T)$	The ordinate of the elastic response spectrum
$A(T)$	Spectral acceleration coefficient
g	Gravitational acceleration
A_0	Coefficient of effective ground acceleration
$S(T)$	Spectrum coefficient
T_A, T_B	Spectrum characteristic periods
$R_a(T)$	Seismic load reduction factor
R	Behaviour factor
S_{MS}	The risk-targeted maximum considered earthquake (MCER) spectral response acceleration parameter at short periods adjusted for site class effects
S_{M1}	The MCER spectral response acceleration parameter at a period of 1 sec adjusted for site class effects
S_{DS}	Design spectral acceleration for short periods
S_{D1}	Design spectral acceleration at a period of 1 sec
S_S	Mapped MCER spectral response acceleration parameter at short periods
S_I	Mapped MCER spectral response acceleration parameter at a period 1 sec
F_a	Corresponding site coefficients for short periods
F_v	Corresponding site coefficients for long periods
T_a	First natural vibration period of the building
T	Fundamental period
T_L	Long-period transition period
W	Wind load
EQ	Earthquake load
Y_{max}	Maximum top displacement limit
V	Base shear force
M	Base bending moment
M_s	Surface wave magnitude of an earthquake
M_w	Moment magnitude of an earthquake

CHAPTER 1

INTRODUCTION

1.1 Background

Among the most unique structures in the most of Islamic cities are the minarets. Minarets are tall and slender structural elements such as towers commonly used in mosque architecture. It is usually built besides to, or attached to the side wall of mosques. Historically minaret was used to recite Azan, where a person ascends to the balcony and calls Muslims to pray five times a day. Since the invention of the loudspeakers, minaret has lost its main function, however still continued to be constructed as a main symbolic element of mosque. Alshehabi, (1993) reported that the first appearance of the minarets was before more than 1300 years in Damascus, Syria at the Umayyad Mosque, which was the largest mosque at that time and had relatively three short, square minarets that are still visible today. Until now the tallest minaret in the world is the minaret of Hassan II Mosque in Casablanca, Morocco, which has 210 m height (Abdullahi, 2014) , but the construction of an another tall minaret with 265 m is still ongoing in the Great Mosque in Algiers (Constantinescu & Köber, 2013). The architectural features of minarets had varied historically by countries. The first style of minarets was inspired by the towers of the churches as a square tower sitting at the corner of the mosque. During the evolution of urban style in Islamic countries, shapes and sizes of minarets were developed. For example, in the 9th century, Abbasids style minarets in Iraq were conical in shape, surrounded by a spiral staircase as shown in Figure 1.1.a. In the 12th century, Moroccan style minarets have been normally square with several storeys, and generally each mosque has a single minaret. An example of this style can be seen in Figure 1.1.b. Egyptian minaret styles in the 15th century were like an octagonal shape with one or two balconies. Egyptian minaret style is shown in Figure 1.1.c. A new style of minarets appeared in the Ottoman period in Turkey. This style of minaret is slim and has a cylindrical main body shape as shown in Figure 1.1.d (Doğangün et al., 2006; Higazy, 2004).

The Ottoman influence in North Cyprus left a particularly rich heritage of beautiful mosques which were all built using brick or stone masonry. Nowadays, in Turkey, North Cyprus and many other countries affected by Ottoman culture, classical Ottoman minaret style is still built while new hybrid style is most commonly in Middle East countries. Hybrid style minarets can be seen in Figure 1.1.e (Alshehabi, 1993).



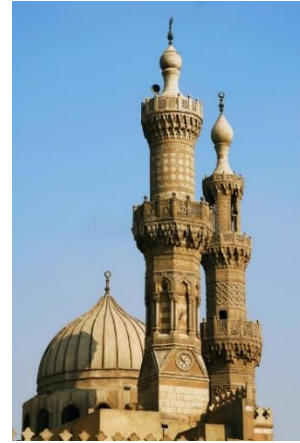
(a) The Malwiya Minaret

Samarra, Iraq



(b) The Koutoubia minaret

Marrakesh, Morocco



(c) Al-Azhar Mosque minaret

Cairo, Egypt



(d) The Blue Mosque minarets

Istanbul, Turkey



(e) Al-Masjid al-Nabawi minarets

Medina, Saudi Arabia

Figure 1.1: Minaret styles of different countries

Majority of the minarets recently constructed are RC structures that enables architects and engineers to design high rise minarets with lower fundamental frequencies of vibration in comparison to masonry minarets. This study is concerned with the RC Ottoman minaret style, which consists of footing, boot, transition segment, main body, balconies, spire, and end ornament, as shown in Figure 1.2 (Ural A. & Firat F. K., 2014).

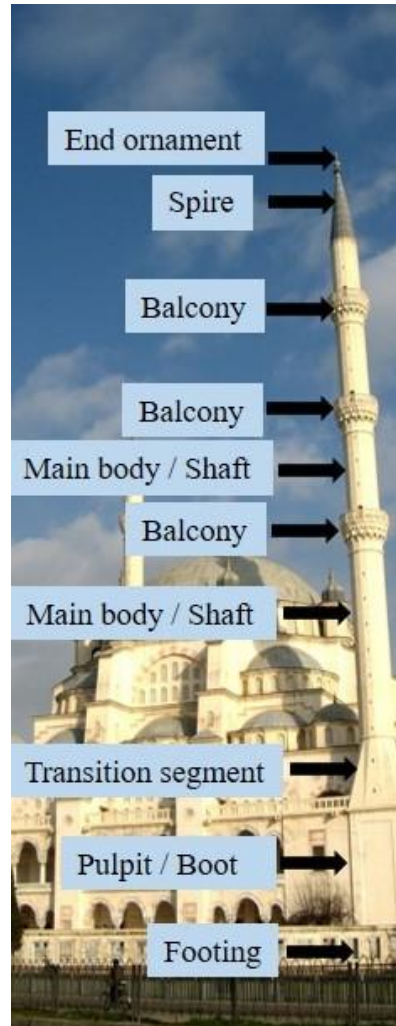


Figure 1.2: Component segments of a typical Ottoman minaret

The footing works as a foundation of the minaret. It is constructed separately or continuously with the mosque structure. The base or boot is the lowermost part of the minaret can be seen above the ground. In general, the boot has a square or polygonal shape and above it there is a transition segment, which connects the larger-diameter boot with a smaller-diameter main body uninterruptedly and smoothly. The main body, which is the main part of the minaret

usually cylindrical and rarely polygonal in shape. Inside the minaret, usually there is a cylindrical column surrounded by spiral staircase running anti-clockwise all the way round the shaft up to the last balcony. The balconies are cantilevers get out from the main body. Historically balconies were used to proclaim prayers, but now they are built for aesthetic appearance and architectural reasons only. It's important to note that door openings in the main body are found where there are balconies. The roof of the minaret is called as the spire and it is usually conical in shape. Above the spire, usually there is an end ornament, which is made of metal and used as an indication noticeable from far to show the direction of qibla (Doğangün et al., 2006).

1.2 Effect of Lateral Loads on Minarets

Minarets, especially the Ottoman minaret style with their unique features such as distinctive shape and high level slenderness is not the same to other known structures. Many minarets were either damaged or collapsed under the effect of destructive earthquakes or strong wind storms, resulting in loss of life and properties. Some of these incidents which happened in the neighbouring country are summarized below:

In 2002 the minaret of Ebubekir Sıddık Mosque in Kayaş, Ankara, Turkey, collapsed during a wind storm and resulted with the death of two people and five injuries. The collapsed minaret is shown in Figure 1.3.

In the same year, the minarets of five mosques collapsed and the minarets of four mosques were damaged during a strong wind storm in Erdemli, Mersin, Turkey, as can be seen in Figure 1.4. The maximum recorded wind speed was 96 km/h. Also in 2003 in the same city a wind storm with a velocity of 100 km/h caused failing of a minaret.

In 2005 during a wind storm with a velocity of 60 km/h in Kahramanmaraş, Turkey, the two minarets of Ulu Mosque, which had a height of 15 m, collapsed and caused some injures as shown in Figure 1.5 (Türkeli, 2014).

Recently, in February 2015, amateur cameras recorded collapse of Şafak Mosque minaret in Izmir, Turkey, during a strong wind storm with a maximum recorded wind speed of 90 km/h. Figure 1.6 shows the minaret during and after the collapse (CUMHURIYET, 2015).



Figure 1.3: The collapsed minaret of the Ebubekir Sıddık Mosque, Kayaş, Ankara, Turkey (Türkeli, 2014)



Figure 1.4: The collapsed minarets in Erdemli, Mersin, Turkey (Türkeli, 2014)

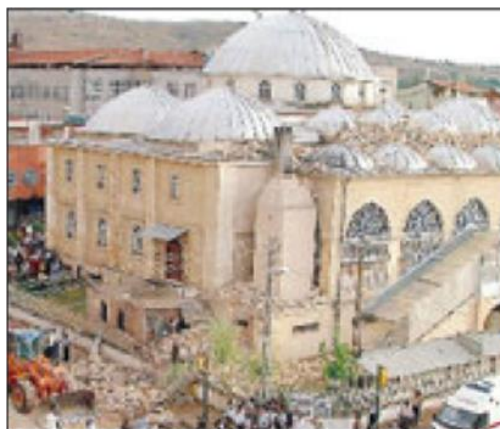


Figure 1.5: The two collapsed minarets of Ulu Mosque, Kahramanmaraş, Turkey (Türkeli, 2014)

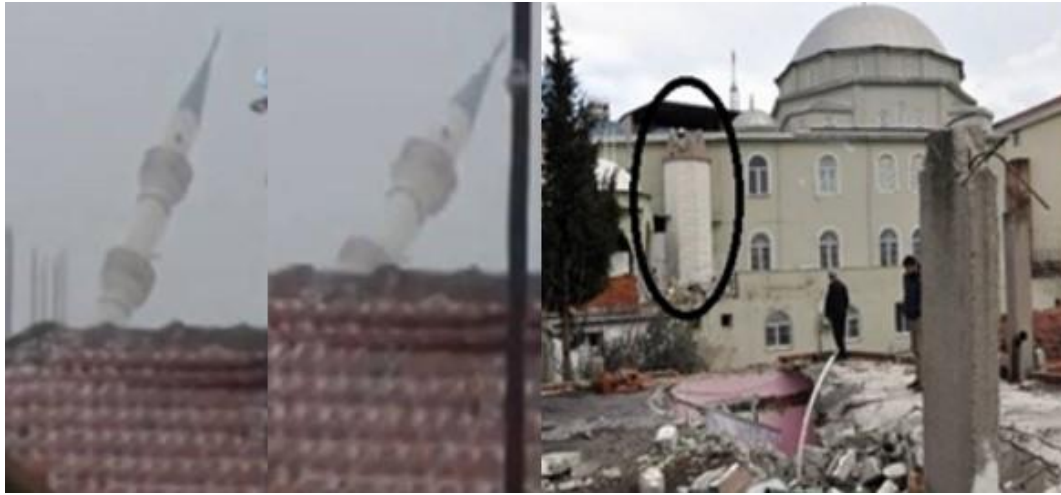


Figure 1.6: The collapsed minaret of Şafak Mosque, Izmir, Turkey (CUMHURIYET, 2015)

On the other hand, earthquake activities were another significant reason of miserable events that occurred in the past. In Turkey, in August and November 1999, about 70% of Düzce's minarets were damaged and knocked down by Kocaeli and Düzce earthquakes having a moment magnitude, M_w of 7.4 and 7.2, respectively. Some of those collapsed minarets are shown in Figure 1.7 (Sezen et al., 2008).

Furthermore, in 23 October, 2011 Van, Turkey, an earthquake with a moment magnitude M_w of 7.2, resulted with the collapse and unrepairable damage of 66% of the minarets. The other minarets had minor repairable damages (Sezen et al., 2008; Sarno et al., 2013).



Figure 1.7: Minarets collapsed during Kocaeli and Düzce earthquakes (Sezen et al., 2008)

1.3 Significance of the Study

Today, in North Cyprus, there is a significant increase in the number of RC minarets. The data obtained from the Cyprus Religious Foundations Administration (Kıbrıs Vakıflar İdaresi) showed that there are 92 new RC minarets constructed, about 71% of them constructed in the last 15 years, as shown in Figure 1.8. The number of newly built minarets has doubled in the last decade, to 92 in 2018 from 26 in 2005. Most of those RC minarets built recently in North Cyprus are designed by using the previous old projects prepared by the Turkish Religious Affairs Administration and are constructed by insufficient skilled workmanship with minimum knowledge about dynamic behaviour of tall and slender structures.

More detailed information about the number of mosques and minarets in North Cyprus can be found in APPENDIX 2.

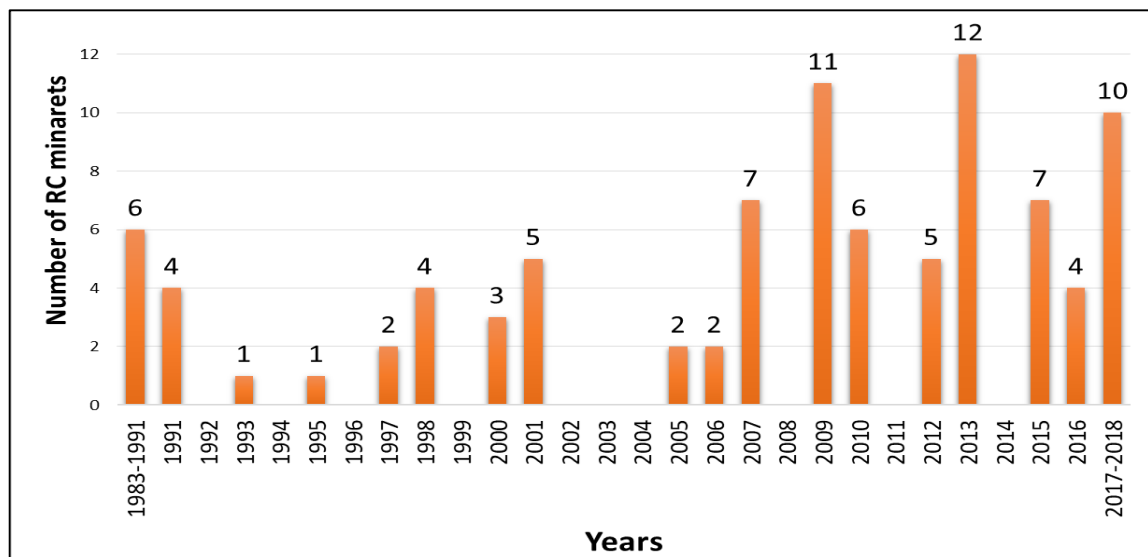


Figure 1.8: Number of constructed RC minarets in North Cyprus since 1983

Cyprus is an island which is located in the Eastern Mediterranean Sea and comprises of many historical structures. The island faces various natural disasters and from the data related to human and economic losses from disasters that have occurred between 1990 and 2014 shows that the biggest economic damage among the disasters has been caused by wind storms as shown in Figures 1.9 - 1.10 (EMDAT, 2009). Sioutas et al. (2006) reported that two multiple

tornadoes hit Cyprus in January 27, 2003 and in January 22, 2004, which was an unusual powerful storm and caused some injuries as a result of collapse of some walls. The maximum recorded wind speed was about 140 km/h. As reported on December 11, 2013, some structures were damaged, sign boards collapsed and one minaret slightly damaged as a result of wind storm with a speed of 80 km/h in North Cyprus. Fortunately, there was no human injured (Abdullahi, 2014).

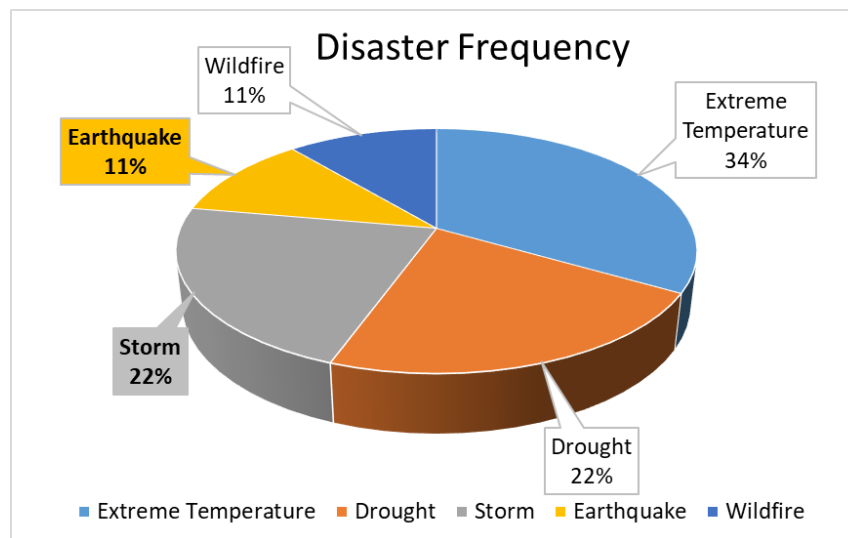


Figure 1.9: Disaster frequency between 1990 and 2014 in Cyprus (EMDAT, 2009).

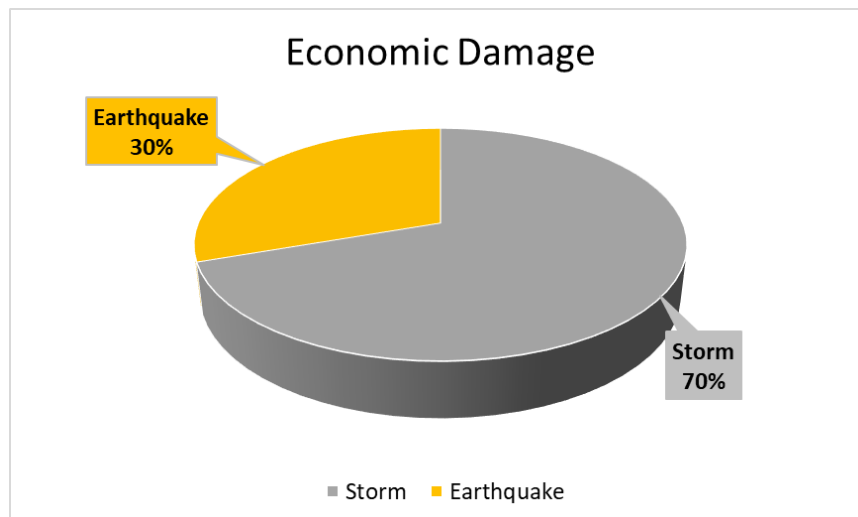


Figure 1.10: Economic damage frequency due to disasters between 1990 and 2014 in Cyprus (EMDAT, 2009)

Moreover, climate change which affects Cyprus is associated with a wide range of consequences, such as changes in rainfall levels, changes in temperatures, and chiefly extreme weather events including wind storms (Zachariadis, 2012; Department of Meteorology, 2006).

On the other hand, earthquake activities were another significant reason of miserable events that occurred in the past as mentioned before.

Since Cyprus is located in a seismically active zone, the island has always vulnerable to earthquakes. Cyprus is situated within the second intensive seismic zone of the earth, where 15% of the world's seismic activities occur in this zone (Cyprus geological heritage educational tool, 2004). Figure 1.11 shows the history of several earthquakes that hit the island.

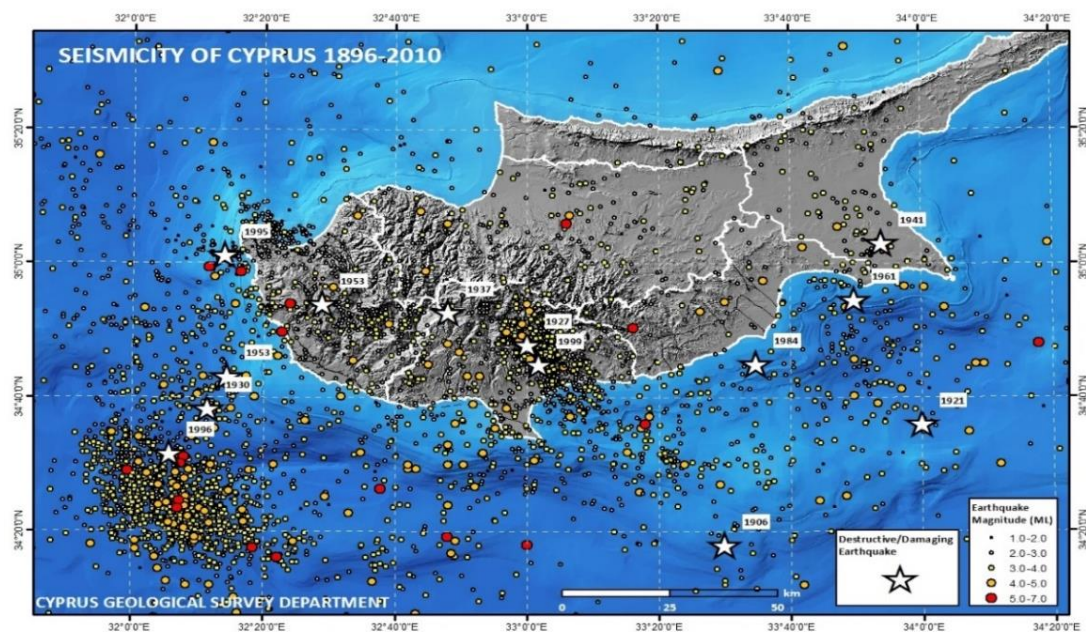


Figure 1.11: Seismicity of Cyprus between 1896 and 2010 (GSD, 2010)

According to Cyprus Geological Survey Department, the main earthquakes occurred in Cyprus with surface wave magnitude larger than 5 ($M_s > 5.0$) between 1947 and 2018 are listed in Table 1.1. The most miserable earthquake hit Cyprus during this period was in 1953 which had a surface wave magnitude of 6.1 and yielded a result of 40 fatalities. (Ambraseys, 2009).

Table 1.1: Largest earthquakes in Cyprus (GSD, 2015)

Years	Location	Surface wave magnitude
1947	Nicosia and Famagusta	5.4
1953	Pafos	6.1
1961	Larnaca	5.7
1995	Pafos	5.7
1996	Pafos	6.5
1999	Lemesos	5.6
2015	Pafos	5.6

The statistical analysis of the historical data expected one destructive earthquake every theoretical return period of 120 years, while the statistical analysis of contributory recordings of the last 100 years gives the results presented in the table below (Cyprus geological heritage educational tool, 2004).

Table 1.2: Statistical analysis of the historical seismicity data in Cyprus (Cyprus geological heritage educational tool, 2004).

Surface wave magnitude	Return period (years)	No. of earthquakes in 100 years
4.6 - 5.0	8	12.5
5.1 - 5.5	26	3.8
5.6 - 6.0	36	2.8
6.1 - 6.5	75	1.3
6.6 - 7.0	166	0.6

No doubt, Cyprus will continue to be hit with earthquakes in the future as well. Furthermore, earthquakes were the second largest reason of the economic damage due to the disasters between 1990 and 2014 as reported by the Centre for Research on the Epidemiology of Disasters (CRED), which can be seen in Figure 1.10.

However, by literature surveying it can be said that, there is no studies investigating the lateral response of RC minarets for the case of Cyprus, especially if it is known that the regulation on buildings to be built in earthquake zones for Northern Cyprus has not been used before in determination of earthquake response of RC minarets. This code, which is the first seismic code in North Cyprus, will be nominated in this thesis as North Cyprus seismic code (NCSC2015).

All these points, in addition to unfortunate events given before in this chapter, compel us to develop our expertise about the lateral response of RC minarets. Therefore, it is interesting to make such a combined study on wind and earthquake analysis of RC minarets.

1.4 Objectives of the Study

The main aim of this study is to investigate the wind and earthquake effects on RC minarets with different heights, located in Nicosia, North Cyprus, and explore the variability of the results obtained from using of Turkish code TS498 (Design Loads for Buildings) and American concrete institute code ACI307-98 (Design and Construction of Reinforced Concrete Chimneys) for wind load, while, NCSC2015 and ACI307-98 are used to determine earthquake load. The procedures that given in the mentioned codes will be followed to verify the internal forces, base reactions and top displacements for the selected minarets under wind and earthquake loads to show the weaknesses of these structures.

CHAPTER 2

LITERATURE REVIEW

2.1 Overview

This chapter presents an overview of previous work related to this study, which gives the indispensable background of this research.

The literature review focuses on a range of studies related to analysis and design RC minarets and similar structures like RC chimneys. The lateral loads effect on RC minarets and chimneys has the most attention in this review. Different codes were followed by authors to determine lateral loads on these structures. The main researches reviewed present as follows:

Sezen, Acar, Dogangun, & Livaoğlu (2008) have presented a study investigated the dynamic analysis and seismic effect on RC minarets. The authors reviewed the failure modes and seismic effects on RC minarets after the earthquakes that occurred in Kocaeli and Duzce, Turkey in 1999. Four 3-D finite element models were represented a RC minaret with 30.0 m height to show the influence of the minaret components such as stairs, balconies, and door openings on the seismic performance of minarets. It is observed from the collapsed minarets during Kocaeli and Duzce earthquakes that the bottom of the main body of minarets and immediately above the transition segment is the weakest section under earthquake load. The use of smooth reinforcement rebars with 180° end hooks at the ends of steel reinforcements and the short height of transition segment are the main practices problems. Another finding in this study was that when balconies or stairs are neglected in the analysis, the maximum shear and bending demands were decreased by about 20 %.

Reddy, Jaiswal, & Godbole (2011) have presented a study dealt with wind and earthquake analysis of tall RC Chimneys. In this study, two RC chimneys were analyzed for wind and earthquake loads. Earthquake analysis is performed according to IS1893 (Part4):2005, while wind analysis is done according to IS4998 (Part 1): 1992. This study presented the comparison of results of wind load analysis with that of earthquake load analysis to decide the most critical loads for the design of the chimneys. The results showed that the earthquake load acting on RC chimney in zone V is close to wind load in a zone with basic wind speed 44 m/s.

Karaca, & Türkeli (2012) have studied wind load and responses of industrial RC chimneys. In this study, the authors followed the procedures given in five different codes to determine wind loads acting to RC chimneys, namely ACI307-98, CICIND2001, DIN1056, Eurocode1 and TS498. By comparing the wind load values that found from the different codes the authors reached that the wind load value according to Eurocode1 is more than the wind load values of other codes by three to four times and they thought that Eurocode1 wants to be more safety in determining wind load acting on RC chimneys. Also, the results show that in order to make a safe and economical design, the effect of slenderness on wind responses of slender industrial RC chimneys should be considered.

Türkeli (2014) has investigated the responses of RC minarets under wind and earthquake effects. The author in this study has followed Turkish codes TS498 and TEC2007 and model code for concrete chimneys, CICIND 2001 to calculate the wind and earthquake loads acting on a representative RC minaret with 61.0 m height. The statically equivalent uniform load was used to analyse the representative minaret under wind load, while two dynamic methods were used to analyse the representative minaret under earthquake load, namely; response spectrum analysis and time history analysis, by using SAP2000 program. The results illustrated that the time history analysis should be used in the determination of lateral loads during designing RC minarets. In addition to this more interest should be taken where cross section changes.

Livaoğlu, Baştürk, Doğangün, & Serhatoğlu (2016) have studied the dynamic behaviour of seven historical masonry minarets in Bursa, Turkey and the effect of geometric features on this behavior. The ambient vibration tests were done to determine modal parameters of the minarets. The finite element program Abaqus Cae was used to make 3-D (solid) models for the studied minarets. Geometric properties effect on the dynamic behaviour of minarets was estimated according to the results found from two ways, experimental investigation and numerical analysis. The results showed that the natural period and frequency of the minarets from the numerical analysis are so close to modal test results.

Haciefendioğlu, Emre, Demir, Dinç, & Birinci (2018) have examined the effect of several kinds of footing soil on seismic behaviour of RC minarets by experimental modal investigation of scale down minaret embedded in different soil types. A model in 1:20 scale was constructed using RC in the laboratory. The foundation soil types, gravel, sand, and clay-gravel mixture, were used to clarify differences in seismic behaviour according to the footing soil type. Test results illustrate that the seismic conduct of RC minaret is strongly affected by the footing soil type.

CHAPTER 3

METHODOLOGY

3.1 Overview

This chapter displays the methodology of this study, discusses the selected case study and presents modelling of RC minaret structures.

3.2 Methodology of the Study

The methodology has been followed in this study to achieve the study aims presents in the following:

The first step is a review of available literatures, related to analysis of RC minarets and similar structures like RC chimneys under the effect of wind and earthquake loads with surveying the codes that used to determine lateral loads in North Cyprus.

The second step is about data collection. RC minarets in North Cyprus vary between low, medium and high rises. Plans and specifications of a wide range of RC minaret projects in North Cyprus were collected from consulting engineering companies, Cyprus Religious Foundations Administration (Kıbrıs Vakıflar İdaresi) and previous studies.

Third step is to determine the case study by selecting the representative RC minarets, and then modelling them in SAP2000 program using shell elements.

Fourth step is to calculate wind and earthquake loads according to the selected codes and applying those loads on the representative RC minarets to compare and evaluate the analysis results.

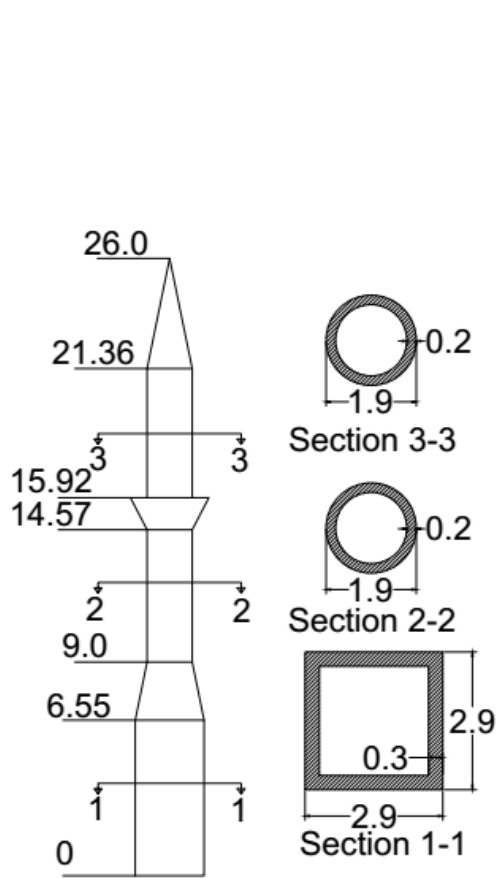
3.3 Case Study

In this study four RC minarets with different heights were selected to be analysed under the effect of wind and earthquake loads. The procedures given in TS498 and ACI308-97 were used to calculate wind load, while NCSC2015 and ACI307-98 specifications were followed to determine earthquake response by using response spectrum method. The representative RC minarets were constructed in Nicosia, North Cyprus. Nicosia is the capital city of north and south Cyprus. Case study is chosen for northern half of Nicosia. All components of Ottoman minaret style are considered in this study including balconies, door openings and stairs. The interference effect is not considered in this study, so the modelled minarets were evaluated that there are no other structures near or around the modelled minarets. The representative minarets base were all accepted as fixed.

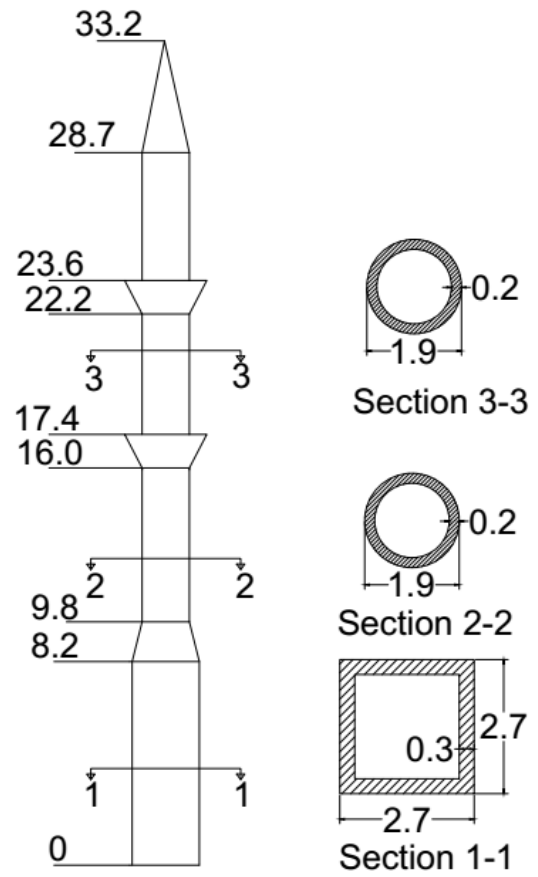
3.4 Modelling of RC Minarets

Four finite element models (FEM) of the four RC minarets, which have different heights and geometrical properties were modelled by using structural analysis program SAP2000 (Wilson, 2000). The height of the minarets are 26.0 m, 33.2 m, 61.45 m and 76.2 m. The geometry and cross sectional properties of four representative minarets are shown in Figures 3.1 (a) (b) (c) and (d). The cross sectional properties and dimensions of selected minarets shown in Figures 3.1 (a) and (b) are considered as a low and medium rise used in a wide range of applications in North Cyprus. For example, the minaret used in the first model consists of a single balcony with total height of 26.0 m, a rectangular base and a cylindrical body. The rectangular base height is 6.55 m where internal diameter is 2.3 m and external diameter is 2.9 m. The height of the transition segment is 2.45 m above which the cross-sectional geometry turns into circular shape with an internal and external diameter decreased to 1.5 m and 1.9 m, respectively, and the wall thickness becomes 0.2 m.

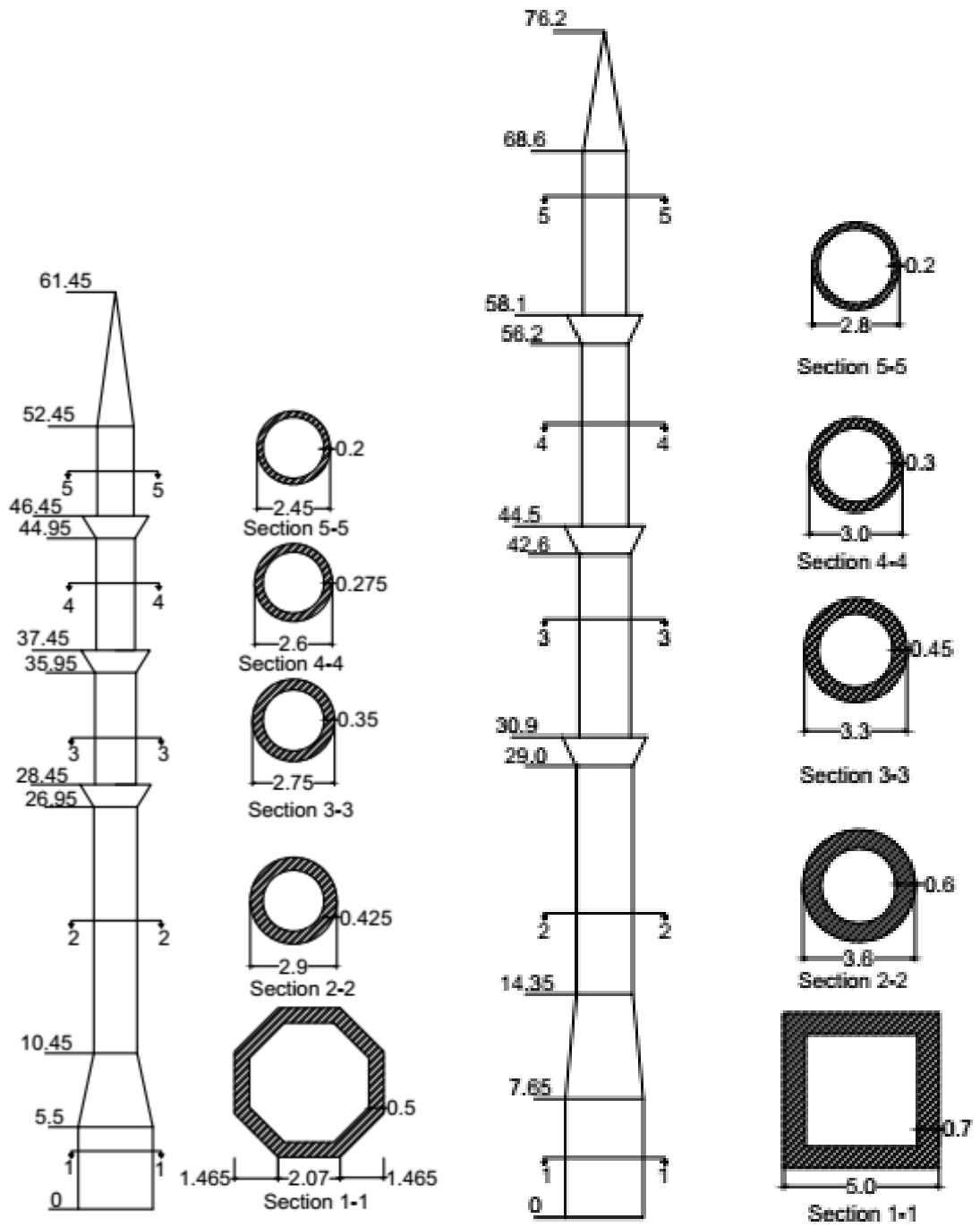
The detailed plans of the selected minarets are shown in APPENDIX 3.



(a) Minaret with a height of 26.0 m



(b) Minaret with a height of 33.2 m



(c) Minaret with a height of 61.45 m

(d) Minaret with a height of 76.2 m

Figure 3.1: Geometrical and cross sectional properties of the selected minarets
(Dimensions are in meters and drawings are not to scale)

Shell elements are used for the finite element model (FEM) of the representative RC minarets (Isgor, 1997). The constructed three dimensional (3-D) FEM of minarets are shown in Figure 3.2. The section property was defined and assigned as shell elements with the thicknesses elucidate in cross sections shown in Figures 3.1 (a) (b) (c) and (d).

The representative RC minarets materials properties are all listed below:

- Weight of unit, $\gamma = 25 \text{ kN/m}^3$.
- Young's modulus, $E = 30000 \text{ MPa}$.
- Poisson's ratio, $\nu = 0.2$.
- Thermal expansion coefficient, $A = 0.0000117$
- Compressive strength of concrete, $f_{ck} = 25 \text{ MPa}$.
- Design strength of concrete, $f_{cd} = 17 \text{ MPa}$.
- Bending reinforced yield stress, $f_y = 420 \text{ MPa}$.
- Expected reinforced yield stress, $f_{yd} = 365 \text{ MPa}$.

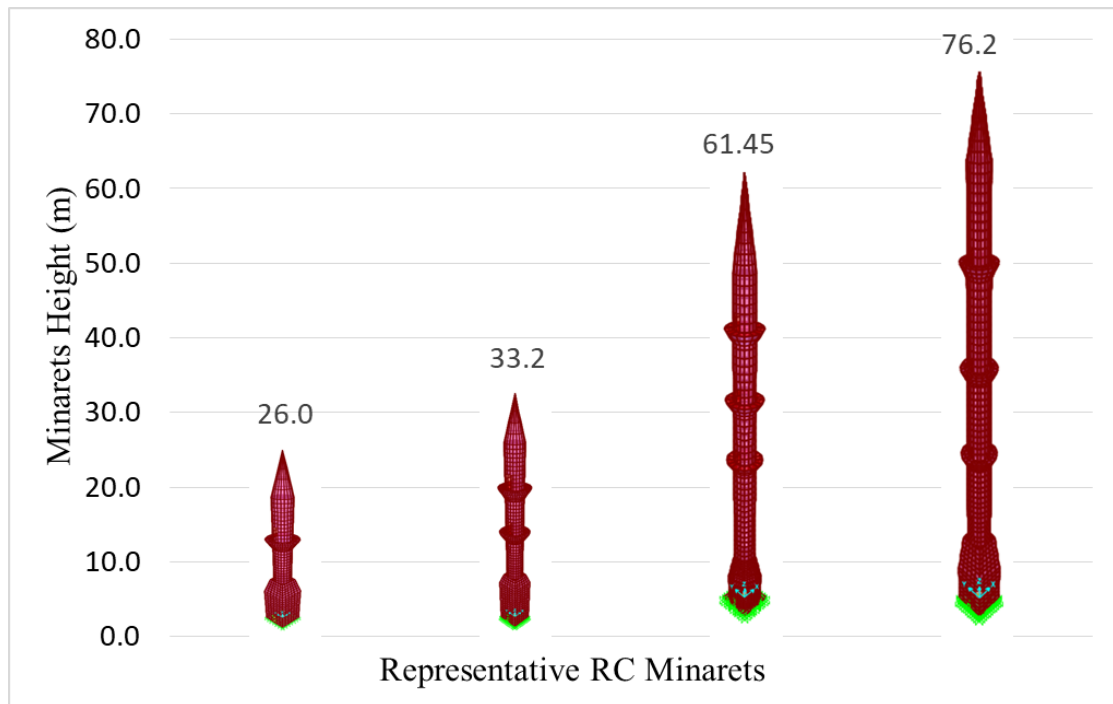
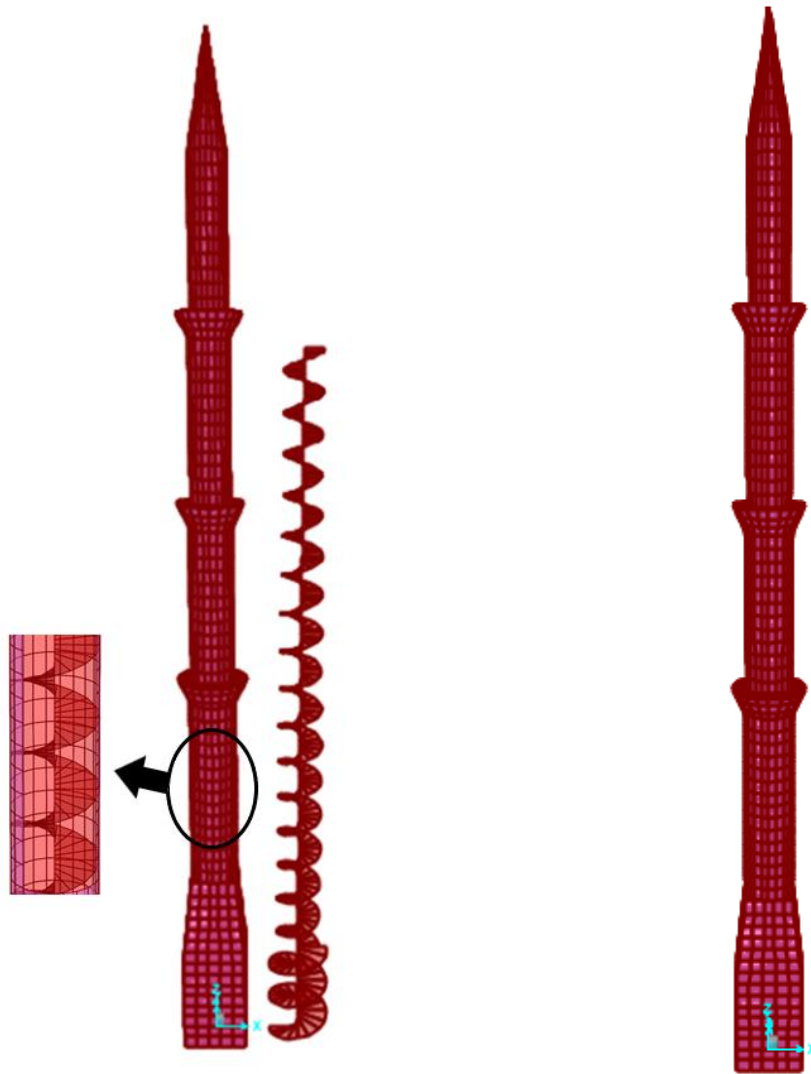


Figure 3.2: 3-D SAP2000 FEM of the representative minarets

3.5 Evaluation of Stairs Effect on the Modal Periods and Frequencies of the Modelled RC Minarets

It is thought that stairs as an additional mass to minaret body affect the dynamic behaviour of these structures. The 76.2 m minaret is selected to show how stairs affect the modal periods and frequencies of the minaret. Table 3.1 presents the modal periods and frequencies of the 76.2 m minaret in two cases; with and without stairs. While Figure 3.3 shows the models in the two cases; with and without stairs. The modal periods and frequencies of the other minarets are given in APPENDIX 6.



(a) With stairs

(b) Without stairs

Figure 3.3: Models of 76.2 m minaret

Table 3.1: Modal periods and frequencies for the 76.2 m minaret.

Mode	Stairs not included		Stairs included	
	Mode Period	Mode frequency	Mode Period	Mode frequency
	T (Sec)	f (Hz)	T (Sec)	f (Hz)
1 st	1.130	0.885	1.184	0.844
2 nd	1.125	0.889	1.182	0.846
3 rd	0.509	1.966	0.560	1.785
4 th	0.313	3.198	0.418	2.394
5 th	0.310	3.226	0.375	2.670
6 th	0.136	7.348	0.330	3.035
7 th	0.135	7.398	0.316	3.161
8 th	0.085	11.752	0.218	4.578
9 th	0.079	12.729	0.208	4.814
10 th	0.078	12.743	0.158	6.316
11 th	0.065	15.457	0.145	6.913
12 th	0.063	15.787	0.138	7.251

It can be noticed that considering stairs in modelling RC minarets affect the natural periods and frequencies. Minaret model including stairs has natural periods larger than minaret model with neglecting stairs. This is mainly because of increase the mass of the structure with fixity of stiffness. Therefore, including stairs increases the effect of earthquake load on RC minarets.

3.6 Slenderness Evaluation of the Modelled RC Minarets

Slenderness ratio is the ratio of the effective length of a structural member to its minimum radius of gyration and usually is considered as the height to width ratio (h/d). Simply, a structure is defined as slender if its height is larger 4 times than its width ($h/d > 4$) (Ali M. & K. Al-Kodmany, 2012). According to this definition all of modelled minarets in this study are slender. In this study, the slenderness definition given in ASCE7-16 (Minimum Design Loads for Buildings and Other Structures) will be considered to evaluate the slenderness of the representative minarets. According to ASCE7-16, the slender structures are the structures that have a first mode natural frequency less than one (Karaca & Türkeli, 2014). First mode natural frequencies of the representative minarets are given in Table 3.2.

Table 3.2: First mode natural frequencies of the representative minarets.

Minaret height (m)	First mode frequency f (Hz)
26.0	5.21
33.2	1.62
61.45	0.87
76.2	0.84

It can be noticed from this table that the high rise minarets (61.45 m and 76.2 m) have a first mode frequency less than 1, so they are considered as slender structures according to ASCE7-16.

CHAPTER 4

WIND LOAD ANALYSIS

4.1 Overview

This chapter presents and discusses the wind load effects on RC minarets, and the procedure given in two different codes, namely TS498 and ACI307-98 to determine wind load on RC minarets.

4.2 Wind Load Effects on RC Minarets

In general, wind load acting on structures has dynamic effects. However, these effects are small in case of non-slender structures and in this case static methods can be applied to determine wind load effects. But in slender structures, like high rise minarets, the dynamic effects are not small to neglect, therefore, these dynamic effects should be taken into consideration. This study does not deal with local effects of wind on the structure. It is just interesting with the effect of wind on the structure as a whole, like a vertical cantilever as shown in Figure 4.1.

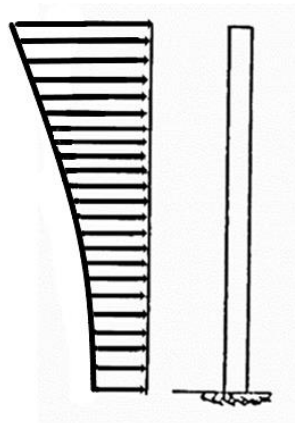


Figure 4.1: Wind load effect on a tall freestanding structure

A tall freestanding structures like minaret is affected by wind load, which can be found in two forms, known as:

- Along wind effect
- Across wind effect

The drag component of wind force causes the along wind load, while the lift component of wind force causes the across wind load. The along wind load is associated with gust hitting causing a dynamic response in the direction of the wind flow, whereas the across wind load is associated with the occurrence of vortex shedding which causes the minaret to fluctuate in a perpendicular direction to wind flow direction as shown in Figure 4.2 (Taranath, 2004; Chenga & Kareem, 1992).

The across wind response mechanism is very complex and the exact analytical method has not been introduced into structural engineering practice. There are some methods to estimate across wind effects in some codes:

- Random response method (IS4998 (Part1): 1992)
- Simplified method (ACI307-98)

While many other codes do not consider across wind effect. (Patidara et al., 2014; Langhe K. & V. R. Rathi, 2016).

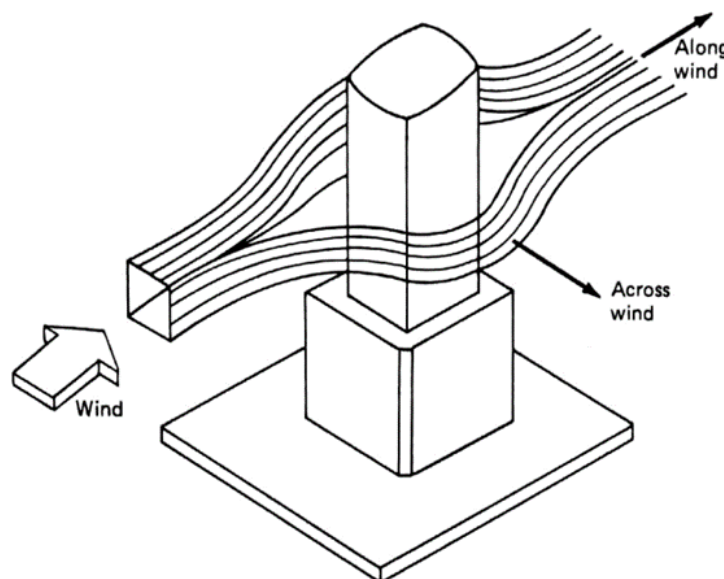


Figure 4.2: Along and across wind directions

In this study the procedures given in two different standards, TS498 and ACI318-97 will be followed to determine wind load effects on the representative minarets.

4.3 Wind Load Calculation Procedure According to TS498

TS498 “Design Loads for Buildings” is used by engineers in North Cyprus to determine load values for designing the structures.

The procedure specified for calculation of wind loads in TS498 is very simple and depends on the aerodynamic factor C_f , which relies on geometrical properties. Wind load resultant magnitude, W (kN) according to this standard is given as the following:

$$W = C_f \cdot q \cdot A \quad (4.1)$$

where, C_f is an aerodynamic factor, q is a wind pressure (kN/m²), A is projected surface (m²).

Wind load value can be also determined as area load (kN/m²) by the following equation:

$$W = C_p \cdot q \quad (4.2)$$

where, C_p is a coefficient depends on structure type and projected area, q is a wind pressure (kN/m²) given as the following:

$$q = \frac{\rho v^2}{2g} \quad (4.3)$$

where, ρ is an air density (1.25 kg/m³), v is a wind velocity and given by the standard for different heights in table 4.1.

Table 4.1: Wind velocity and wind pressure for different heights (TS498, 1997)

Height (m)	Wind velocity v (m/s)	Wind pressure q (kN/m ²)
0 - 8	28.0	0.50
9 - 20	36.0	0.80
21 - 100	42.0	1.10
Above 100	46.0	1.30

In the case of tall body structures with circular cross sections like minarets, C_p coefficient is equal to 1.2 in pressure and 0.4 in suction as shown in Figure 4.3.

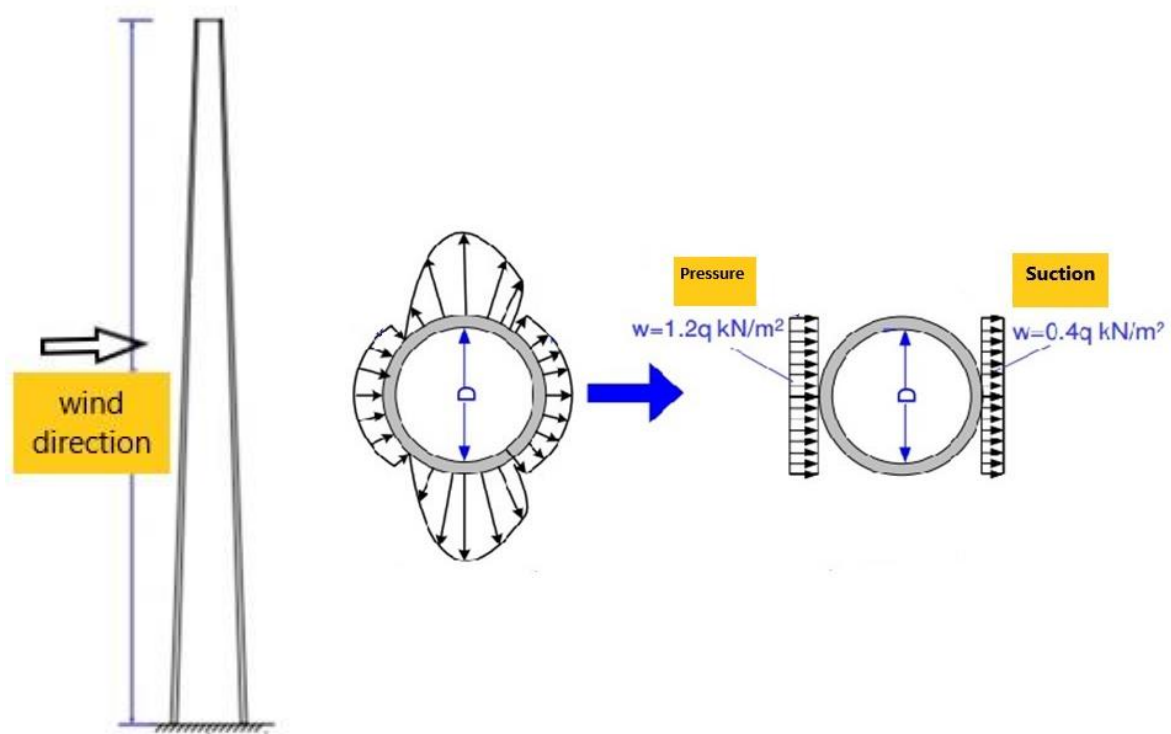


Figure 4.3: Wind profile for tall body structures with circular section

It can be noticed that TS498 doesn't consider the effect of across wind load.

4.4 Wind Load Calculation Procedure According to ACI307-98

ACI307-98 defines the design and construction requirements of circular RC chimneys. In many respects, chimneys are very analogous to RC minarets. Therefore, many parts of this standard can be applied directly on RC minarets.

According to ACI307-98, RC chimneys and similarly RC minarets should be designed to resist the wind load in both forms along wind and across wind effects. The procedures for determining both of them are set out in ACI307-98.

Both along and across wind load calculations in ACI307-98 require the reference design wind speed V_R in km/h and the mean hourly design speed \bar{V}_z in m/s. The reference design wind speed V_R (km/h) can be defined by the following:

$$V_R = (I)^{0.5} \cdot V \quad (4.4)$$

where,

- V is the basic wind speed in km/h, which is the (3-sec) gust speed at height 10 m above the ground level. Figure 4.4 shows the basic wind speed map for Cyprus. It can be notice that the maximum basic wind speed in South Cyprus is 40 m/s while it isn't exceed 30 m/s in North Cyprus. In this study the basic wind speed will be taken as 35 m/s.
- I is the importance factor for wind design and shall be as specified by ASCE7-16 as shown in Table 4.2.

All chimneys and similar structures like minarets shall be classified as Category IV as defined in ASCE7-16.

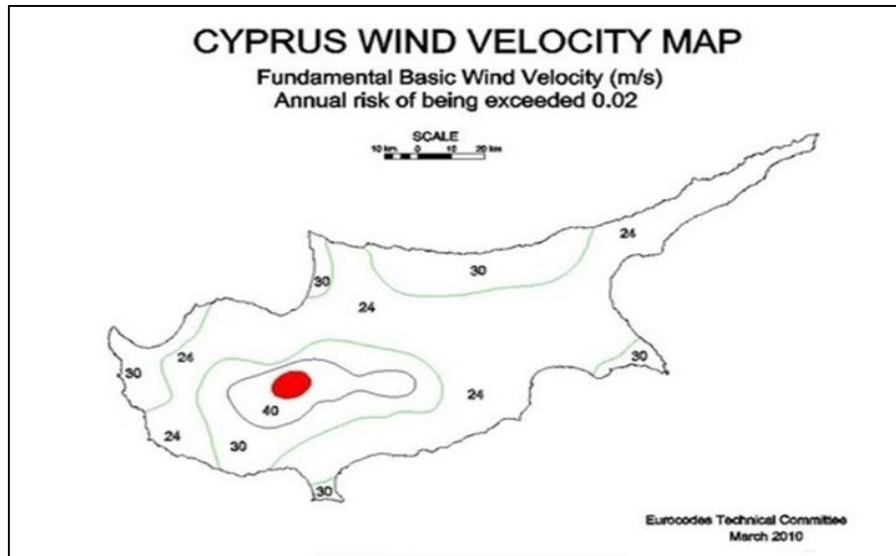


Figure 4.4: Basic wind speed map for Cyprus (Eurocodes Technical Committee, 2010)

Table 4.2: Importance factor for wind design (I) (ASCE7-16)

Category	Non-Hurricane Prone Regions and Hurricane Prone Regions with $V = 85 - 100$ mph	Hurricane Prone, Regions with $V > 100$ mph
I	0.87	0.77
II	1.00	1.00
III	1.15	1.15
IV	1.15	1.15

At a height z (m) above ground level, the mean hourly design speed \bar{V}_z in m/s can be calculated from Equation (4.5).

$$\bar{V}_z = 0.2784 V_R \left(\frac{z}{10} \right)^{0.154} \quad (0.65) \quad (4.5)$$

where, V_R is the reference design wind speed in km/h.

4.4.1 Along wind load calculation procedure

Along wind effect is caused by the frontal hitting action, when the wind acts on the face of a structure. To estimate these loads, the minaret is considered as a vertical cantilever, fixed at its base to the ground. The wind is then considered to act on an exposed face of a minaret. Additional complexity emerge from the fact that the wind does not generally act in a same rate. Wind generally impact as gusts. This needs that the identical loads, and hence the response is to be taken as dynamic. Most codes use an “equivalent static” procedure known as the gust factor method to estimate along wind loads. This method is immensely widespread and used in ACI307-98.

According to ACI307-98, the along wind load, $W(z)$ as a uniform distributed load at any height, z (m), ought to be the gathering of the mean load, $\bar{w}(z)$ and the fluctuating load, $w'(z)$. Schematic representation of mean and gust wind effects can be shown in Figure 4.5.

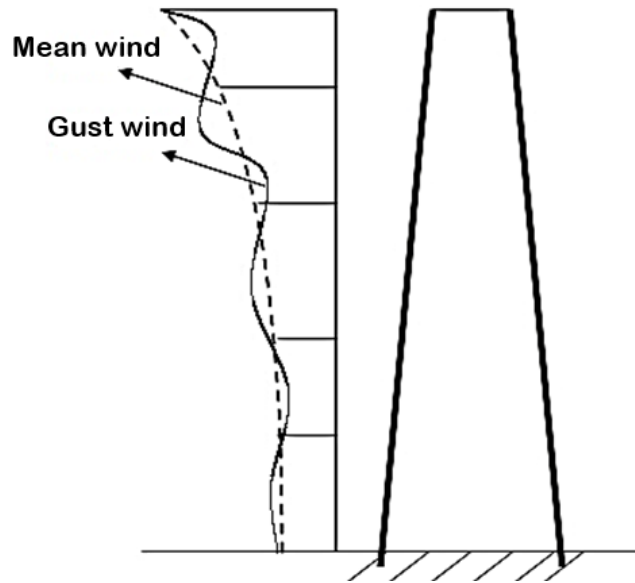


Figure 4.5: Simplified representation of mean and gust wind effects (Taranath, 2004)

The mean load, $\bar{w}(z)$ in N/m shall be found from Equation (4.6).

$$\bar{w}(z) = C_{dr}(z) \cdot d(z) \cdot \bar{p}(z) \quad (4.6)$$

where,

- $C_{dr}(z)$ is drag coefficient and can be determined by the following:

$$C_{dr}(z) = 0.65 \quad \text{when } z < h - 1.5 d(h) \quad (4.7)$$

$$C_{dr}(z) = 1.0 \quad \text{when } z \geq h - 1.5 d(h)$$

where, h is the height of minaret above ground level (m) and $d(h)$ is the external diameter at the top (m).

- $\bar{p}(z)$ is pressure due to mean hourly design wind speed at height z (Pa) and can be determined by Equation (4.8):

$$\bar{p}(z) = 0.67 [\bar{V}(z)]^2 \quad (4.8)$$

where, \bar{V}_z is the mean hourly design speed (m/s).

- $d(z)$ is the outside diameter at elevation Z (m).

The fluctuating load $w'(z)$ in N/m shall be taken equal to:

$$w'(z) = \frac{3.0 z \cdot G_{w'} \cdot M_{\bar{w}}(b)}{h^3} \quad (4.9)$$

where,

- $M_{\bar{w}}(b)$ is the base bending moment due to mean along wind load, $\bar{w}(z)$ (N.m)
- $G_{w'}$ is the gust factor for along wind fluctuating load and can be calculated as the following:

$$G_{w'} = 0.30 + \frac{19.227 [T_1 \cdot \bar{V}(10)]^{0.47}}{(3.2808 \cdot h + 16)^{0.86}} \quad (4.10)$$

where,

- T_1 is the natural period in sec/cycle, can be estimated using Equation (4.11):

$$T_1 = 5.32808 \frac{h^2}{\bar{d}(b)} \sqrt{\frac{\rho_{ck}}{E_{ck} * 1099.2}} \left[\frac{t(h)}{t(b)} \right]^{0.3} \quad (4.11)$$

where,

- $\bar{d}(b)$ is the mean diameter at bottom (m).
- ρ_{ck} is the concrete mass density (mg-sec²/m⁴).
- E_{ck} is the concrete modulus of elasticity (MPa).
- $t(h)$ is the top thickness of minaret (m).
- $t(b)$ is the bottom thickness of minaret (m).
- $\bar{V}(10)$ is determined from Equation (4.5) for $z = 10$ m.

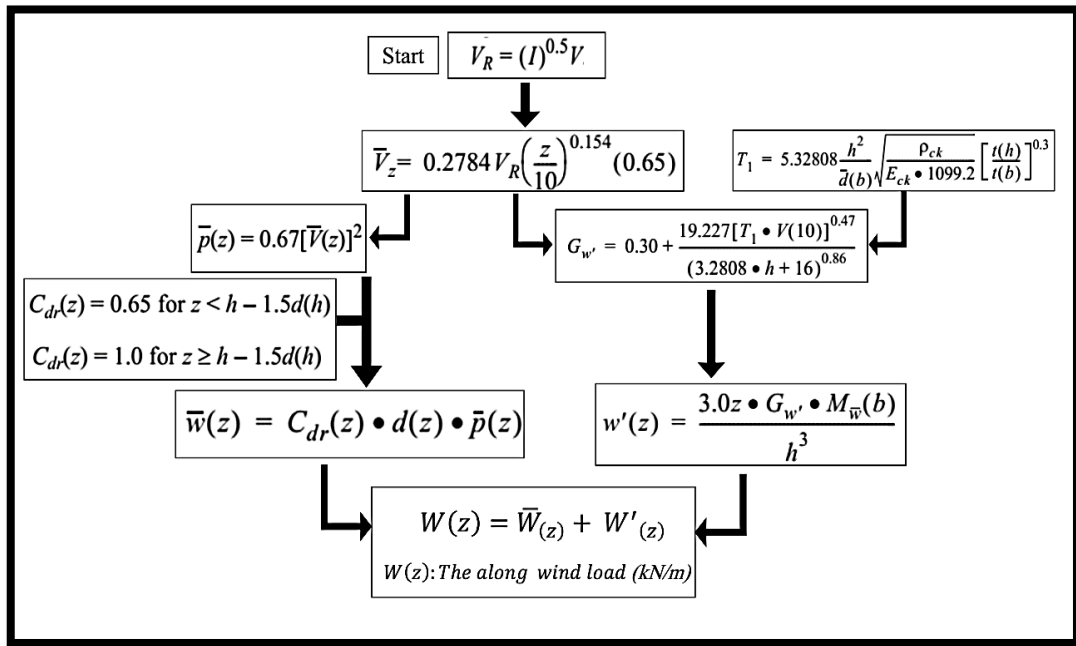


Figure 4.6: Schematic representations for along wind load calculations as per ACI307-98

4.4.2 Across wind load calculation procedure

A tall body like a minaret is a bluff body as opposite of a streamlines body. The streamlined body causes the wind flow to go smoothly past it and hence any extra forces is not happen. While the bluff body causes the wind to break away from the body. This separated flow causes high negative zone in the wake zone in back of the minaret. The wake zone is a greatly turbulent zone that give rise to lift forces that act in a direction perpendicular to the wind direction as shown in Figure 4.7. These lift forces cause the minaret to fluctuate in a perpendicular direction to the wind flow. (Patidara et al., 2014).

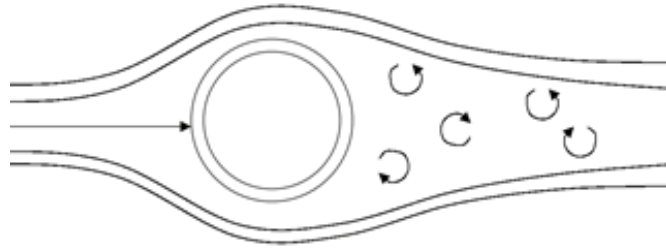


Figure 4.7: Across wind effect “Vortex shedding”

ACI307-98 considers across wind loads due to vortex shedding when the critical wind speed V_{cr} is between 0.50 and $1.30 \bar{V}(Z_{cr})$ and otherwise it is ignored.

The critical wind speed V_{cr} (m/s) can be computed as the following:

$$V_{cr} = \frac{f d(u)}{S_t} \quad (4.12)$$

where,

- f is the frequency for first-mode (Hz).
- $d(u)$ is the mean external diameter of higher third of minaret (m).
- S_t is Strouhal number, which can be found as the following:

$$S_t = 0.25 F_1(A) \quad (4.13)$$

where,

$$F_1(A) = 0.333 + 0.206 \log_e \frac{h}{d(u)} \quad (4.14)$$

but not > 1.0 or < 0.60 .

$\bar{V}(Z_{cr})$ is the mean design wind speed at $Z_{cr} = 5/6 h$ (m), and can be calculated from Equation (4.5)

Across wind loads according to ACI307-98 is calculated using Equation (4.15) which states the peak base moment M_a (N.m)

$$M_a = G \cdot S_s \cdot C_L \cdot \frac{\rho_a}{2} \cdot V_{cr}^2 \cdot d(u) \cdot h^2 \cdot \sqrt{\frac{\pi}{4(\beta_s + \beta_a)}} \cdot S_p \cdot \sqrt{\frac{2L}{\frac{h}{d(u)} + C_E}} \quad (4.15)$$

where,

- G is peak factor and should be considered as 4.0.
- S_s is mode shape factor. $S_s = 0.57$ for first mode, $S_s = 0.18$ for second mode.
- C_L is RMS lift coefficient, which can be calculated as the following:

$$C_L = C_{Lo} F_1(B) \quad (4.16)$$

where,

- C_{Lo} is RMS lift coefficient modified for local turbulence and can be found as the following:

$$C_{Lo} = -0.243 + 5.648i - 18.182 i^2 \quad (4.17)$$

where,

$$i = \frac{1}{\log_e \frac{5/6h}{Z_c}} \quad (4.18)$$

where, Z_c is exposure length = 0.0183 m.

- $F_1(B)$ is lift coefficient parameter and equals to:

$$F_1(B) = -0.089 + 0.377 \log_e \frac{h}{d(u)} \quad (4.19)$$

but not > 1.0 or < 0.20 .

- ρ_a is the air density, $\rho_a = 1.2 \text{ kg/m}^3$.
- β_s is fraction of critical damping and is calculated as follows:

$$\beta_s = 0.01 + \frac{0.10 [\bar{V} - \bar{V}_{(Z_{cr})}]}{\bar{V}_{(Z_{cr})}} \quad (4.20)$$

but not < 0.01 or > 0.04 .

- β_a is aerodynamic damping and is calculated as follows:

$$\beta_a = \frac{K_a \rho_a d(u)^2}{\overline{wt}(u)} \quad (4.21)$$

where,

- K_a is aerodynamic damping parameter and can be found as follows:

$$K_a = K_{ao} \cdot F_1(B) \quad (4.22)$$

where, K_{ao} is the mass damping parameter of small capacities and is calculated as the following:

$$K_{ao} = \frac{-1.0}{(1 + 5i) \left(1 + \frac{|k - 1|}{i + 0.10} \right)}, k = \frac{\bar{V}}{V_{cr}} \quad (4.23)$$

- $\overline{wt}(u)$ is average weight in top third of minaret (kg/m).
- S_p is spectral parameter and can be found by Equation (4.24):

$$S_p = \frac{k^{\frac{3}{2}}}{B^{\frac{1}{2}} \pi^{\frac{1}{4}}} \exp \left[-\frac{1}{2} \left(\frac{1 - k^{-1}}{B} \right)^2 \right] \quad (4.24)$$

where, B is band width parameter and equal to $0.10 + 2i$.

- L is correlation length coefficient and should be considered as 1.2.
- C_E is end effect factor and should be considered as 3.

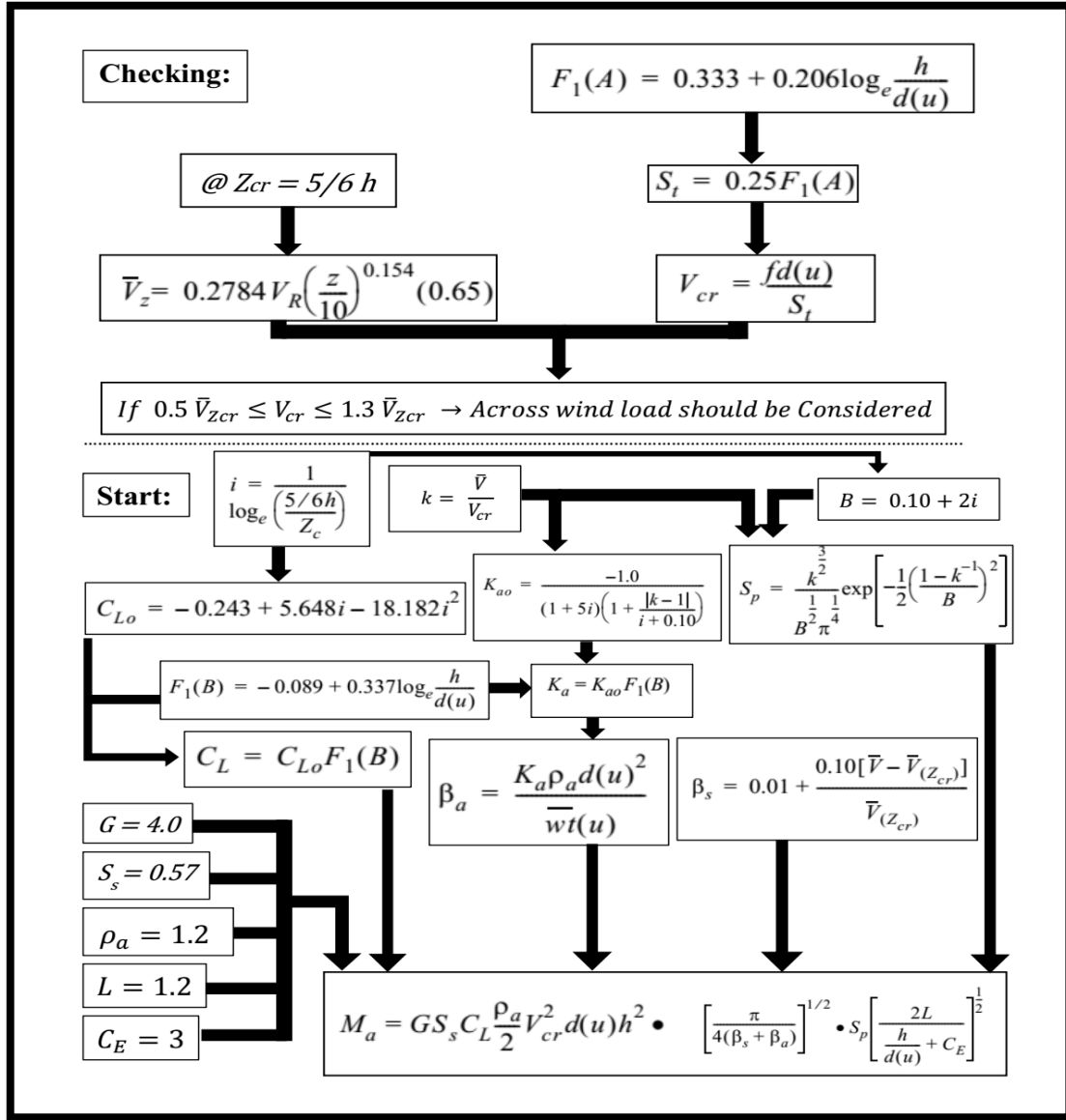


Figure 4.8: Schematic representations for across wind load calculations as per ACI307-98

Sadeghi (2001) states another method to find across wind load due to vortex shedding for tall structures, and it can be found in APPENDIX 5.

4.4.3 Combination of across wind and along wind load

Across wind loads and along wind loads occurring at the same time should be combined with each other by Equation (4.25), which define the combined design moment at any section (z):

$$M_w(z) = \sqrt{[M_a(z)]^2 + [M_l(z)]^2} \quad (4.25)$$

where,

- $M_a(z)$ is the moment produce by across wind loads, given in Equation (4.15).
- $M_l(z)$ is the moment produce by the average along wind load, $w_l(z)$.

where,

$$w_l(z) = \bar{w}(z) \left[\frac{\bar{V}}{\bar{V}(z_{cr})} \right]^2 \quad (4.26)$$

where,

- $\bar{w}(z)$ is the mean along wind load.
- \bar{V} is the mean wind velocity.
- $\bar{V}(Z_{cr})$ is the mean design wind speed at Z_{cr} and can be calculated by Equation (4.5).

CHAPTER 5

EARTQUAKE LOAD ANALYSIS

5.1 Overview

This chapter presents a summary about earthquake load acting on RC minarets and the procedure to estimate earthquake load effect on the representative minarets by using response spectrum method in accordance with two different codes, NCSC2015 and ACI307-98.

5.2 Earthquake Load Effect on RC Minarets

Earthquake load on RC minarets forms an additional source of natural loads on the RC minaret. Earthquake or seismic action is a short and strong violent shaking of the ground. Any structure under earthquake loading is subjected to repeated loading for a short interval of time. During an earthquake ground oscillated (moves) in all directions. The horizontal component of the ground vibration is generally stronger than that of the vertical components during earthquakes. The earthquake is generally random in nature and the random peaks of several directions may not occur altogether. Hence, for design purposes at one time, it is assumed that only the horizontal component acts in any one direction. All structures are designed to resist their own weight. This could be considered as though a vertical acceleration of 1g is applied to the different masses of the structure system. Since the design vertical forces suggested in the codes are small as compared to the acceleration of 1 gravity, the same importance has not been given to the vertical forces as compared to the horizontal forces. Therefore vertical earthquake forces are considered to be neglected (Gupta A. K., 1990).

There are many seismic analysis methods to estimate earthquake load effect on structures, and can be divided into two groups, linear and non-linear methods. Linear methods can be divided into two different methods, static and dynamic methods, which called as equivalent lateral force method and response spectrum method, respectively. Also, non-linear methods can be divided into static and dynamic methods, which called as pushover and time history analysis, respectively. In this study, response spectrum method is selected to estimate seismic load on the representative RC minarets (Touqan & Salawdeh, 2013; Rashmi & Kumar, 2017).

5.3 Response Spectrum Method

Response spectrum method (RSM) mainly depends on designing of a graph called spectrum. This graph is obtained from subjecting a specific earthquake or ground motion to a set of structures having different natural periods, T , getting the maximum response of each structure, and plotting this as a function of T as shown in Figure 5.1.

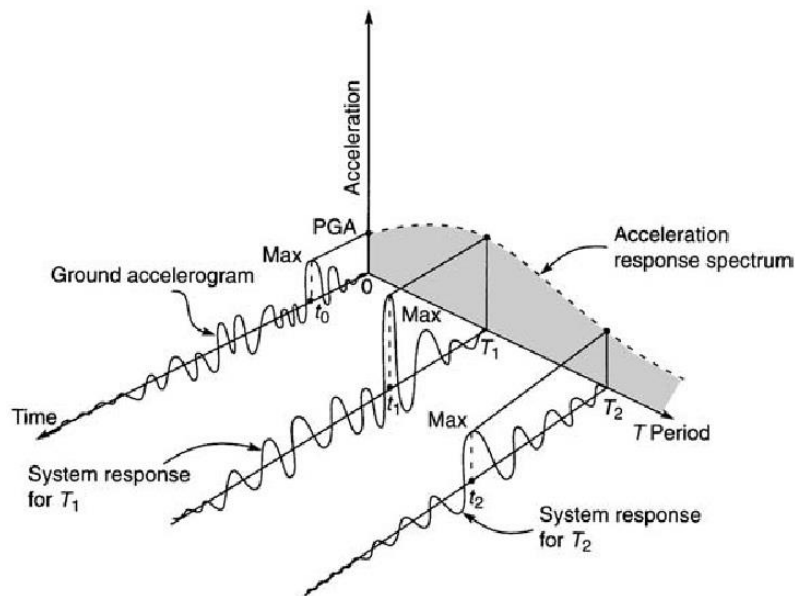


Figure 5.1: Graphical description of response spectrum (Taranath, B. S., 2004)

Earthquakes records will give various response spectrums. However earthquakes which have same magnitude tend to produce spectrums with similar characteristics. This has permitted

the structural codes to adopt standard response spectra that combine these characteristics, and which would be expected at a construction site during a design earthquake. Structural codes averaged the peaks and valleys in the spectrums which have got from records, then form smooth response spectra to be used (Taranath, B. S., 2004).

A typical situation of elastic design spectrum is shown in Figure 5.2, where T is natural period of the structure and S_e is spectral acceleration. It can be noticed that the graph is of four phases, the elastic stage between points A and B, the constant acceleration stage between points B and C, the constant velocity stage between points C and D and the last stage is the constant displacement phase between D and E (Chandak, N. R., 2013).

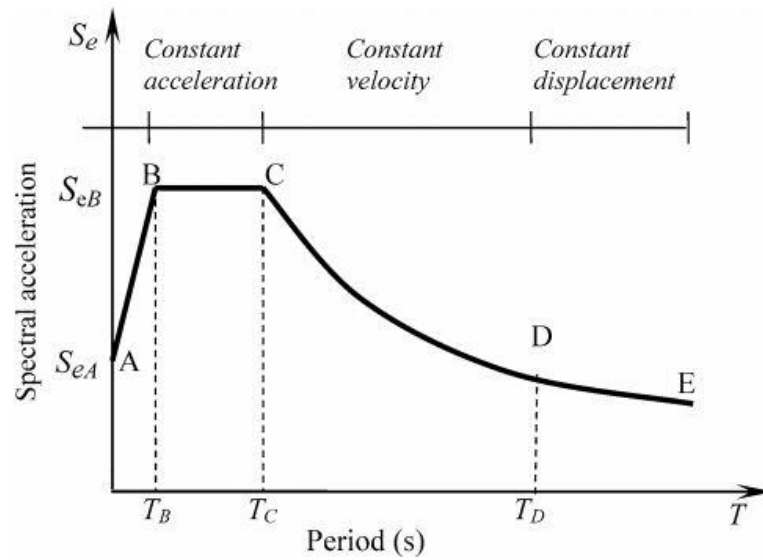


Figure 5.2: A typical design spectrum (Chandak, N. R., 2013)

5.4 Response Spectrum Method According to NCSC2015

In NCSC2015, the ordinate of the elastic response spectrum can be found by Equation (5.1):

$$S_{pa}(T) = \frac{A(T) \cdot g}{R_a(T)} \quad (5.1)$$

where,

- $A(T)$ refers to the spectral acceleration coefficient
- $R_a(T)$ refers to the earthquake load reduction factor
- g is the gravitational acceleration

The spectral acceleration coefficient, $A(T)$ is considered to be the basis for the expectation of seismic load and can be calculated as the following:

$$A(T) = A_0 I S(T) \quad (5.2)$$

where,

- A_0 is the coefficient of effective ground acceleration
- I is the importance factor
- $S(T)$ is the spectrum coefficient

The effective ground acceleration coefficient, A_0 is related with the seismic zones as specified in Table 5.1.

Table 5.1: The effective ground acceleration coefficient (Chamber of Civil Engineers, 2015)

Seismic Zone	A_0
1	0.40
2	0.30
3	0.20
4	0.10

Figure 5.3 shows the seismic zoning map that has been adapted to the northern part of the island with a PGA value between 0.2 – 0.3 g for Nicosia city (Chamber of Civil Engineers, 2015).

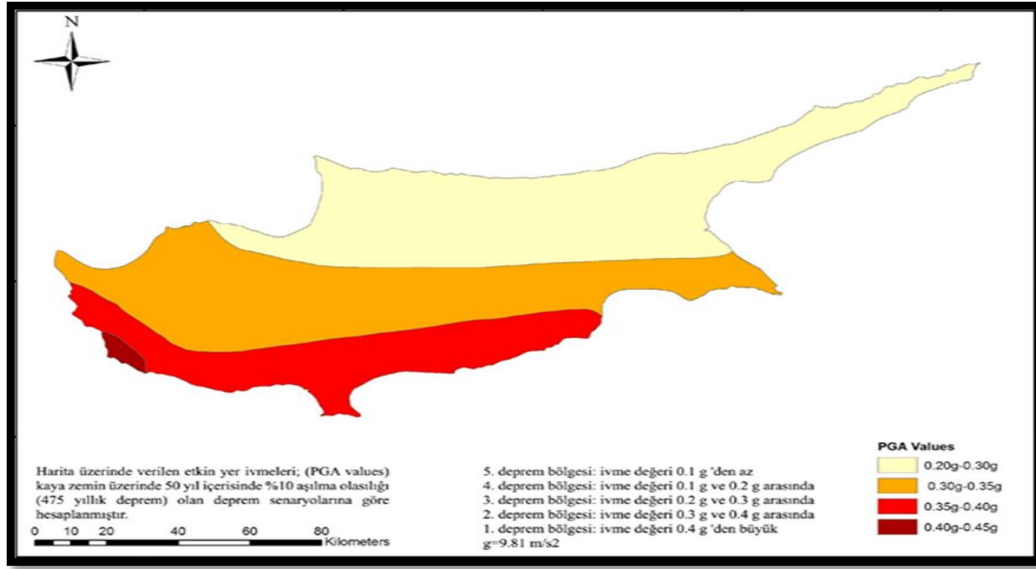


Figure 5.3: Seismic map zones according to NCSC2015 (Chamber of Civil Engineers, 2015)

The importance factor, I is specified according to structure's function as shown in Table 5.2.

The spectrum coefficient, $S(T)$ depends on the local site conditions and the building's natural period, T . $S(T)$ can be calculated by the following:

$$S(T) = 1 + 1.5 \frac{T}{T_A} \quad 0 \leq T \leq T_A \quad (5.3)$$

$$S(T) = 2.5 \quad T_A < T \leq T_B \quad (5.4)$$

$$S(T) = 2.5 \left(\frac{T_B}{T} \right)^{0.8} \quad T_B < T \quad (5.5)$$

where, T_A and T_B are the spectrum characteristic periods in seconds. Table 5.3 gives T_A and T_B values depending on local soil classes.

Soil types according to NCSC2015 are given in Table 5.4 depending on shear wave velocity (m/s), while local site classes are presented in Table 5.5.

Table 5.2: Building importance factor (Chamber of Civil Engineers, 2015)

Occupancy or Type of Building	Importance Factor (<i>I</i>)
1. Buildings are required to be utilised after the earthquake and buildings containing hazardous materials	
a. Buildings required to be utilized immediately after the earthquake.(Hospitals, dispensaries, health wards, fire fighting buildings and facilities, PTT and other telecommunication facilities, transportation stations and terminals, power generation and distribution facilities; governorate, county and municipality administration buildings, first aid and emergency planning station)	1.5
b. Buildings are containing or storing toxic, explosive and flammable materials, etc.	
2. Intensively and long-term occupied buildings and buildings preserving valuable goods.	
a. Schools, other educational buildings and facilities, dormitories and hostels, military barracks, prisons, etc.	1.4
b. Museums.	
3. Intensively but short-term occupied buildings.	
a. Sports facilities, cinema, theatre and concert halls, etc.	1.2
4. Other buildings	
a. Buildings other than above defined buildings. (Residential and office buildings, hotels, building like industrial structures, etc.)	1.0

Table 5.3: The spectrum characteristic periods (Chamber of Civil Engineers, 2015)

Local Site Soil Class	T _A (second)	T _B (second)
Z1	0.10	0.30
Z2	0.15	0.40
Z3	0.15	0.60
Z4	0.20	0.90

Table 5.4: Ground (soil) types (Chamber of Civil Engineers, 2015)

Ground Type	Soil Description	Shear Wave Velocity V _{S30} (m/s)
A	I. Massive volcanic rocks, unweathered sound metamorphic rocks, stiff cemented sedimentary rocks	> 1000
	II. Very dense sand, gravel	> 700
	III. Hard clay and silty clay	> 700
B	I. Soft volcanic rocks such as tuff and agglomerate, weathered cemented sedimentary rocks with planes of discontinuity	700 – 1000
	II. Dense sand, gravel	400 - 700
	III. Very stiff clay and silty clay	300 - 700
C	I. Highly weathered soft metamorphic rocks and cemented sedimentary rocks with planes of discontinuity.	400 - 700
	II. Medium dense sand and gravel	200 - 400
	III. Stiff clay and silty clay	200 - 300
D	I. Soft, deep alluvial layers with high groundwater level	< 300
	II. Loose sand	< 200
	III. Soft clay and silty clay	< 200

Table 5.5: Local site classes (Chamber of Civil Engineers, 2015)

Local Site Class	Soil Group and Topmost Soil Layer Thickness (h_1)
	Group (A) soils
Z1	Group (B) soils with $h_1 < 15.0$ m
	Group (B) soils with $h_1 > 15.0$ m
Z2	Group (C) soils with $h_1 < 15.0$ m
	Group (C) soils with $15.0 \text{ m} < h_1 < 50.0 \text{ m}$
Z3	Group (D) soils with $h_1 < 10.0$ m
	Group (C) soils with $h_1 > 50.0$ m
Z4	Group (D) soils with $h_1 > 10.0$ m

The earthquake load reduction factor, $R_a(T)$ can be found by the following:

$$R_a(T) = 1.5 + (R - 1.5) \frac{T}{T_A} \quad 0 \leq T \leq T_A \quad (5.6)$$

$$R_a(T) = R \quad T > T_A \quad (5.7)$$

where,

- R refers to the structural system behavior factor, as given in Table 5.6
- T is the natural period

Table 5.6: Structural behaviour factor R for non-building structures (Chamber of Civil Engineers, 2015)

Structural Type	R
Elevated liquid tanks pressurized tanks, bunkers, vessels carried by frames of high ductility level or steel eccentric braced frames	4
Elevated liquid tanks, pressurized tanks, bunkers, vessels carried by frames of nominal ductility level or steel centric braced frames	2
Cast-in-situ RC silos, industrial chimneys and suchlike structural systems with uniformly distributed mass along height	3
RC cooling towers	3
Space truss steel towers, steel silos and industrial chimneys with uniformly distributed mass along height	4
Guyed steel high posts and guyed steel	2
Inverted pendulum type structures carried by a single structural element with mass concentrated at the top	2
Industrial type steel storage racks	4

Figure 5.4 shows the design acceleration spectra, which relating spectrum coefficients, $S(T)$ with the natural time periods.

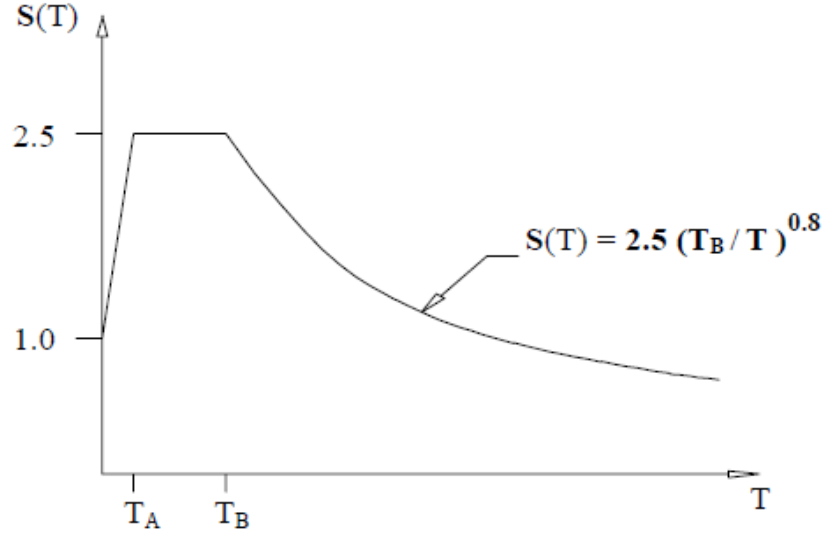


Figure 5.4: Design acceleration spectra according to NCSC2015 (Chamber of Civil Engineers, 2015)

5.5 Response Spectrum Method According to ACI307-98

ACI307-98 states that the local specific response spectrum shall be based on a 90% probability of not being transcended in 50 years with 5% damping. The design spectral response acceleration, S_a , depends on two parameters, S_{DS} and S_{D1} , which are the design earthquake spectral response acceleration parameters at short period and at 1 second period, respectively and can be calculated by the following:

$$S_{DS} = \left(\frac{2}{3}\right) S_{MS} \quad (5.8)$$

$$S_{D1} = \left(\frac{2}{3}\right) S_{M1} \quad (5.9)$$

where, S_{MS} and S_{M1} are the risk-targeted maximum considered earthquake, MCE_R for short periods and at 1 second, respectively, adjusted for site class effects, and shall be determined as the following:

$$S_{MS} = F_a S_S \quad (5.9)$$

$$S_{M1} = F_v S_1 \quad (5.10)$$

where,

- F_a and F_v are site coefficients
- S_S and S_1 are parameters shall be determined from the 0.2 and 1 second spectral response accelerations and can be found as follows: (Lubkowski and Aluisi, 2012)

$$S_S / PGA = 0.3386 PGA + 2.1696 \quad (5.11)$$

$$S_1 / PGA = 0.5776 PGA + 0.5967 \quad (5.12)$$

There are six types of soil to be considered to represent the most common soil conditions as given in Table 5.7 depending on shear wave velocity. Wherever, the shear wave velocity is unknown to determine the soil class, shall be used soil class D.

Once the soil site class is assigned, the corresponding site coefficients for short and long periods, F_a and F_v , respectively, are determined using Table 5.8 and 5.9.

Table 5.7: Soil site class (ASCE7, 2016)

Site Class	Soil Description	Shear Wave Velocity V_{S30} (m/s)
A	Hard rock	$V_S > 1500$
B	Rock	$760 < V_S < 1500$
C	Very dense soil and soft rock	$360 < V_S < 760$
D	Stiff soil (default site class)	$180 < V_S < 360$
E	Soft clay soil	$V_S < 180$
F	Liquefiable soils, quick highly sensitive clays, collapsible weakly cemented soils. These require site response analysis.	

Table 5.8: The corresponding site coefficients at short period F_a (ASCE7, 2016)

Site Class	$S_S \leq 0.25$	$S_S = 0.5$	$S_S = 0.75$	$S_S = 1.0$	$S_S \geq 1.25$
A	0.8	0.8	0.8	0.81	0.8
B	1.0	1.0	1.0	1.0	1.0
C	1.2	1.2	1.1	1.0	1.0
D	1.6	1.4	1.2	1.1	1.0
E	2.5	1.7	1.2	0.9	0.9
F	A site response analysis must be performed				

Table 5.9: The corresponding site coefficients at long period F_v (ASCE7, 2016)

Site Class	$S_I \leq 0.1$	$S_I = 0.2$	$S_I = 0.3$	$S_I = 0.4$	$S_I \geq 0.5$
A	0.8	0.8	0.8	0.8	0.8
B	1.0	1.0	1.0	1.0	1.0
C	1.7	1.6	1.5	1.4	1.3
D	2.4	2.0	1.8	1.6	1.5
E	3.5	3.2	2.8	2.4	2.4
F	A site response analysis must be performed				

The response spectrum curve should be designed as shown in Figure 5.5 and as specified in the following:

$$S_a = S_{DS} \left[0.4 + 0.6 \frac{T}{T_0} \right] \quad T < T_0 \quad (5.13)$$

$$S_a = S_{DS} \quad T_0 \leq T \leq T_S \quad (5.14)$$

$$S_a = \frac{S_{D1}}{T} \quad T_S < T \leq T_L \quad (5.15)$$

$$S_a = \frac{S_{D1} T_L}{T^2} \quad T_L < T \quad (5.16)$$

where,

- T is the fundamental period of the structure in seconds
- T_0 (sec) is calculated by Equation (5.17)
- T_S (sec) is calculated by Equation (5.18)

- T_L is the long period transition period (sec) and can be determined from Table 5.10.

$$T_0 = 0.2 \frac{S_{D1}}{S_{DS}} \quad (5.17)$$

$$T_s = \frac{S_{D1}}{S_{DS}} \quad (5.18)$$

Table 5.10: Long period, transition period (Council, 2015)

M_s	T_L (sec)
6.0 - 6.5	4
6.5 - 7.0	6
7.0 - 7.5	8
7.5 - 8.0	12
8.0 - 8.5	16
8.5 - 9.0	20

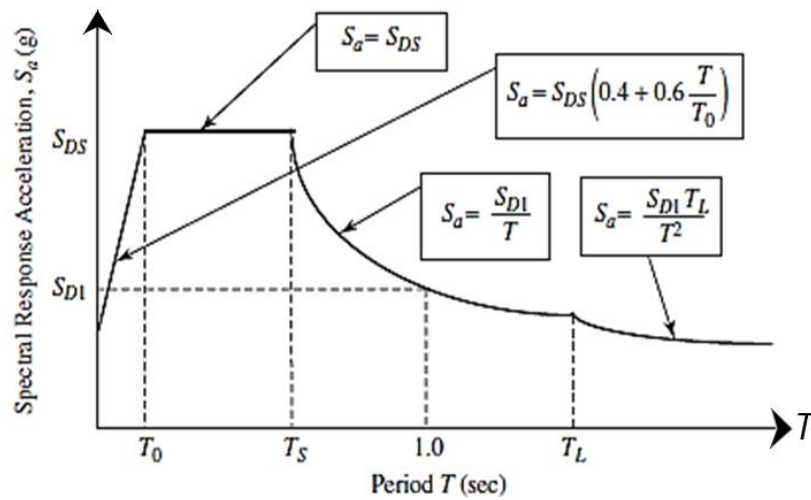


Figure 5.5: Design response spectrum according to ACI307-98 (McCormac, 2005)

CHAPTER 6

CALCULATIONS AND RESULTS

6.1 Overview

This chapter discusses applying wind and earthquake loads on the modelled minarets and then presents the analysis results according to the cited codes and the comparison between these results.

6.2 Wind Load Calculation

Wind load in this study is determined according to two codes, TS498 and ACI307-98.

6.2.1 Wind load calculation according to TS498

As stated before, TS498 uses a simple method to estimate wind load. Calculations of wind loads on the four modelled minarets according to TS498 are presented in Tables 6.1 - 6.4.

Table 6.1: Wind load calculation for 26.0 m minaret according to TS498

Section no.	Height (m)	Diameter, d (m)	C_p coefficient	Wind pressure, q (kN/m ²)	Wind load, W (kN/m)
1	0-6.55	2.9	1.2	0.5	1.74
2	6.55-8	2.6	1.6	0.5	2.08
3	8-9	2.1	1.6	0.8	2.69
4	9-20	1.9	1.6	0.8	2.43
5	20-21.36	1.9	1.6	1.1	3.34
6	21.36-26	1.9	1.6	1.1	3.34

Table 6.2: Wind load calculation for 33.2 m minaret according to TS498

Section no.	Height (m)	Diameter, d (m)	C_p coefficient	Wind pressure, q (kN/m ²)	Wind load, W (kN/m)
1	0-8	2.7	1.2	0.5	1.62
2	8-9.8	2.3	1.6	0.5	1.84
3	9.8-20	1.9	1.6	0.8	2.43
4	20-28.7	1.9	1.6	1.1	3.34
5	28.7-33.2	1.9	1.6	1.1	3.34

Table 6.3: Wind load calculation for 61.45 m minaret according to TS498

Section no.	Height (m)	Diameter, d (m)	C_p coefficient	Wind pressure, q (kN/m ²)	Wind load, W (kN/m)
1	0-5.5	5	1.6	0.5	4.0
2	5.5-8	3.95	1.6	0.5	3.16
3	8-10.45	3.95	1.6	0.8	5.06
4	10.45-20	2.9	1.6	0.8	3.71
5	20-28.45	2.9	1.6	1.1	5.10
6	28.45-37.45	2.75	1.6	1.1	4.84
7	37.45-46.45	2.6	1.6	1.1	4.58
8	46.45-52.45	2.45	1.6	1.1	4.31
9	52.45-61.45	2.45	1.6	1.1	4.31

Table 6.4: Wind load calculation for 76.2 m minaret according to TS498

Section no.	Height (m)	Diameter, d (m)	C_p coefficient	Wind pressure, q (kN/m ²)	Wind load, W (kN/m)
1	0-7.65	5.0	1.2	0.5	3.0
2	7.65-14.35	4.3	1.6	0.5	5.50
3	14.35-20	3.6	1.6	0.8	4.61
4	20-30.9	3.6	1.6	0.8	6.34
5	30.9-44.45	3.3	1.6	1.1	5.81
6	44.45-58	3	1.6	1.1	5.28
7	58-68.5	2.8	1.6	1.1	4.93
8	68.5-76.2	2.8	1.6	1.1	4.93

6.2.2 Wind load calculation according to ACI307-98

As stated before, ACI307-98 states the procedure to determine wind load in both cases along and across wind load.

The basic wind speed for calculation of both along and across wind load is accepted as 35 m/s, while the importance factor shall be considered as 1.15 for the case of chimneys and similar structures like minarets.

6.2.2.1 Along wind load calculation according to ACI307-98

The along wind load calculations for the modelled minarets are given in the Tables 6.5 - 6.16.

Table 6.5: Mean wind load calculation for 26.0 m minaret according to ACI307-98

Section no.	Z (m)	d (m)	$\bar{V}(z)$ (m/s)	$Cdr(z)$	$\bar{p}(z)$ (Pa)	$\bar{w}(z)$ (N/m)*
1	6.55	2.9	22.91	0.65	351.63	662.82
2	9	2.4	24.06	0.65	387.78	604.94
3	21.36	1.9	27.48	0.65	506.05	624.98
4	26	1.9	28.33	1	537.64	1021.5

* Z: Height, d: Diameter, $\bar{V}(z)$: Mean design speed, $Cdr(z)$: Drag coefficient, $\bar{p}(z)$: Mean pressure, $\bar{w}(z)$: Mean along wind load.

Table 6.6: Fluctuating wind load calculation for 26.0 m minaret according to ACI307-98

Section no.	Z (m)	d (m)	$G_{w'}$	$M_{\bar{w}}(b)$ (N.m)	$w'(z)$ (N/m)*
1	6.55	2.9	1.972	255241.48	562.76
2	9	2.4	1.972	255241.48	773.26
3	21.36	1.9	1.972	255241.48	1835.21
4	26	1.9	1.972	255241.48	2233.87

* Z: Height, d: Diameter, $G_{w'}$: Gust Factor, $M_{\bar{w}}(b)$: Base bending moment due to mean load, $w'(z)$: Fluctuating along load.

Table 6.7: Along wind load calculation for 26.0 m minaret according to ACI307-98

Section no.	Z (m)	$\bar{w}(z)$ (N/m)	$w'(z)$ (N/m)	$W(z)$ (kN/m)*
1	6.55	662.82	562.76	1.23
2	9	604.94	773.26	1.38
3	21.36	624.98	1835.21	2.46
4	26	1021.5	2233.87	3.26

* Z: Height, $\bar{w}(z)$: Mean along wind load, $w'(z)$: Fluctuating along load, $W(z)$: Along wind load.

Table 6.8: Mean wind load calculation for 33.2 m minaret according to ACI307-98

Section no.	Z (m)	d (m)	$\bar{V}(z)$ (m/s)	$C_{dr}(z)$	$\bar{p}(z)$ (Pa)	$\bar{w}(z)$ (N/m)
1	8.2	2.7	23.72	0.65	376.82	661.32
2	9.8	2.3	24.38	0.65	398.09	595.14
3	28.7	1.9	28.76	0.65	554.25	684.50
4	33.2	1.9	29.41	1	579.68	1101.4

Table 6.9: Fluctuating wind load calculation for 33.2 m minaret according to ACI307-98

Section no.	Z (m)	d (m)	$G_{w'}$	$M_{\bar{w}}(b)$ (N.m)	$w'(z)$ (N/m)
1	8.2	2.9	2.05	433238.52	596.75
2	9.8	2.4	2.05	433238.52	713.19
3	28.7	1.9	2.05	433238.52	2088.63
4	33.2	1.9	2.05	433238.52	2416.11

Table 6.10: Along wind load calculation for 33.2 m minaret according to ACI307-98

Section no.	Z (m)	$\bar{w}(z)$ (N/m)	$w'(z)$ (N/m)	$W(z)$ (kN/m)
1	8.2	661.32	596.75	1.26
2	9.8	595.14	713.19	1.31
3	28.7	684.50	2088.63	2.77
4	33.2	1101.4	2416.11	3.52

Table 6.11: Mean wind load calculation for 61.45 m minaret according to ACI307-98

Section no.	Z (m)	d (m)	$\bar{V}(z)$ (m/s)	$C_{dr}(z)$	$\bar{p}(z)$ (Pa)	$\bar{w}(z)$ (N/m)
1	5.5	5	22.30	0.65	333.20	1082.91
2	10.45	3.95	24.62	0.65	406.04	1042.50
3	28.45	2.9	28.72	0.65	552.76	1041.95
4	37.45	2.75	29.96	0.65	601.59	1075.35
5	46.45	2.6	30.98	0.65	642.85	1086.42
6	52.45	2.45	31.56	0.65	667.36	1062.77
7	61.45	2.45	32.34	1	700.72	1716.76

Table 6.12: Fluctuating wind load calculation for 61.45m minaret according to ACI307-98

Section no.	Z (m)	d (m)	$G_{w'}$	$M_{\bar{w}}(b)$ (N.m)	$w'(z)$ (N/m)
1	5.5	5	4.30	2346641.6	717.09
2	10.45	3.95	4.30	2346641.6	1362.46
3	28.45	2.9	4.30	2346641.6	3709.29
4	37.45	2.75	4.30	2346641.6	4882.70
5	46.45	2.6	4.30	2346641.6	6056.11
6	52.45	2.45	4.30	2346641.6	6838.39
7	61.45	2.45	4.30	2346641.6	8011.80

Table 6.13: Along wind load calculation for 61.45 m minaret according to ACI307-98

Section no.	Z (m)	$\bar{w}(z)$ (N/m)	$w'(z)$ (N/m)	$W(z)$ (kN/m)
1	5.5	1082.91	717.09	1.80
2	10.45	1042.50	1362.46	2.40
3	28.45	1041.95	3709.29	4.75
4	37.45	1075.35	4882.70	5.96
5	46.45	1086.42	6056.11	7.14
6	52.45	1062.77	6838.39	7.90
7	61.45	1716.76	8011.80	9.73

Table 6.14: Mean wind load calculation for 76.2 m minaret according to ACI307-98

Section no.	Z (m)	d (m)	$\bar{V}(z)$ (m/s)	$C_{dr}(z)$	$\bar{p}(z)$ (Pa)	$\bar{w}(z)$ (N/m)
1	7.65	5.00	23.46	0.65	368.85	1198.75
2	14.35	4.30	25.85	0.65	447.70	1251.33
3	30.90	3.60	29.09	0.65	567.00	1326.79
4	44.45	3.30	30.77	0.65	634.20	1360.35
5	58.00	3.00	32.05	0.65	688.36	1342.30
6	68.50	2.80	32.89	0.65	724.56	1318.69
7	76.20	2.80	33.43	1	748.72	2096.42

Table 6.15: Fluctuating wind load calculation for 76.2 m minaret according to ACI307-98

Section no.	Z (m)	d (m)	$G_{w'}$	$M_{\bar{w}}(b)$ (N.m)	$w'(z)$ (N/m)
1	7.65	5.00	7.05	2250249.7	822.34
2	14.35	4.30	7.05	2250249.7	1542.55
3	30.90	3.60	7.05	2250249.7	3321.59
4	44.45	3.30	7.05	2250249.7	4778.14
5	58.00	3.00	7.05	2250249.7	6234.70
6	68.50	2.80	7.05	2250249.7	7363.39
7	76.20	2.80	7.05	2250249.7	8191.10

Table 6.16: Along wind load calculation for 76.2 m minaret according to ACI307-98

Section no.	Z (m)	$\bar{w}(z)$ (N/m)	$w'(z)$ (N/m)	$W(z)$ (kN/m)
1	5.5	1198.75	822.34	2.02
2	10.45	1251.33	1542.55	2.79
3	28.45	1326.79	3321.59	4.65
4	37.45	1360.35	4778.14	6.14
5	46.45	1342.30	6234.70	7.58
6	52.45	1318.69	7363.39	8.68
7	61.45	2096.42	8191.10	10.29

6.2.2.2 Across wind load calculation according to ACI307-98

As stated before, ACI307-98 considers across wind loads when the critical wind speed V_{cr} is between 0.50 and $1.30 \bar{V}(Z_{cr})$ and otherwise it is ignored. Table 6.17 shows verification of this condition on the modelled minarets. From the table, it can be noticed that the across wind load is ignored in all of the modelled minarets.

Table 6.17: Condition of consideration of across wind load according to ACI307-98

Minaret height (m)	V_{cr} (m/s)	$\bar{V}(Z_{cr})$ (m/s)	$0.5 \bar{V}(Z_{cr})$	$1.3 \bar{V}(Z_{cr})$	Across wind load considering
26.0	38.95	21.67	13.77	35.81	Not needed
33.2	14.0	27.67	14.3	37.18	Not needed
61.45	11.59	31.44	15.72	40.88	Not needed
76.2	9.85	32.50	16.25	42.25	Not needed

It can be noticed that across wind load according to ACI307-98 can be neglected in this case study.

6.2.3 Comparison between wind load calculation results according to TS498 & ACI307-98

Wind load intensities, for the modelled minarets which are found according to the mentioned standards, TS498 and ACI307-98, are presented and compared to each other in Tables 6.18 - 6.21 and Figures 6.1 - 6.4.

Table 6.18: Comparison of wind load intensities for 26.0 m minaret

Height (m)	W-TS498 (kN/m)	W-ACI307-98 (kN/m)	Difference %
0	0	0	-
6.55	1.74	1.226	29.6%
8	2.08	1.378	33.7%
9	2.688	1.378	48.7%
20	2.432	2.460	1.1%
21.36	3.344	2.460	26.4%
26	3.344	3.255	2.6%

* W-TS498: Wind load intensity according to TS498, W-ACI307-98: Wind load intensity according to ACI307-98.

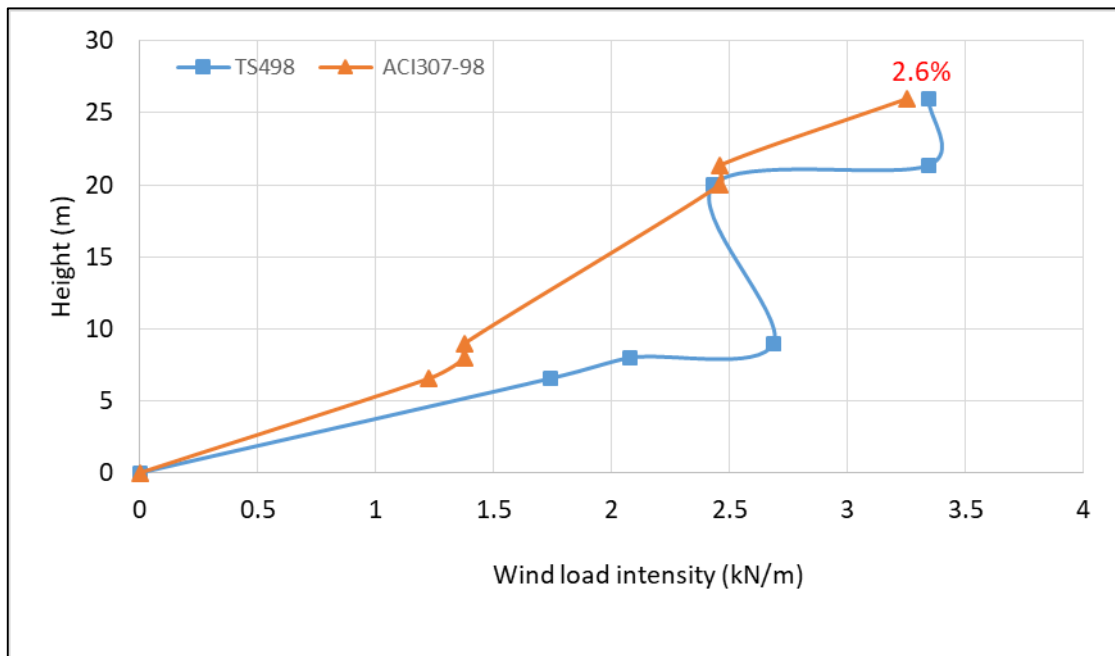


Figure 6.1: Comparison of wind load intensities for 26.0 m minaret

From the results shown in Figure 6.1, it can be seen that the wind load intensity shows an upward sloping curve with respect to ACI307-98. According to TS498, it can be noticed that there is a variable slope curve due to the C_p coefficient, the wind pressure and the change of minaret outer diameter values.

According to TS498, the wind load intensity at a height of 6.55 m is 29.6% higher than ACI307-98. This difference increases to 33.7% at an elevation of 8.0 m, due to the increase in the C_p coefficient value from 1.2 for rectangular shapes to 1.6 for circular shapes. At a height of 9.0 m, the difference increases to 48.7% because the wind pressure value increases from 0.5 kN/m^2 to 0.8 kN/m^2 . The difference decreases to 1.1% at 20.0 m in height due to the fixity of the outer diameter and wind pressure values. After 20.0 m in height, wind pressure value increases to 1.1 kN/m^2 and the difference increases to 2.6% at the top of the minaret.

Generally, it is observed that the resultant wind load according to TS498 in 26.0 m minaret is larger than ACI307-98. It can be said that, the distribution of wind load intensity according to ACI307-98 is more appropriate.

Table 6.19: Comparison of wind load intensities for 33.2 m minaret

Height (m)	W-TS498 (kN/m)	W-ACI307-98 (kN/m)	Difference %
0	0	0	-
8	1.62	1.258	22.3%
9.8	1.84	1.308	28.9%
20	2.432	2.773	12.3%
28.7	3.344	3.20	4.3%
33.2	3.344	3.518	4.9%

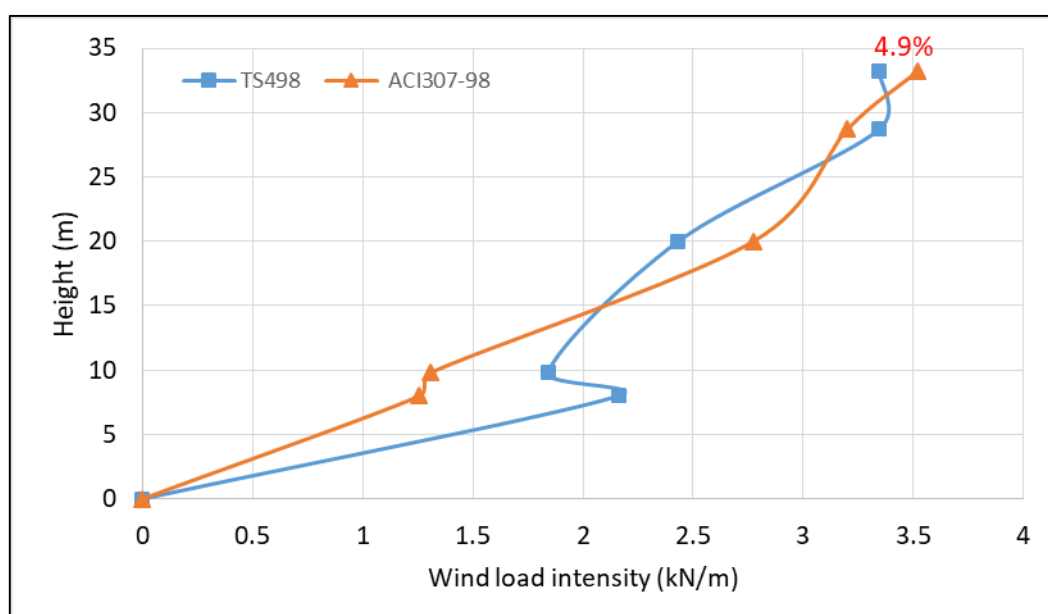


Figure 6.2: Comparison of wind load intensities for 33.2 m minaret

The results presented in Figure 6.2 show that the wind load intensity has an upward sloping curve according to ACI307-98. While, TS498, has a variable slope curve depending on the C_p coefficient, the wind pressure and the change in outside diameter values.

The wind load intensity at 8.0 m in TS498 is about 22.3% higher than ACI307-98. As the C_p coefficient increases after the base, this difference increases to 28.9% at 9.8 m in height. At a height of 20.0 m, the wind load intensity according to ACI307-98 is higher than TS498 by about 12.3% because of the constant wind pressure value between 9.0 m and 20.0 m in height. Due to increase wind pressure after 20.0 m to 1.1 kN/m^2 , the wind intensity according to TS498 at a height of 28.7 m is higher than ACI307-98 by about 4.3%. At the top of the minaret, the wind load intensity according to ACI307-98 is higher than TS498 by about 4.9%, due to constancy of wind pressure value as 1.1 kN/m^2 .

Generally, the resultant wind load values according to TS498 and ACI307-98 in 33.2 m minaret are very close to each other. It can be said that the distribution of wind load intensity according to ACI307-98 is more appropriate.

Table 6.20: Comparison of wind load intensities for 61.45 m minaret

Height (m)	W-TS498 (kN/m)	W-ACI307-98 (kN/m)	Difference %
0	0	0	-
5.5	4	1.391	65.2%
8	3.16	1.628	48.5%
10.45	5.056	1.628	67.8%
20	3.712	2.637	29.0%
28.45	5.104	2.637	48.3%
37.45	4.84	3.234	33.2%
46.45	4.576	3.816	16.6%
52.45	4.312	4.199	2.6%
61.45	4.312	5.477	21.3%

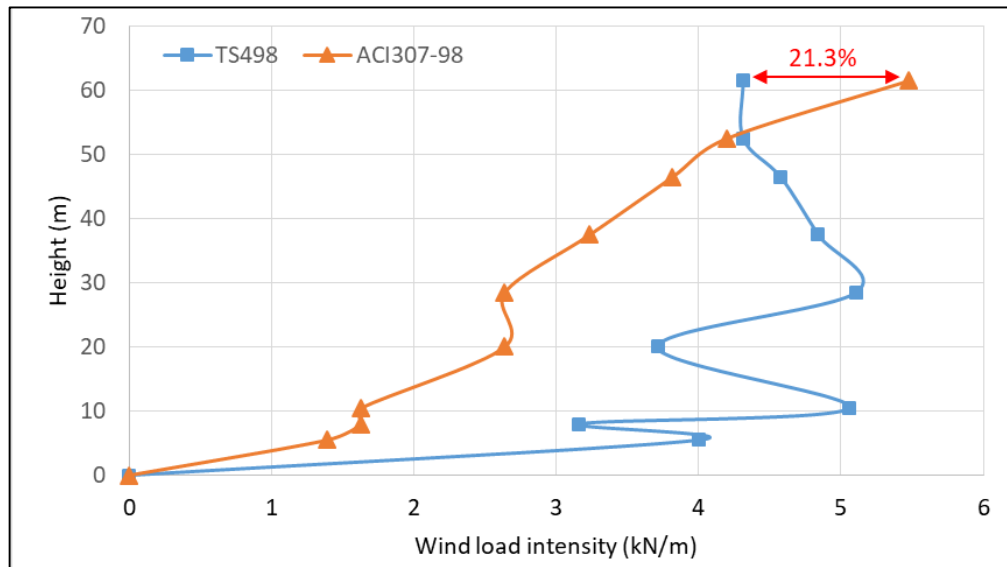


Figure 6.3: Comparison of wind load intensities for 61.45 m minaret

From the results shown in Figure 6.3, it can be seen that the wind load intensity shows an upward sloping curve with respect to ACI307-98. According to TS498, it can be noticed that there is a variable slope curve due to the wind pressure and the change of minaret outer diameter values.

The wind load intensity at 5.5 m in height according to TS498 is larger than ACI307-98 by about 65.2%. As the outer diameter decreases during the transition segment, this difference decreases to 48.5% at a height of 8.0 m. Since the wind pressure increases after 8 m, the difference increases to 67.8% at a height of 10.45 m. Between 9.0 m and 20.0 m in height, the wind pressure has a constant value causes a decrease in the difference to 29% at a height of 20 m. After that, wind pressure value increases causing increasing in the difference at a height of 28.45 m to 48.3%. At a height of 37.45 m, the wind load intensity according to TS498 is larger than ACI307-98 by about 33.2% because of the decrease in the outer diameter. Another decrease in the outer diameter at a height of 46.45 m causes decrease in the difference to 16.6%. At the top of the minaret, the wind load intensity according to ACI307-98 is greater than TS498 by about 21.3 %.

Generally, it is observed that the resultant wind load according to TS498 in 61.45 m in high minaret is larger than ACI307-98. But, it can be said that, the distribution of wind load intensity according to ACI307-98 is more appropriate.

Table 6.21: Comparison of wind load intensities for 76.2 m minaret

Height (m)	W-TS498 (kN/m)	W-ACI307-98 (kN/m)	Difference %
0.00	0.00	0.00	-
7.65	3.00	1.438	52.1%
14.35	5.50	2.324	57.8%
20.00	4.61	3.652	20.7%
30.90	6.34	3.652	42.4%
44.45	5.81	4.706	19.0%
58.00	5.28	5.707	7.5%
68.50	4.93	6.474	23.9%
76.20	4.93	7.831	37.1%

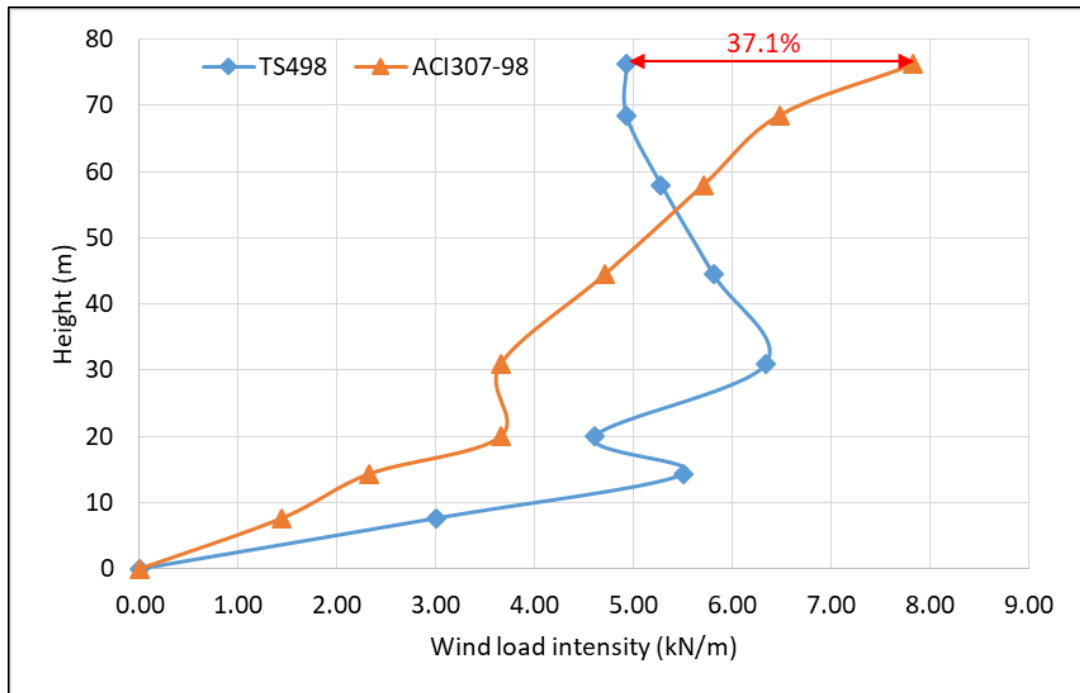


Figure 6.4: Comparison of wind load intensities for 76.2 m minaret

From the results shown in Figure 6.4, it can be seen that the wind load intensity shows an upward sloping curve with respect to ACI307-98. While, TS498, has a variable slope curve depending on the C_p coefficient, the wind pressure and the change in outside diameter values.

The wind load intensity according to TS498 at 7.65 m height is greater than ACI307-98 by about 52.1%. Since the C_p coefficient increases after the base, this difference increases to 57.8% at a height of 14.35 m. The wind load intensity according to TS498 is higher than ACI307-98 by about 20.7% at a height of 20.0 m because of the constant wind pressure value between 9.0 m and 20.0 m in height. After that, wind pressure value increase causes an increase in the difference at a height of 30.9 m to 42.4%. At a height of 44.45 m, the outer diameter decreases caused decrease in the difference to 19.0%. Another decrease in the outer diameter at a height of 58.0 m causes decrease in the difference to 7.5%. At a height of 68.5 m, the wind load intensity according to ACI307-98 is larger than TS498 by about 23.9%. While, at the top of the minaret, this difference increases to 37.1%.

Generally, it is observed that the resultant wind load according to TS498 in 76.2 m minaret is larger than ACI307-98. But, it can be said that, the distribution of wind load intensity according to ACI307-98 is more appropriate.

6.3 Earthquake Load Calculation

As stated before, earthquake load in this study is determined according to two codes, NCSC2015 and ACI307-98, as presents in the following.

6.3.1 Earthquake load calculation according to NCSC2015

Response spectrum method is used to evaluate the earthquake response of the modelled minarets. In this study, the seismic zone is determined as zone 2 and the soil class is assumed as Z3. The values, $R_a(T)$, the seismic load reduction factor, A_0 , the effective ground acceleration coefficient and I , the importance factor are evaluated as 3, 0.3 and 1.2, respectively. The earthquake load is evaluated by using SAP2000, v19.0 package program and response spectrum function definition is shown in Figure 6.5, while response spectrum curve is shown in Figure 6.6.

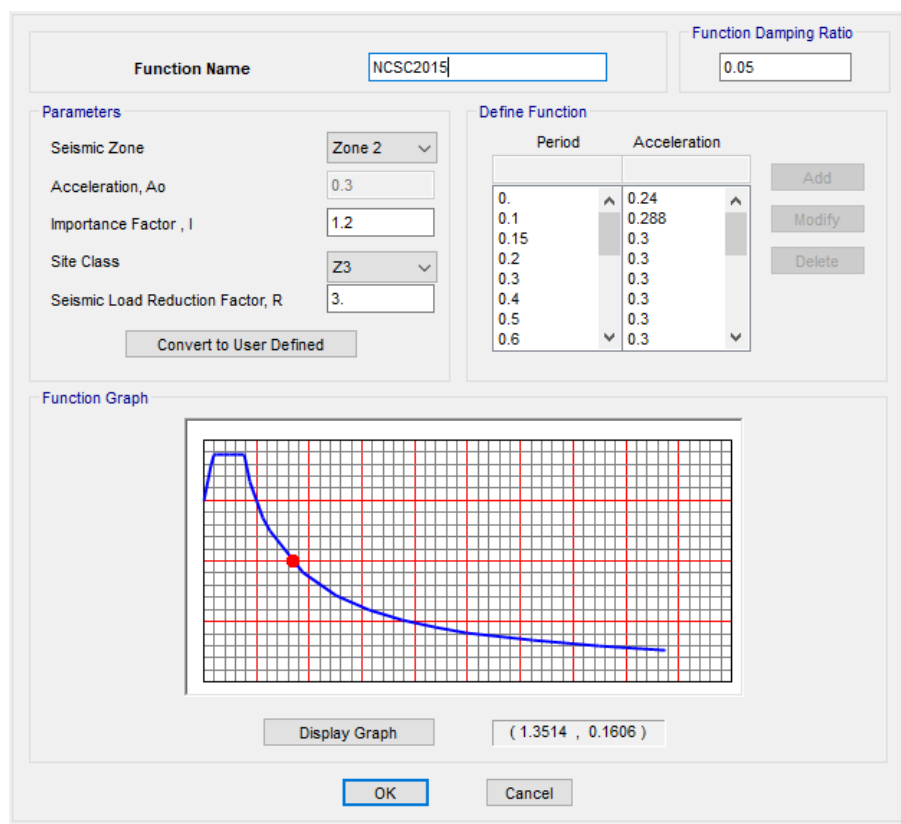


Figure 6.5: Response spectrum function definition on SAP2000 according to NCSC2015

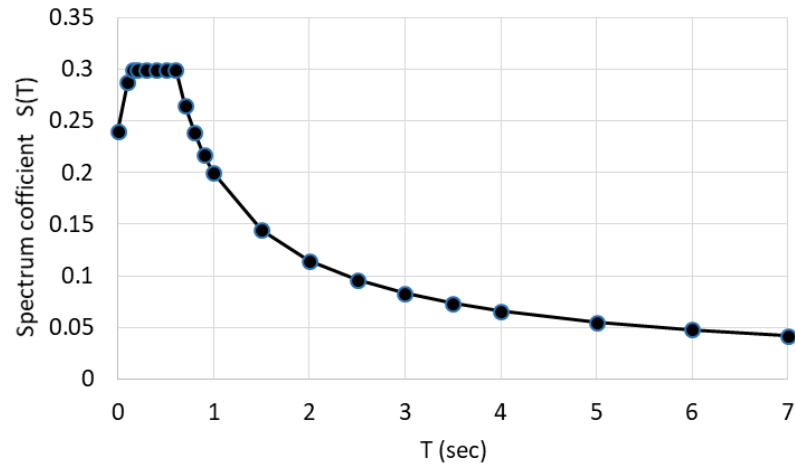


Figure 6.6: Response spectrum curve according to NCSC2015

6.3.2 Earthquake load calculations according to ACI307-98

Design response spectrum according to ACI307-98 depends on the parameters S_S and S_1 and the soil class. In the case of this study S_S , S_1 and soil class are accepted as 0.681, 0.231 and class D, respectively. The earthquake load evaluated by using SAP2000, v19.0 package program and response spectrum function definition is shown in Figure 6.7, while response spectrum curve is shown in Figure 6.8.

Function Name: Function Damping Ratio:

Parameters

☐ Ss and S1 from USGS - by Lat./Long.
☐ Ss and S1 from USGS - by Zip Code
☒ Ss and S1 User Specified

Site Latitude (degrees):
 Site Longitude (degrees):
 Site Zip Code (5-Digits):
 0.2 Sec Spectral Accel, Ss:
 1 Sec Spectral Accel, S1:
 Long-Period Transition Period:
 Site Class:
 Site Coefficient, Fa:
 Site Coefficient, Fv:
 Calculated Values for Response Spectrum Curve
 SDS = (2/3) * Fa * Ss:
 SD1 = (2/3) * Fv * S1:

Define Function

Period	Acceleration
0.	0.2279
0.1047	0.5699
0.5237	0.5699
0.8	0.3731
1.	0.2985
1.2	0.2487
1.4	0.2132
1.6	0.1865

Function Graph

Figure 6.7: Response spectrum function definition on SAP2000 according to ACI307-98

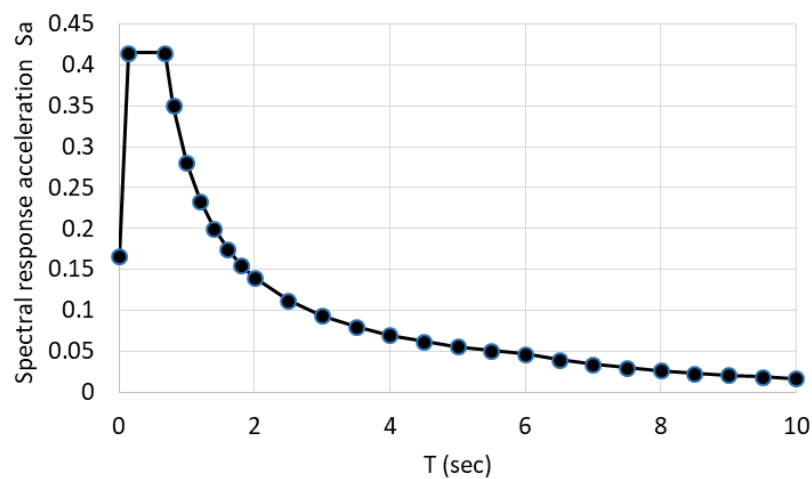


Figure 6.8: Response spectrum curve according to ACI307-98

6.4 Applying Wind and Earthquake Loads on the Modelled Minarets

Wind loads that are found from both TS498 and ACI307-98 are applied to the minaret models as statically equivalent uniformly distributed load (kN/m) in X-direction, where there are door openings, as shown in Figures 6.9 and 6.10, while earthquake load is applied directly by the program also in X-direction.

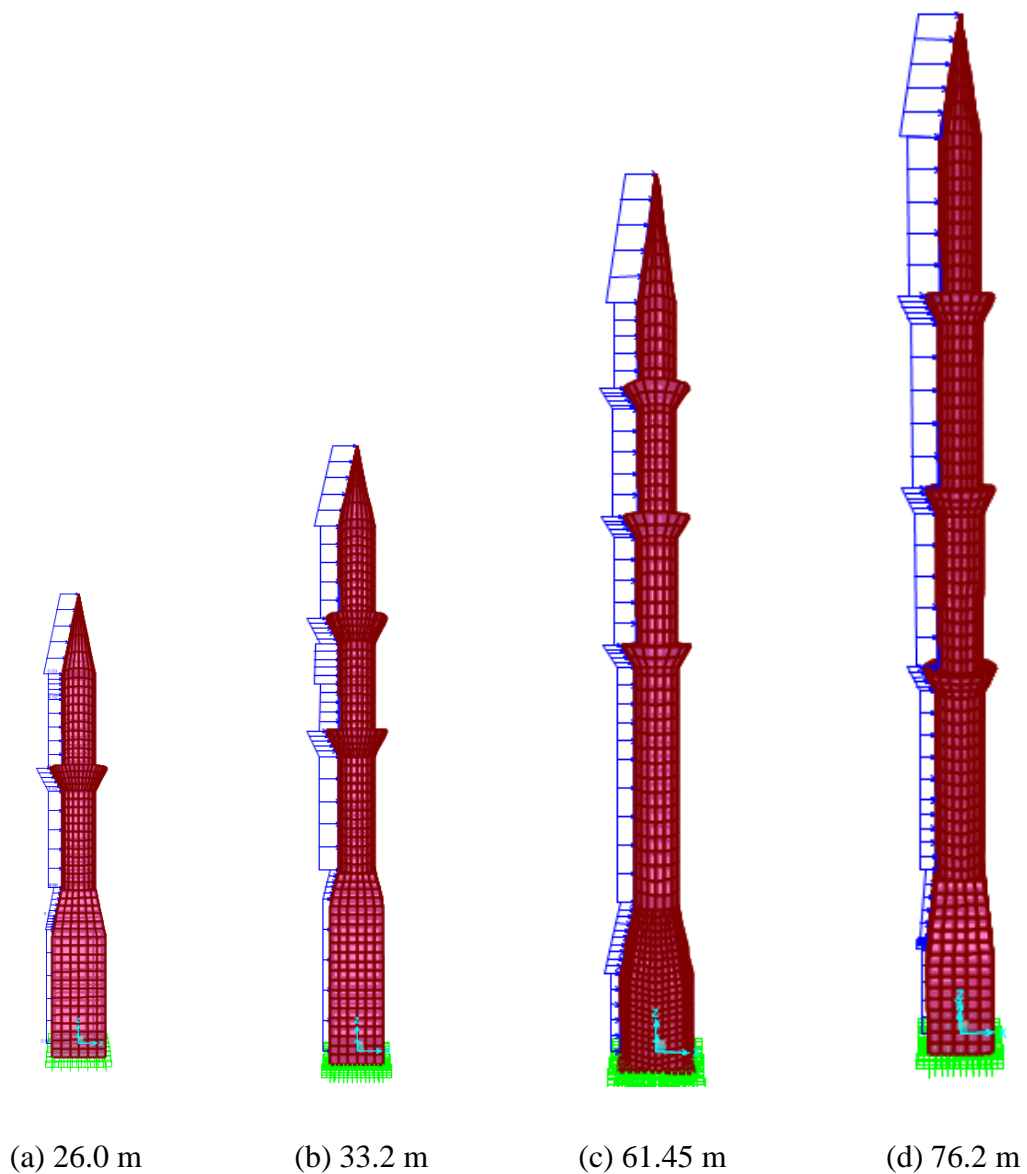
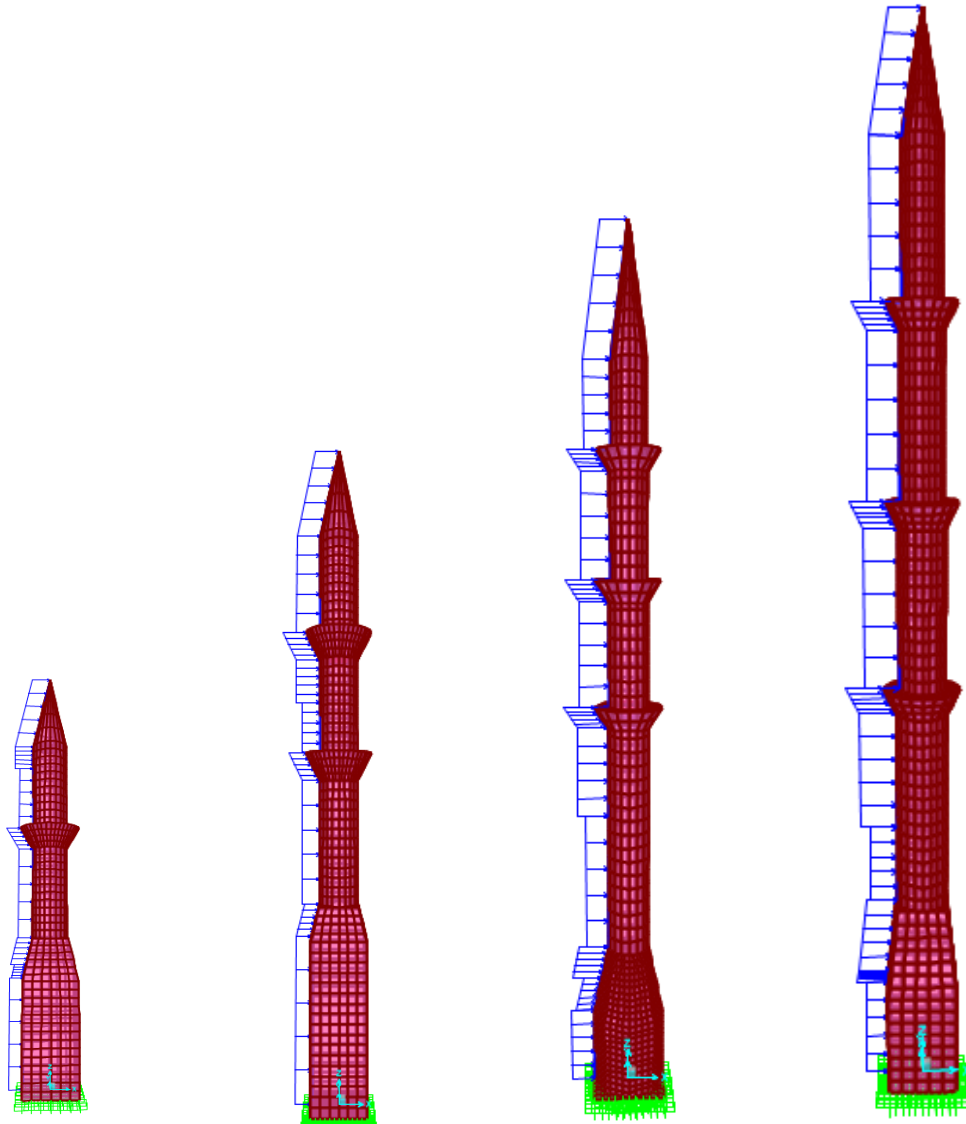


Figure 6.9 : Applying wind loads according to ACI307-98 on the modelled minarets



(a) 26.0 m

(b) 33.2 m

(c) 61.45 m

(d) 76.2 m

Figure 6.10: Applying wind loads according to TS498 on the modelled minarets

6.5 Analysis Results

The analysis results obtained from both wind and earthquake analysis are presented in the form of top displacements, base reactions and stress distribution. The deformed shapes of the modelled minarets after applying the loads can be seen below.

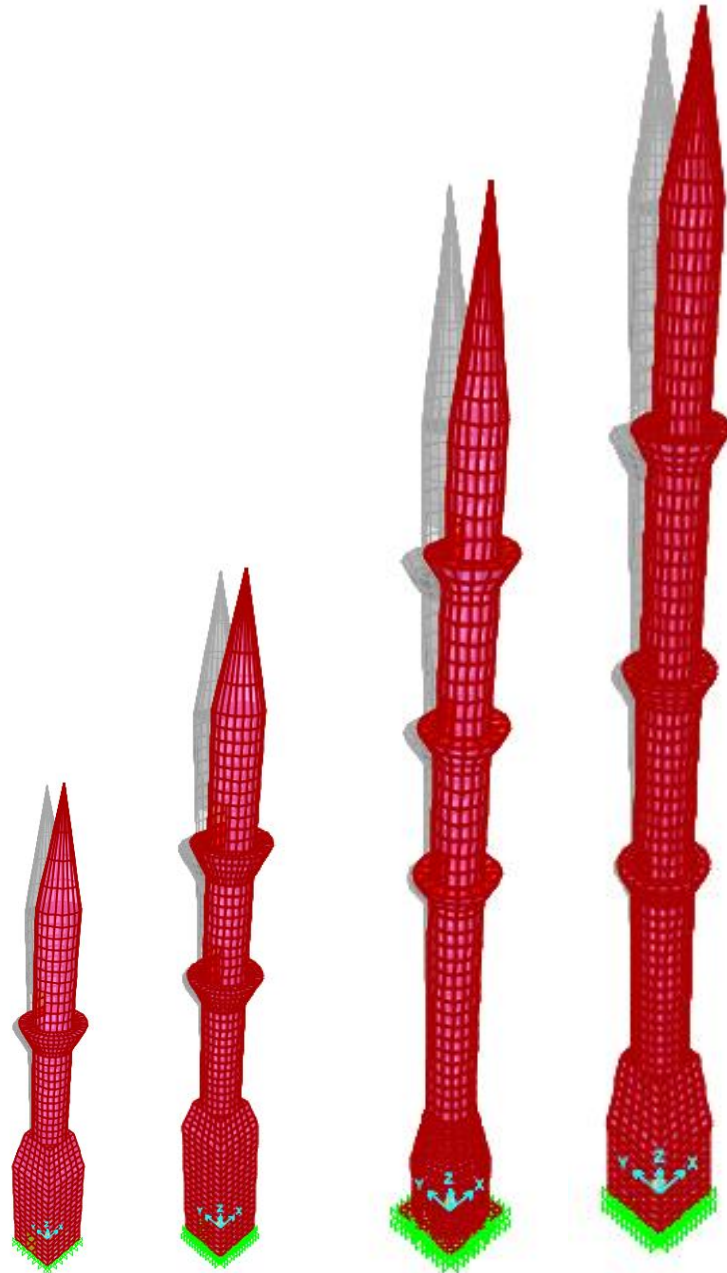


Figure 6.11: Deformed shapes of the modelled minarets after applying the loads

6.5.1 Top displacements

The displacements over the height of the modelled minarets in X-direction due to the wind and earthquake loads that cited before, are presented in Figures 6.11 – 6.14.

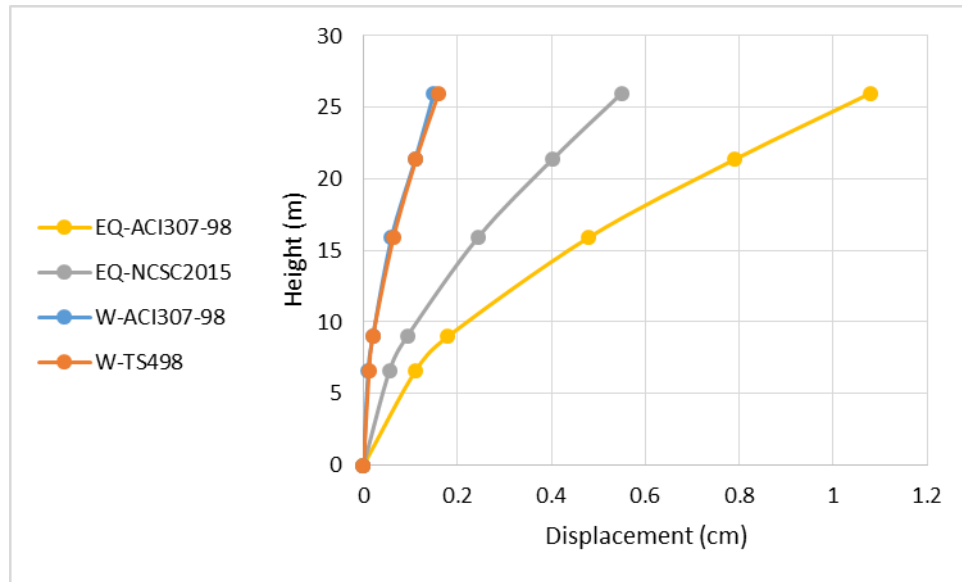


Figure 6.11: Displacements over the height of 26.0 m Minaret

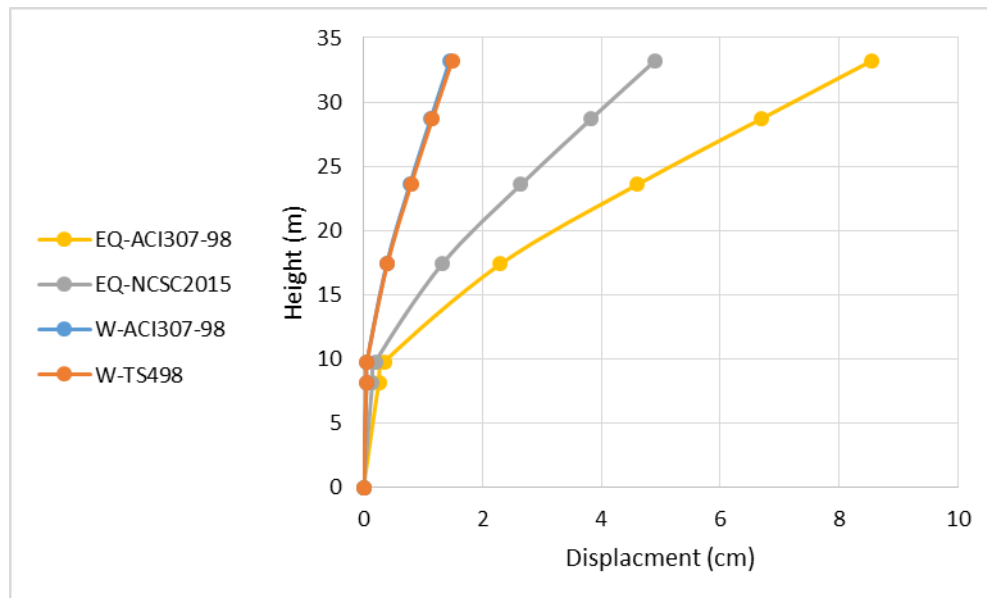


Figure 6.12: Displacements over the height of 33.2 m Minaret

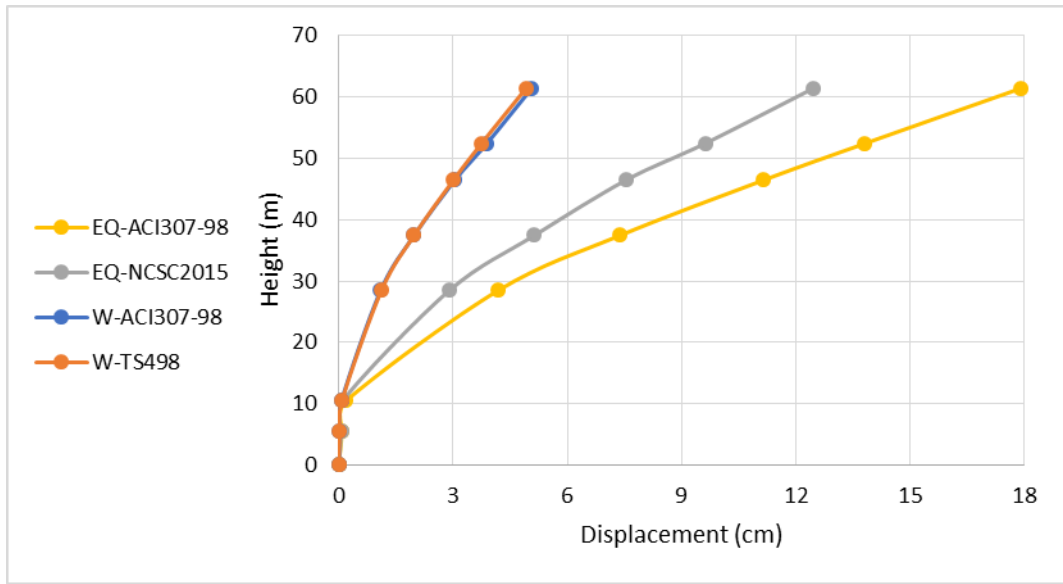


Figure 6.13: Displacements over the height of 61.45 m Minaret

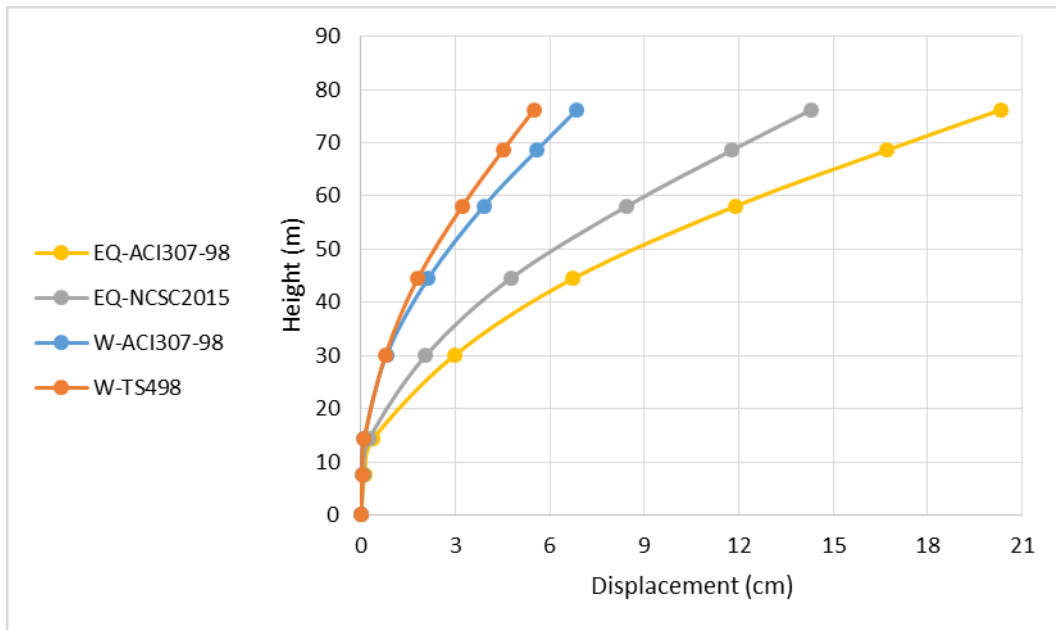


Figure 6.14: Displacements over the height of 76.2 m Minaret

The displacements at the top of the minarets in X-direction due to the wind and earthquake loads, are presented in Table 6.22 and Figure 6.15.

Table 6.22: Top displacements due to wind and earthquake loads.

Height of minaret (m)	Top displacement (cm)			
	W-TS498	W-ACI307-98	EQ-NCSC2015	EQ-ACI307-98*
26.0	0.16	0.15	0.55	1.08
33.2	1.49	1.45	4.9	8.54
61.45	4.92	5.07	12.5	17.9
76.2	5.49	6.86	14.3	20.32

* W-TS498: Wind load according to TS498, W-ACI307-98: Wind load according to ACI307-98, EQ-NCSC2015: Earthquake load according to NCSC2015, EQ-ACI307-98: Earthquake load according to ACI307-98.

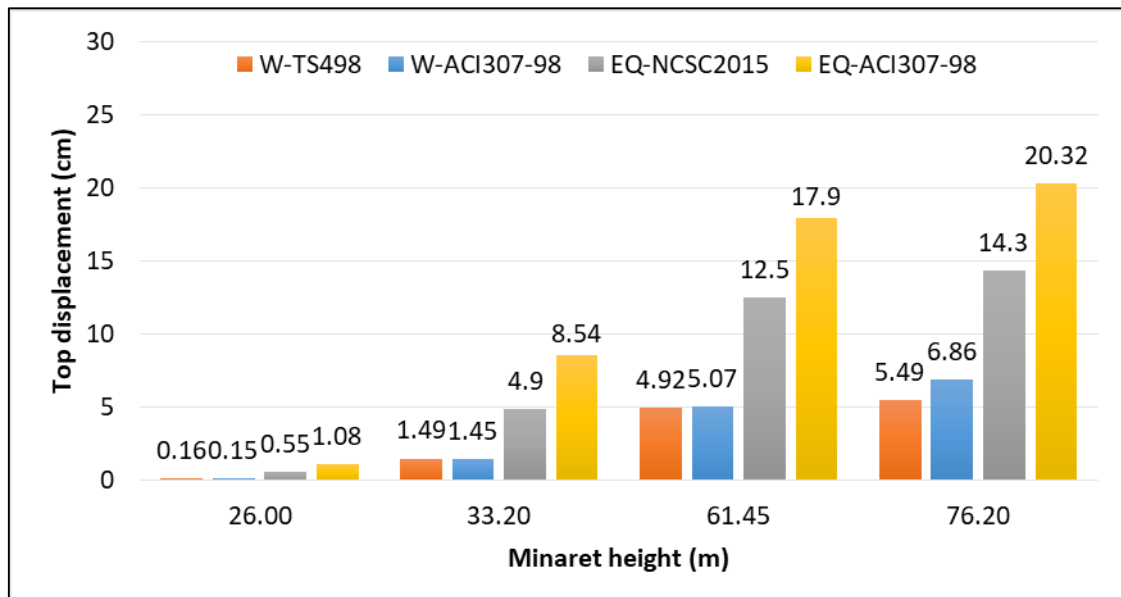


Figure 6.15: Top displacements due to wind and earthquake load

From the displacement results, it can be said that, the displacements due to the wind load according to TS498 are more than ACI307-98 in 26.0 m and 33.2 m minarets. The displacements due to wind load according to ACI307-98 are more than TS498 in 61.45 m and 76.2 m minarets. This is mainly because the displacement does not depend only on the

wind load resultant, but also it affects by the distribution of the load, thus, the resultant force position.

The displacements due to earthquake load are more than those due to wind load in all of the studied minarets. Furthermore, the displacements due to earthquake load according to ACI307-98 are larger than NCSC2015 in all of the studied minarets.

In evaluating the deflection, ACI307-98 states that the maximum lateral deflection of the top of a minaret under all service conditions prior to the application of load factors shall not exceed the limits set forth by Equation 6.1.

$$Y_{max} = 3.33 \times h \quad (6.1)$$

where, Y_{max} is the maximum top displacement limit (mm) and h is the minaret height (m).

Maximum top displacement limit for the modelled minarets according to ACI307-98 are presented in Table 6.23.

Table 6.23: Maximum top displacement limit for the modelled minarets.

Height of minaret (m)	Max. top displacement limit (cm)
26.0	8.06
33.2	11.06
61.45	20.46
76.2	25.37

6.5.2 Base reactions

Maximum shear forces and bending moments that occurred at the base of modelled minarets due to different load cases are presented in Table 6.24.

Table 6.24: Shear force and bending moment values due to wind and earthquake loads.

Height of minaret (m)	W-TS498		W-ACI307-98		EQ-NCSC2015		EQ-ACI307-98	
	V (kN)	M (kN.m)	V (kN)	M (kN.m)	V (kN)	M (kN.m)	V (kN)	M (kN.m)*
26.0	65.27	951.5	57.7	886.1	228.7	3509.4	441.9	6909.8
33.2	87.06	1659.6	83.6	1622.9	257.8	5288.1	461.6	9274.1
61.45	274.8	8615.43	230.5	8169.8	590.9	19584.9	895.8	28944.5
76.2	406.8	15574.2	360.8	16810.4	1154.1	41779.1	1950.9	62916.6

* W-TS498: Wind load according to TS498, W-ACI307-98: Wind load according to ACI307-98, EQ-NCSC2015: Earthquake load according to NCSC2015, EQ-ACI307-98: Earthquake load according to ACI307-98, V: Base shear force, M: Base bending moment.

The base reaction results show that, shear force values due to wind load according to TS498 are more than ACI307-98 in all of the studied minarets. This is mainly because, wind load resultant values according to TS498 are larger than ACI307-98. The bending moment values due to wind load according to TS498 are larger than ACI307-98 in 26.0 m, 33.2 m and 61.45 m minarets. While, that inverses in 76.2 m minaret. This is mainly because bending moment affects by the distribution of wind load, thus the resultant position. The resultant wind load according to ACI307-98 is in a position higher than TS498. Therefore, the moment arm is larger, and the bending moment value due to wind load according ACI307-98 is larger than TS498. On the other hand, shear force and bending moment values due to earthquake load are larger than those due to wind load in all of the studied minarets. Furthermore, shear force and bending moment values due to earthquake load according to ACI307-98 are larger than NCSC2015 in all of the studied minarets.

6.5.3 Stress contours analysis

It can be clearly seen that the maximum top displacement and maximum base reactions occurred due to earthquake load according to ACI307-98. Therefore this load case is selected to show the stress distribution over the length of the highest minaret. Figures 6.12 & 6.13 show respectively the normal and shear stress distributions over the length of the 76.2 m minaret under the earthquake load according to ACI307-98.

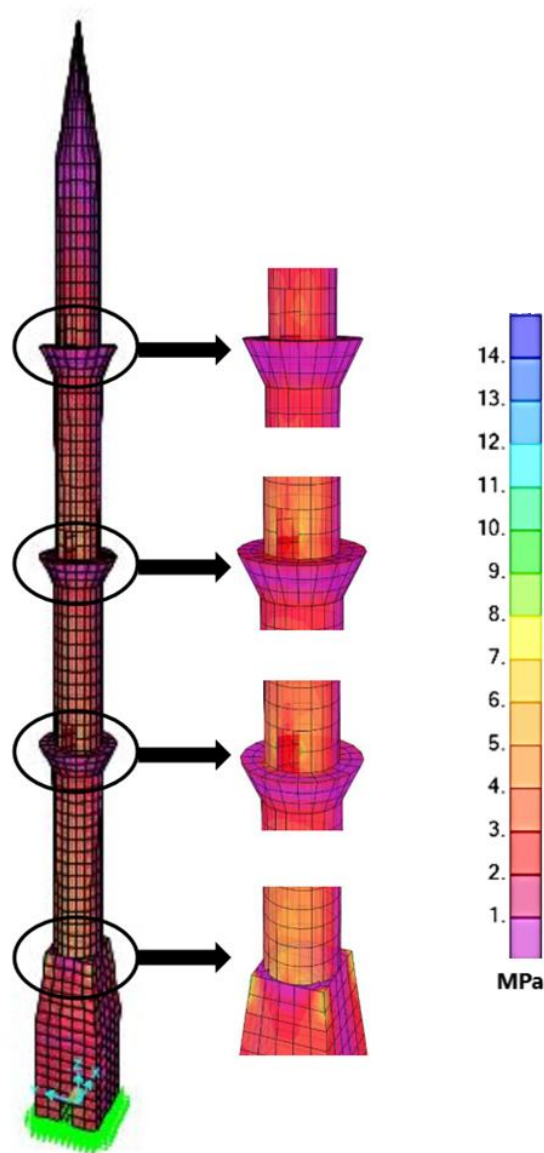


Figure 6.12: Normal stress distribution of 76.2 m minaret

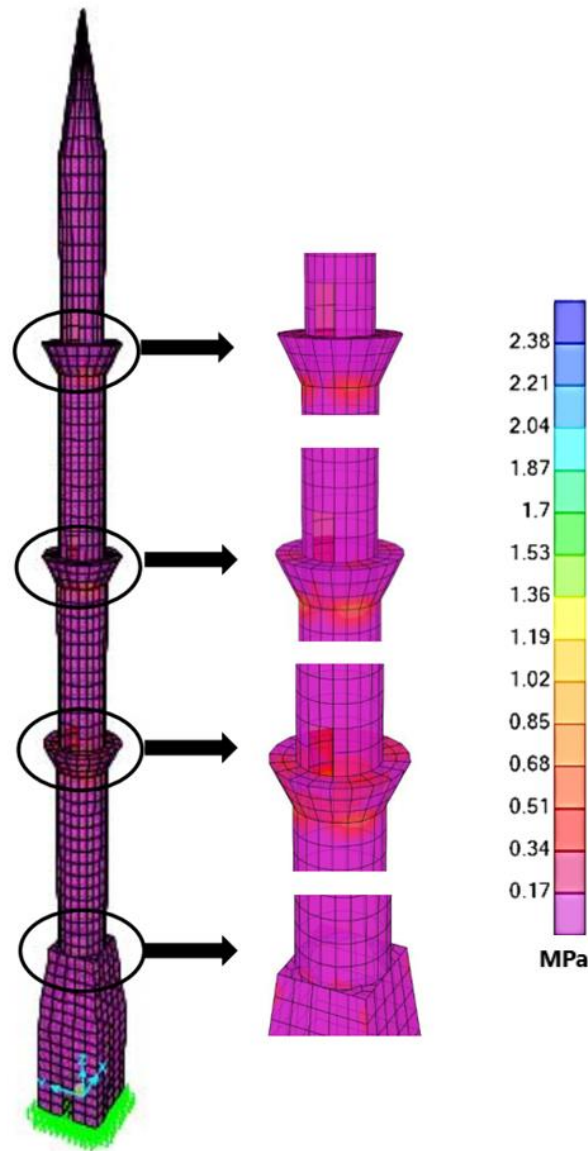


Figure 6.13: Shear stress distribution of 76.2 m minaret

It can be seen from the stress distribution contours that there are high stress values in two positions; at the top of transition segment where there is a change in the cross-sectional size and at the balconies where the door openings and extra mass are found.

The maximum stress value that occurred at the top of transition segment is about 9.8 MPa. While, the design strength of concrete used in this study is 17 MPa. It can be noticed that the maximum stress is less than concrete design strength.

CHAPTER 7

CONCLUSIONS

The main purpose of this study is to analyse several RC minarets existing in North Cyprus under wind and earthquake loads according to different codes to compare the results and determine the major lateral load in minarets design. In the light of this study, the derived evaluations and suggestions are presented as follows:

- The distribution of wind load intensity according to ACI307-98 is more appropriate, since, it shows an upward sloping curve. While, TS498 has a variable slope curve depending on the C_p coefficient, the wind pressure and the change in outside diameter values. TS498 code does not consider the gust buffeting and across wind effects, which can be effective in high rise structures. Also TS498 regulations consider a constant value for wind velocities in determination of wind load values without considering the regional effect. All these points should be evaluated and added to TS498 code.
- Low, medium and high rise minarets are accepted as slender in accordance to the general definition of slenderness (a slender structure is a structure which has a height larger 4 times than its width, $h/d > 4$), while only high rise minarets are accepted as slender in accordance to the structures dynamic properties (a slender structure is a structure which has a first mode frequency not more than one). The dynamic definition of slenderness should be evaluated and added to TS498 code.
- The displacement results show that the top displacements due to varied load cases that are studied in this thesis in low and medium rise minarets have the following order from the maximum to the minimum: EQ-ACI307-98, EQ-NCSC2015, WTS498 and then W-ACI307-98, while in high rise minarets the top displacements have the following order: EQ-ACI307-98, EQ-NCSC2015, W-ACI307-98 and then W-TS498. The maximum top displacements in all minaret heights occur in the load case EQ-ACI307-98. However, the maximum top displacements satisfy ACI307-98 top displacement limitation criteria.

- The base shear force values due to wind load according to TS498 are larger than ACI307-98. This is mainly because, wind load resultant values according to TS498 are larger than ACI307-98. The bending moment values due to wind load according to TS498 are larger than ACI307-98 in 26.0 m, 33.2 m and 61.45 m minarets. The large wind load intensity according to ACI307-98 at the higher parts of 76.2 m minarets, causes bending moment value in case of ACI307-98 larger than TS498. On the other hand, shear force and bending moment values due to earthquake load are larger than those due to wind load. Furthermore, the maximum base reactions occur due to earthquake load according to ACI307-98.
- The analyses results showed that statically wind load is undervaluing the deflections and the base reactions. Therefore, in designing RC minarets statically wind load should be averted. Moreover, seismic elastic response spectrum function according to NCSC2015 should be evaluated because it gives lower values compared with ACI307-98. Moreover, in this study, statically equivalent wind loads according to TS498 and ACI307-98 and dynamic elastic response spectrum function according to NCSC2015 are not forming the major lateral load in designing RC minarets. But rather, dynamic elastic response spectrum method according to ACI307-98 is forming the major lateral load in designing RC minarets.
- It is apparent from the stress distribution contours that high stress values are noticed in two positions; at the top of transition segment where there is a change in the cross-sectional size and at the balconies where the door openings and extra mass are found. An additional concern should be given to these crucial points in order to preserve flexibility of the structure.

Finally, RC minarets which have increased recently in North Cyprus have unique characteristics and should be provided by a sufficient flexibility to prevent damage or collapse these structures under lateral loads. This study concerns four RC minarets with different heights and the results obtained cover a wide range of minaret heights in North Cyprus. Cyprus contains a number of historical masonry minarets. Since this study concern RC minarets, it is recommended to study the lateral load effects on masonry minarets as well.

REFERENCES

- ACI 307-98 (1998). *Design and construction of RC chimneys*, American Concrete Institute; Farmington Hills, MI, USA.
- Ali Mir M. & Kheir Al-Kodmany, (2012). Tall buildings and urban habitat of the 21st century: a global perspective. *Buildings*, 2(4), 384-423.
- Alshehabi, K. (1993) *Damascene Minarets; History & Style. Publications of the Ministry of Culture in the Syrian Arab Republic*, Damascus, Syria.
- Ambraseys, N. (2009). *Earthquakes in the Mediterranean and Middle East: a multidisciplinary study of seismicity up to 1900*. Cambridge University Press.
- ASCE 7-95, (1996), *Minimum design loads for buildings and other structures*, American Society of Civil Engineers, New York, USA.
- ASCE 7, (2016). *Minimum design loads for buildings and other structures*. American Society of Civil Engineers. New York, USA.
- Chamber of Civil Engineers. (2015). *KKTC Deprem Bölgelerinde Yapılacak Binalar Hakkında Yönetmelik*. Lefkoşa: İnşaat Mühendisleri Odası Chamber of Civil Engineers.
- Chandak, N. R. (2013). Effect of base isolation on the response of reinforced concrete building. *Journal of Civil Engineering Research*, 3(4), 135-142.
- Chenga, C-M., & Kareem, A. (1992). Across wind Response of Reinforced Concrete Chimneys. *Journal of Wind Engineering and Industrial Aerodynamics*, 43(1-3), 2141-2152.
- Constantinescu, D., & Köber, D. (2013). The minaret of the great mosque in Algiers, a structural challenge. *Open Journal of Civil Engineering*, 03(2), 27-39.
- Council, B. S. S. (2015). *Investigation of an identified short-coming in the seismic design procedures of ASCE 7-10 and development of recommended improvements for ASCE*

7-16.

CSI. (2014). *Modal analysis - Technical Knowledge Base - Computers and Structures, Inc.*
- *Technical Knowledge Base*.

Cyprus geological heritage educational tool. (2004). Historical records and instrumental recordings of earthquakes for Cyprus from
http://www.cyprusgeology.org/english/5_3_seismicity.htm

Doğangün, A., Tuluk, Ö., İ., Livaoğlu R., & Acar, R. (2006). Traditional Turkish minarets on the basis of architectural and engineering concepts, In *1st International Conference on Restoration of Heritage Masonry Structures*, Cairo, Egypt, April.

Department of Meteorology. (2006). Republic of Cyprus, Ministry of Agriculture, Rural Development and Environment, Department of Meteorology. Annual reports from
http://www.moa.gov.cy/moa/ms/ms.nsf/DMLcyclimate_en/DMLcyclimate_en?OpenDocument

EMDAT. (2009), International Disaster Database, Centre for Research on the Epidemiology of Disasters – CRED, Belgium. <http://www.emdat.be/>

GSD. (2004). Geological Survey Department- Seismic Zoning Map of Cyprus. Retrieved from
<http://www.moa.gov.cy/moa/gsd/gsd.nsf/All/90B0EFABDA274E8FC22579B200406F6E?OpenDocument>

GSD. (2010). Earthquakes - Historic Earthquakes. Retrieved from
[http://www.moa.gov.cy/moa/gsd/gsd.nsf/All/3CBA830B3B598132C225787000374313/\\$file/cyprus-seismicity-upto2010-engl.jpg?OpenElement](http://www.moa.gov.cy/moa/gsd/gsd.nsf/All/3CBA830B3B598132C225787000374313/$file/cyprus-seismicity-upto2010-engl.jpg?OpenElement)

GSD. (2015). Geological Survey Department - Historic Earthquakes. Retrieved from
http://www.moa.gov.cy/moa/gsd/gsd.nsf/dmlHistEarthquakes_en/dmlHistEarthquakes_en?OpenDocument

- Gupta, A. K. (1990). *Response spectrum method in seismic analysis and design of structures*. Blackwell scientific publications Inc., Cambridge, England.
- Hacıfendioğlu Kemal, Emre Alpaslan, Gökhan Demir, Burcu Dinç & Fahri Birinci, (2018). Experimental modal investigation of scaled minaret embedded in different soil types. *GRADEVINAR*, 70(3), 201-212.
- Higazy, E. M., (2004). Vulnerability of historical minarets; investigation of their seismic assessment & retrofitting. *Emirates Journal for Engineering Research*, 9(2), 59-64.
- Isgor, O. B. (1997). Analysis and Design of Reinforced Concrete Shell Elements. M.Sc. Thesis. Carleton University, Ottawa, Ontario, Canada.
- Karaca, Z., & Türkeli, E. (2012). Determination and comparison of wind loads for industrial reinforced concrete chimneys. *Struct. Design Tall Spec. Build.*, 21(2), 133-154.
- Karaca, Z., & Türkeli, E. (2014). The slenderness effect on wind response of industrial reinforced concrete chimneys. *Wind and Structures*, 18(3), 281-294.
- Langhe Kaluram & Vijaykumar R. Rathi, (2016). Analysis of self supported reinforced concrete chimney with geometry variation. *International Research Journal of Engineering and Technology (IRJET)*, 03(07), 1298-1304.
- Livaoğlu, R., Baştürk, M. H., Doğançün, A., & Serhatoğlu, C. (2016). Effect of geometric properties on dynamic behavior of historic masonry minaret. *KSCE Journal of Civil Engineering*, 20(6), 2392-2402.
- McCormac, J. C. (2005). *Design of reinforced concrete. ACI 318-05 Code Edition/Jack C. McCormac, James K. Nelson.*— USA.
- Rashmi M P & D. S. Sandeep Kumar, (2017) Seismic performance study on RC chimney. *International Research Journal of Engineering and Technology (IRJET)*, 04(06), 2920-2925.
- Reddy, B. S. K., Padmavathi, V. R., & Srikanth, Ch. (2012), Study of wind load effects on tall RC chimneys. *International Journal of Advanced Engineering Technology*, 03(02),

0976-3945.

- Reddy, K. R. C., Jaiswal, O. R., & Godbole, P. N. (2011). Wind and earthquake analysis of tall RC chimneys. *International Journal of Earth Sciences and Engineering ISSN*, 04(06), 508-511.
- Sadeghi, K. (2001). *Coasts ports and offshore structures engineering*, Power and Water University of Technology.
- Sarno, L. D., Yenidogan C., & Erdik, M. (2013). Field evidence and numerical investigation of the Mw = 7.1 October 23 Van, Tabanlı and the Mw > 5.7 November earthquakes of 2011, *Bull Earthquake Eng.*, 11(1), 313-346.
- Sezen, H., Acar, R., Doğangün, A., & Livaoğlu, R. (2008). Dynamic analysis and seismic performance of RC minarets. *Eng. Struct.*, 30(8), 2253-2264.
- Abdullahi, S. (2014), Structural behaviour of reinforced concrete minaret under wind effect using sap2000 v.15, M.Sc. Thesis, Near East University, Nicosia, North Cyprus.
- Sioutas, M., Doe, R., Michaelides, S., Christodoulou, M., & Robins, R. (2006). Meteorological conditions contributing to the development of severe tornadoes in southern Cyprus. *Weather*, 61(1), 10-16.
- Taranath, B. S. (2004). *Wind and earthquake resistant buildings; structural analysis and design*. John A. Martin & Associates, Inc. Los Angeles, California, USA.
- Touqan, A. R., & Salawdeh, S. (2013). Major Steps Needed Towards Earthquake Resistant Design. *The 6 Th Jordanian International Civil Engineering Conference (JICEC06)*, 1, 1–24.
- Türkeli, E., (2014) Determination and comparison of wind and earthquake responses of reinforced concrete minarets. *Arab J Sci. Eng.*, 39(5), 3665-3680.
- Turkish Earthquake Code. (2007). *Specification for structures to be built in disaster areas*. Ministry of Public Works and Settlement Government of Republic of Turkey. Ankara, Turkey.

Turkish standard, TS498. (1997). *The calculation values of loads used in designing structural elements*, Turkish Standard Institute. Ankara, Turkey.


Ural A., & Firat, F. K., (2014). Evaluation of masonry minarets collapsed by a strong wind under uncertainty. *Natural Hazards*, 76(2), 999-1018.

Zachariadis T., (2012). Climate change in Cyprus: impacts and adaptation policies. *Cyprus Economic Policy Review*, 6(1), 21-37.

APPENDICES

APPENDIX 1

MINISTRY OF LABOUR AND SOCIAL SECURITY BUILDING, SOIL INVESTIGATION REPORT



KKTC
Çevre ve Doğal Kaynaklar Bakanlığı
Jeoloji ve Maden Dairesi

**ÇALIŞMA VE SOSYAL GÜVENLİK
BAKANLIĞI BİNASI
ZEMİN ETÜD RAPORU**

Hazırlayan
Hatice KAŞER
Jeoloji Yüksek Mühendisi

KASIM, 2007
Lefkoşa

Temel Zeminine Ait Mekanik Parametreler:

1. İnceleme alanı **2. Derece** deprem bölgesindedir.
2. Temel zemin grubu (C)
3. Yerel zemin sınıfı (Z_2)
4. Zeminin spektrum karakteristik periyotları $T_A=0.15sn$,
 $T_B=0.40sn$
5. Kayma dalgası hızı **200-400 m/s** alınabilir.
6. Deprem hesaplarında kullanılacak etkin yer ivmesi katsayısı $A_0 = 0.30$ 'dur.
7. Yatak Katsayısı $K_0=2000 \text{ ton/m}^3$
8. Bina önem katsayısı $I=1.4$


Hatice Kaşer

Jeoloji Yüksek Mühendisi

APPENDIX 2

CYPRUS RELIGIOUS FOUNDATIONS ADMINISTRATION (KIBRIS VAKIFLAR İDARESİ), LIST OF NORTH CYPRUS MOSQUES

KKTC GENELİNDE CAMİ ARAZİ DAĞILIM ENVANTERİ LİSTESİ

Sıra No	Açıklama	Dönemi	Adet
1-	Osmanlı Döneminde Yapılan Camiler	Osmanlı	133
2-	KKTC Döneminde Yapılan Camiler	Yeni	70
3-	Kilise olup Cami Olarak Kullanılanlar	Kilise	33
4-	Kilise Olarak Kullanılanlar	Kilise	2
5-	Askeri Bölge	-	11
6-	Camisi Olmayan Köyler	-	9
		TOPLAM	258

Figure 2.1 Number of all mosques in North Cyprus until 2016

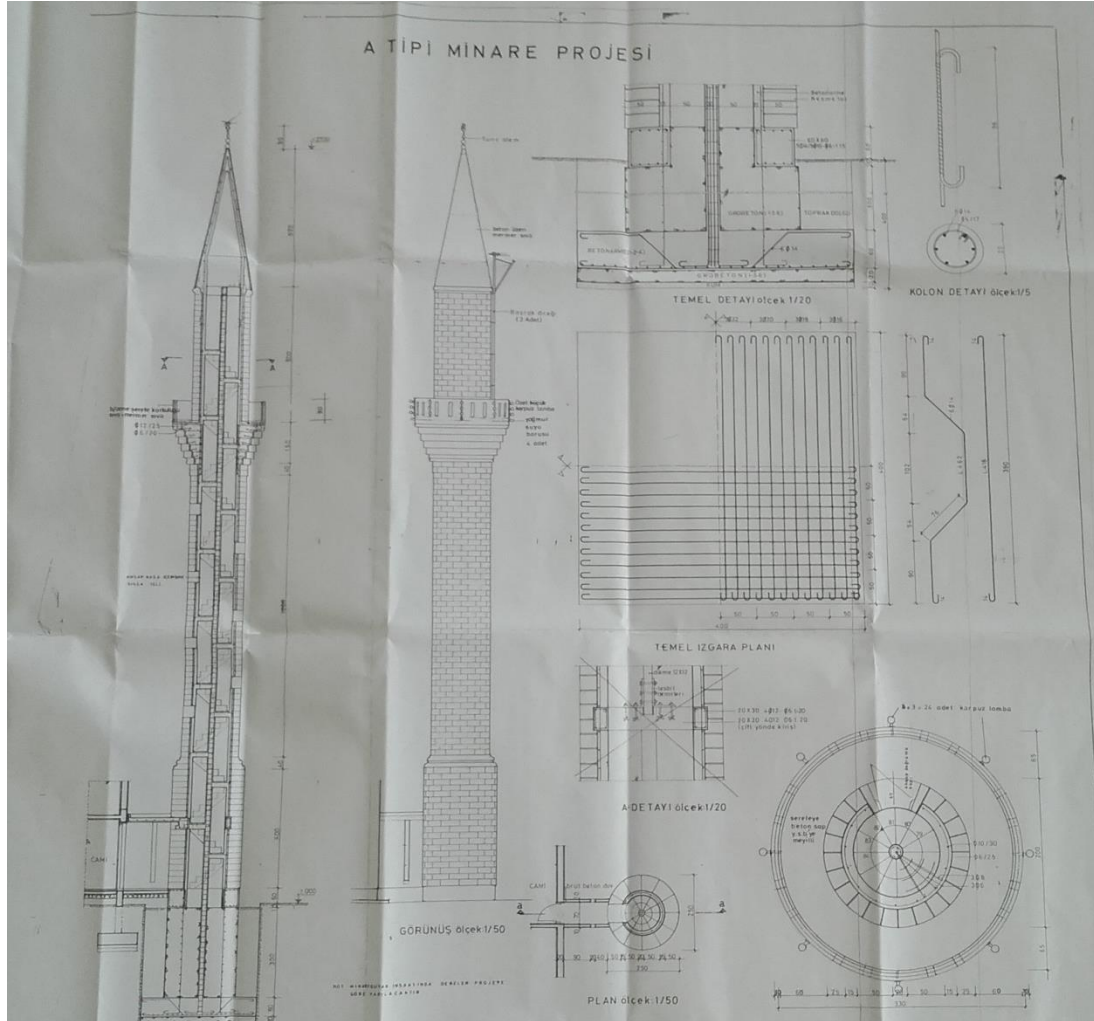
Vakıflar İdaresinin TC Yardım Heyeti Finansmanı İle Yaptırdığı Yeni Camiler Ve İhale Yılları

Sayı	Caminin Adı	Minare sayısı	Yılı		Sayı	Caminin Adı	Minare sayısı	Yılı
1	Boltaşlı Camisi	1	1991		34	Pamuklu Camisi	1	2010
2	Yarköy Camisi	1	1991		35	Düzova Camisi	1	2010
3	Dıpkarpaz Camisi	2	1991		36	Mormenekşe Camisi	2	2010
4	Yedidalga Camisi	1	1993		37	Kayalar Camisi	1	2010
5	Değirmenlik Camisi	1	1995		38	Sadrazamköy Camisi	1	2012
6	Yeni iskele Camisi	2	1997		39	Doğanköy Camisi	2	2012
7	Türkmenköy Camisi	1	1998		40	Karaoğlanoğlu Camisi	2	2012
8	Nurettin Ersin Camisi	2	1998		41	Aygün Camisi	1	2013
9	Çayönü Camisi	1	1998		42	Korkuteli Camisi	1	2013
10	Dörtöyl Camisi	2	2001		43	Güvercinlik Camisi	1	2013
11	Ziyamet Camisi	1	2000		44	Yıldırım Camisi	1	2013
12	Kumyalı Camisi	1	2000		45	Mersinlik Camisi	1	2013
13	Bafra Camisi	1	2000		46	Kalecik Camisi	1	2013
14	Derince Camisi	1	2001		47	Şahinler Camisi	1	2013
15	Gelincik Camisi	1	2001		48	Dikmen Camisi	2	2013
16	Sipahi Camisi	1	2001		49	Yeni Boğaziçi Camisi	2	2013
17	O. Fazıl Camisi	2	2005		50	Serhatköy Camisi	1	2013
18	Yedikonuk Camisi	1	2006		51	Turnalar Camisi	2	2015
19	Geçitkale Camisi	1	2006		52	Yamaç Köy Camisi	1	2015
20	Boğaztepe Camisi	1	2007		53	Tirmen Köyü Camisi	1	2015
21	Tuzluca Camisi	1	2007		54	Kurudere Köyü Camisi	2	2015
22	Taşlıca Camisi	1	2007		55	Ardahan Köyü Camisi	1	2015
23	Ağıllar Camisi	1	2007		56	Başpınar Camisi	2	2015
24	Tatlısu Camisi	1	2007		57	Gürpınar Camisi	1	2016
25	Yeni Erenköy Camisi	2	2007		58	Aslanköy Camisi	2	2016
26	Beyarmudu Camisi	2	2009		59	Akova Camisi	2	2016
27	Ötüken Camisi	1	2009		60	Kozanköy Camisi	2	2016
28	Harika Mahal. Camisi	2	2009		61	Bostancı Camisi	2	2017
29	Gemikonağı Camisi	2	2009		62	Akdoğan Camisi	2	2017
30	Alayköy Camisi	2	2009		63	İncirli Camisi	2	2017
31	Ulukışla Camisi	2	2009		64	Lefkoşa Sanayi Camisi	2	2017
32	Yayla Camisi	1	2009		65	Pınarlı Camisi	2	2017
33	Adaçay Camisi	1	2010					

Figure 2.2 List of new mosques in North Cyprus with the number of minarets attached to each one

APPENDIX 3

CYPRUS RELIGIOUS FOUNDATIONS ADMINISTRATION (KIBRIS VAKIFLAR İDARESİ), A TYPICAL MINARET PROJECT PLAN



APPENDIX 4

THE STUDIED MINARETS PLANS

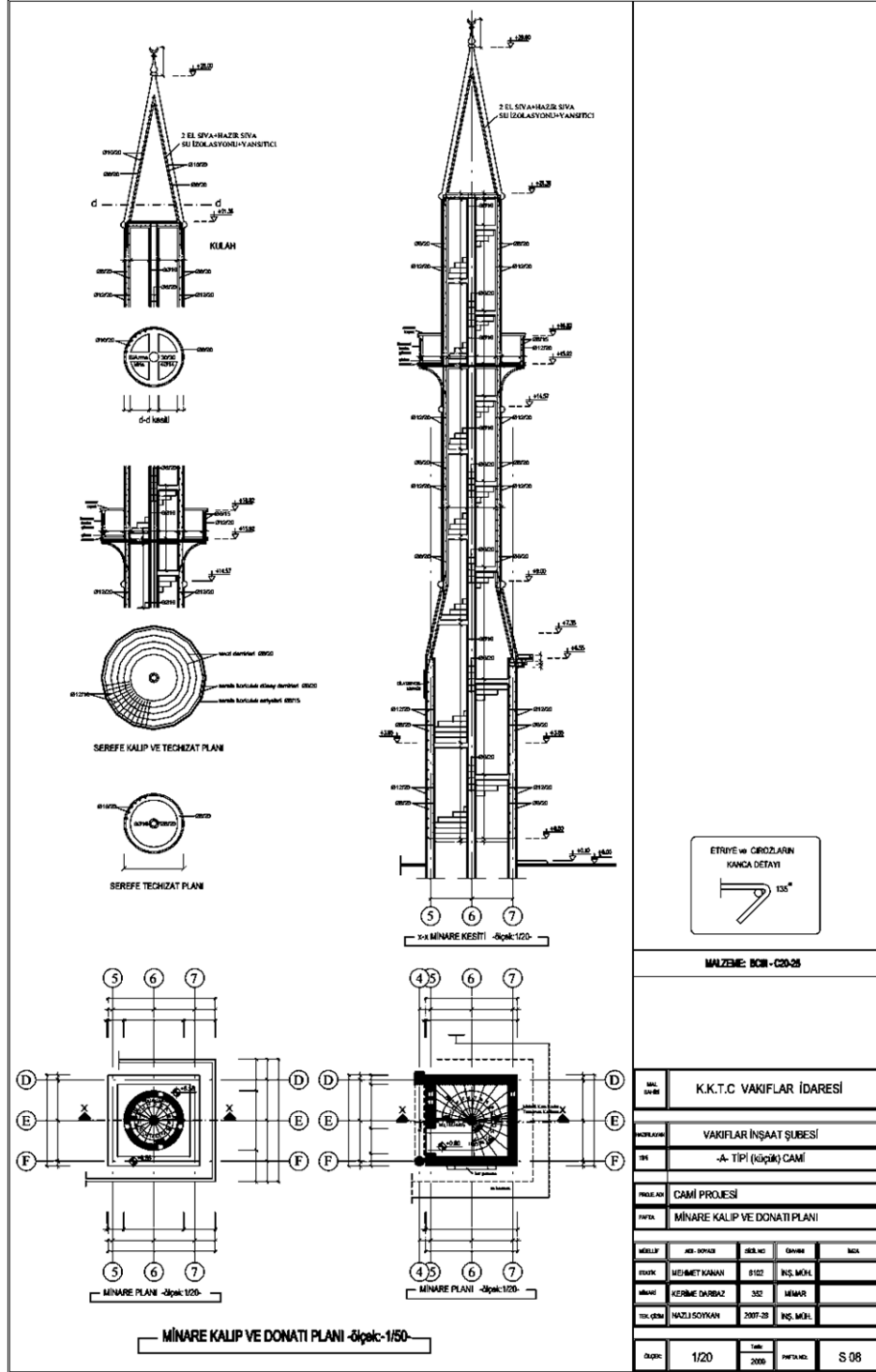


Figure 4.1 Detailed plan for the 26.0 m minaret

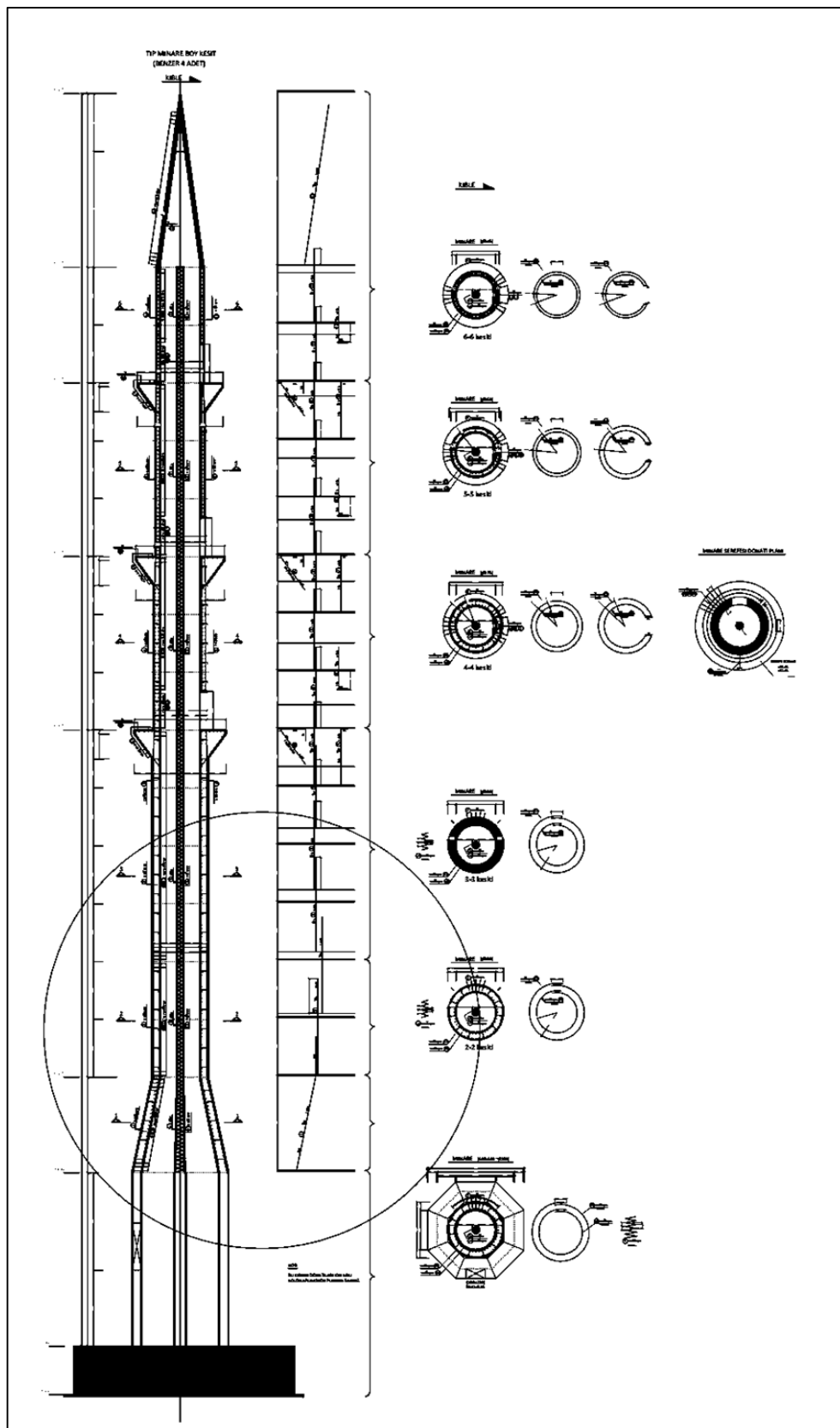


Figure 4.3 Detailed plan for the 61.45 m minaret

APPENDIX 5

ESTIMATING OF VORTEX SHEDDING EFFECTS ON TALL STRUCTURES

For the estimation of across load due to vortex shedding on tall structures, the following relation can be used:

$$F_L = F_{Lm} \cos 2\theta = C_L \frac{\rho g}{2} D H^2 K_{Dm} \cos 2\theta$$

where,

F_L is the equivalent across force

F_{Lm} is the maximum across force

$$\theta = \left(\frac{2\pi x}{L} - \frac{2\pi l}{T} \right)$$

And the next figures show the curves that relate the ratio (C_L/C_D) with the value ($\frac{U_{max} T}{D}$) (Sadeghi, 2001)

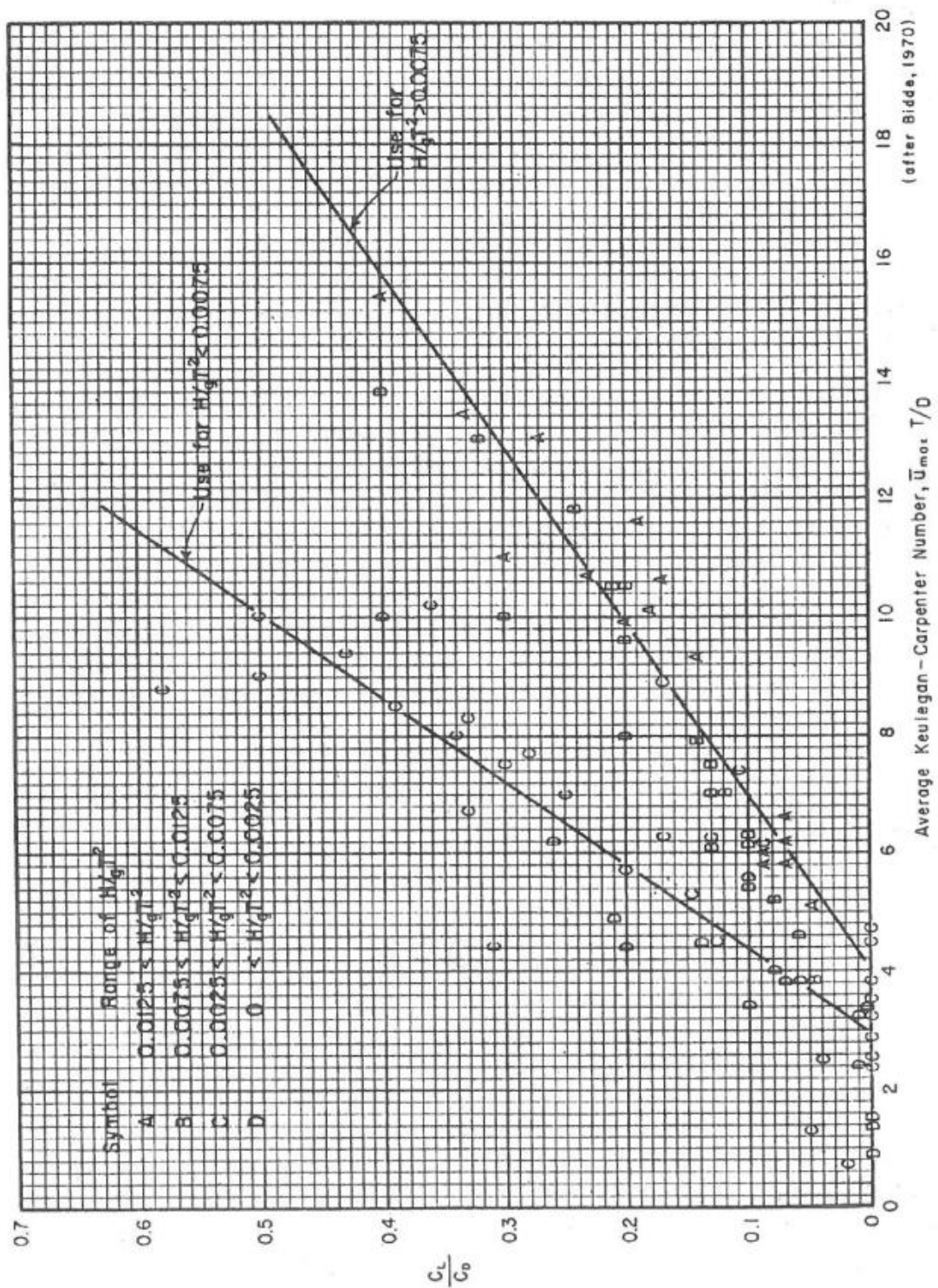


Figure 6.1: Relation curves between the ratio (C_L/C_D) and the value $(\frac{U_{max} T}{D})$ (Sadeghi,

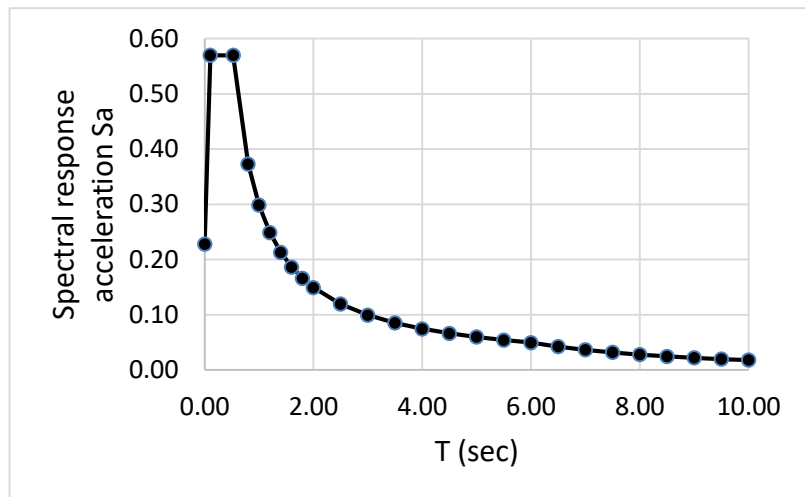
2001)

APPENDIX 6

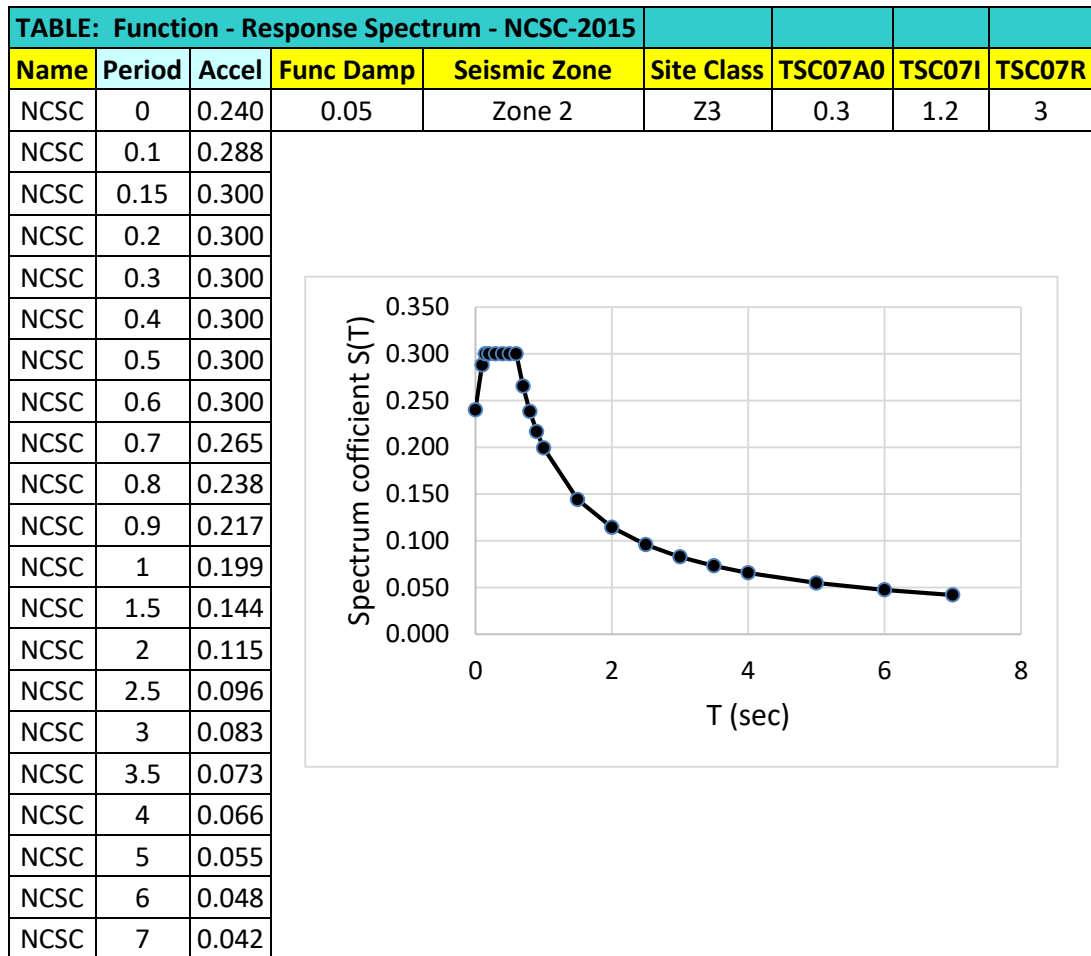
SAP2000 ANALYSIS AND RESULTS

1- Response spectrum function according to ACI307-98 by using SAP2000

TABLE: Function - Response Spectrum - ACI307-98												
Name	Period	Accel	Func Damp	Acc Option	Ss	S1	TL	Site Class	Fa	Fv	SDS	SD1
ACI307	0.00	0.23	0.05	User	0.68	0.2	6	D	1.26	1.9	0.57	0.30
ACI307	0.10	0.57										
ACI307	0.52	0.57										
ACI307	0.80	0.37										
ACI307	1.00	0.30										
ACI307	1.20	0.25										
ACI307	1.40	0.21										
ACI307	1.60	0.19										
ACI307	1.80	0.17										
ACI307	2.00	0.15										
ACI307	2.50	0.12										
ACI307	3.00	0.10										
ACI307	3.50	0.09										
ACI307	4.00	0.07										
ACI307	4.50	0.07										
ACI307	5.00	0.06										
ACI307	5.50	0.05										
ACI307	6.00	0.05										
ACI307	6.50	0.04										
ACI307	7.00	0.04										
ACI307	7.50	0.03										
ACI307	8.00	0.03										
ACI307	8.50	0.02										
ACI307	9.00	0.02										
ACI307	9.50	0.02										
ACI307	10.00	0.02										



2- Response spectrum function according to NCSC2015 by using SAP2000



3- Modal periods and frequencies for the studied minarets

TABLE: Modal Periods And Frequencies For 26.2 m Minaret				
OutputCase	StepType	StepNum	Period	Frequency
Text	Text	Unitless	Sec	Cyc/sec
MODAL	Mode	1	0.192	5.210
MODAL	Mode	2	0.190	5.256
MODAL	Mode	3	0.115	8.709
MODAL	Mode	4	0.101	9.852
MODAL	Mode	5	0.064	15.7
MODAL	Mode	6	0.059	16.85
MODAL	Mode	7	0.052	19.287
MODAL	Mode	8	0.048	20.915
MODAL	Mode	9	0.048	21.044
MODAL	Mode	10	0.044	22.712
MODAL	Mode	11	0.038	26.626
MODAL	Mode	12	0.034	29.055

TABLE: Modal Periods And Frequencies For 33.2m Minaret				
OutputCase	StepType	StepNum	Period	Frequency
Text	Text	Unitless	Sec	Cyc/sec
MODAL	Mode	1	0.616	1.624
MODAL	Mode	2	0.590	1.696
MODAL	Mode	3	0.258	3.874
MODAL	Mode	4	0.123	8.161
MODAL	Mode	5	0.116	8.595
MODAL	Mode	6	0.110	9.122
MODAL	Mode	7	0.083	12.033
MODAL	Mode	8	0.075	13.308
MODAL	Mode	9	0.069	14.435
MODAL	Mode	10	0.060	16.665
MODAL	Mode	11	0.054	18.640
MODAL	Mode	12	0.053	18.824

TABLE: Modal Periods And Frequencies For 61.45m Minaret				
OutputCase	StepType	StepNum	Period	Frequency
Text	Text	Unitless	Sec	Cyc/sec
MODAL	Mode	1	1.149	0.871
MODAL	Mode	2	1.136	0.881
MODAL	Mode	3	0.632	1.582
MODAL	Mode	4	0.326	3.068
MODAL	Mode	5	0.279	3.590
MODAL	Mode	6	0.267	3.742
MODAL	Mode	7	0.258	3.873
MODAL	Mode	8	0.245	4.080
MODAL	Mode	9	0.189	5.289
MODAL	Mode	10	0.154	6.505
MODAL	Mode	11	0.143	6.998
MODAL	Mode	12	0.125	7.993

TABLE: Modal Periods And Frequencies For 76.2m Minaret				
OutputCase	StepType	StepNum	Period	Frequency
Text	Text	Unitless	Sec	Cyc/sec
MODAL	Mode	1	1.184	0.844
MODAL	Mode	2	1.182	0.846
MODAL	Mode	3	0.560	1.785
MODAL	Mode	4	0.418	2.394
MODAL	Mode	5	0.375	2.670
MODAL	Mode	6	0.330	3.035
MODAL	Mode	7	0.316	3.161
MODAL	Mode	8	0.218	4.578
MODAL	Mode	9	0.208	4.814
MODAL	Mode	10	0.158	6.316
MODAL	Mode	11	0.145	6.914
MODAL	Mode	12	0.138	7.251

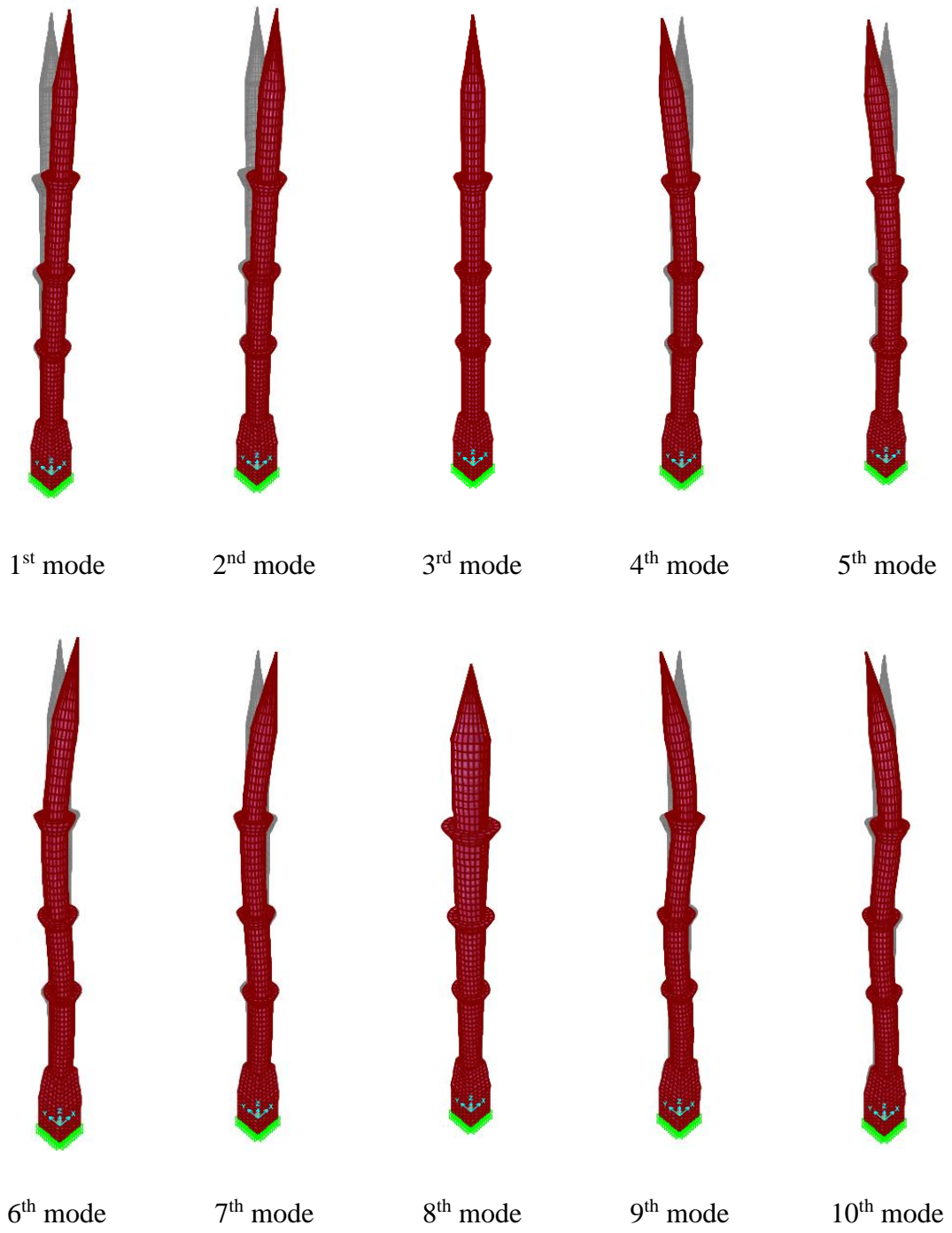


Figure 6.1: First 10 modal shapes for the 76.2 m minaret.